UNIVERSITI TEKNOLOGI MARA

MODELING OF FIRE HAZARD INDEX FROM MULTISPECTRAL INDICES FOR ESTIMATING WILDFIRE HAZARD ZONES IN PERLIS

AFIQAH ZAHIDAH BINTI ANWARZAINI

MSc

August 2026

UNIVERSITI TEKNOLOGI MARA

MODELING OF FIRE HAZARD INDEX FROM MULTISPECTRAL INDICES FOR ESTIMATING WILDFIRE HAZARD ZONES IN PERLIS

AFIQAH ZAHIDAH BINTI ANWARZAINI

Thesis submitted in fulfilment
of the requirements for the degree of
Master of Science
(Built Environment)

Faculty of Built Environment

August 2026

CONFIRMATION BY PANEL OF EXAMINERS

I certify that a Panel of Examiners has met on 8th May 2026 to conduct the final examination of Afiqah Zahidah Binti Anwarzaini on her Masters of Science thesis entitled "Modeling of Fire Hazard Index from Multispectral Indices for Estimating Wildfire Hazard Zones in Perlis" in accordance with Universiti Teknologi MARA Act 1976 (Akta 173). The Panel of Examiners recommends that the student be awarded the relevant degree. The Panel of Examiners was as follows:

Irwan Mohammad Ali, PhD
Associate Professor
Faculty of Built Environment
Universiti Teknologi MARA
(Chairman)

Faradina Marzukhi, PhD
Senior Lecturer
Faculty of Built Environment
Universiti Teknologi MARA
(Internal Examiner)

Mohd Farid Mohd Ariff, PhD
Senior Lecturer
Faculty of Built Environment & Surveying
Universiti Teknologi Malaysia
(External Examiner)

PROF DR HJH ZURAEDA BINTI IBRAHIM
Dean
Institute of Postgraduates Studies
Universiti Teknologi MARA

Date: 18 August 2026

AUTHOR'S DECLARATION

I declare that the work in this thesis was carried out in accordance with the regulations of Universiti Teknologi MARA. It is original and is the result of my own work, unless otherwise indicated or acknowledged as referenced work. This thesis has not been submitted to any other academic institution or non-academic institution for any degree or qualification.

I hereby acknowledge that I have been supplied with the Academic Rules and Regulations for Postgraduate, Universiti Teknologi MARA, regulating the conduct of my study and research.

Name of Student	:	Afiqah Zahidah Binti Anwarzaini
Student ID. No.	:	2023227964
Programme	:	Master of Science (Built Environment) – CFAP781
Faculty	:	Built Environment
Thesis Title	:	Modeling of Fire Hazard Index from Multispectral Indices for Estimating Wildfire Hazard Zones In Perlis
Signature of Student	:	
Date	:	August 2026

ABSTRACT

Wildfire is an uncontrolled burning that occurs in natural vegetation, including forests, grasslands, and peatlands. Fueled by climate change, land-use changes, and prolonged droughts, wildfires pose significant threats to ecosystems, human lives, and property worldwide. Over the past decade, wildfire occurrences in Perlis have increased in frequency and intensity, particularly during March and April. According to the data from the Perlis State Fire and Rescue Department, 55% of wildfire incidents involving agricultural fields, woodlands, and shrub lands occurred in March, between 2012 and 2024. Previous studies conducted in Malaysia have frequently utilized Land Surface Temperature (LST), the Normalized Difference Vegetation Index (NDVI), and the Normalized Burn Ratio (NBR) as predictors of wildfire occurrence. However, the use of multispectral indices in wildfire prediction remains limited in some studies. Therefore, this study aims to develop a framework that incorporates multispectral indices for the predictive modelling of the wildfire hazard zone in Perlis. The objectives of this study are: (i) to examine the changing trend of LST and wildfire occurrence from the year 2014 to the year 2024, (ii) to determine the correlations among NDVI, NDWI, NDMI, NDDI, NBR, and LST for the year 2024, and (iii) to model the potential wildfire occurrences within the state of Perlis using the Fire Hazard Index (FHI). This study utilizes satellite imagery to derive remote sensing indices, while the statistical data on the frequency and locations of wildfire occurrences were obtained from the Fire and Rescue Department. Multiple Linear Regression (MLR) was employed to evaluate the strength of the relationship between LST and each index in relation to wildfire occurrence, and Kernel Density Estimation (KDE) was conducted to identify the wildfire hazard zone. The results indicate an increasing trend in wildfire occurrence associated with elevated temperatures and arid conditions. NDVI, NBR, and NDDI exhibited positive relationships with LST, whereas NDMI and NDWI showed inverse relationships. Hazard zone mapping shows that the Kangar political zone was classified as a “Very High Hazard” zone based on the number of reported wildfire cases. These findings may assist decision-makers in implementing preventive strategies to mitigate the risks and impacts of wildfires, while also contributing to the academic understanding of the application of spatial indices in estimating wildfire occurrence.

ACKNOWLEDGEMENT

I would like to express my deepest gratitude to my thesis advisor, Sr Dr Nazirah Md Tarmizi, for her invaluable guidance, insightful feedback, and unwavering support throughout this research journey. Her expertise, patience, and encouragement have been instrumental in shaping this work and my development as a researcher.

My appreciation also extends to the Faculty of Built Environment, UiTM Perlis branch, whose academic environment and institutional support provided the resources and opportunities necessary to complete this research. I would also like to acknowledge the UiTM Research Management Centre for their financial assistance and support, which made this work possible.

I am deeply thankful to my colleagues, peers, and friends for their encouragement, insightful discussions, and companionship throughout this process. Their support helped make the challenges of graduate study both manageable and rewarding.

Finally, I owe my greatest thanks to my family for their unconditional love, patience, and belief in me. Their constant encouragement and sacrifices have been a source of strength and motivation during every stage of this journey. This achievement would not have been possible without their support.

To all who contributed, directly or indirectly, to the completion of this thesis, I offer my sincere gratitude.

TABLE OF CONTENTS

		Page
CONFIRMATION BY PANEL OF EXAMINERS		**ii**
AUTHOR'S DECLARATION		**iii**
ABSTRACT		**iv**
ACKNOWLEDGEMENT		**v**
TABLE OF CONTENTS		**vi**
LIST OF TABLES		**ix**
LIST OF FIGURES		**xi**
LIST OF PLATES		**xii**
LIST OF ABBREVIATIONS		**xv**
CHAPTER 1 INTRODUCTION		**1**
1.1	Research Background	1
1.2	Problem Statement	5
1.3	Study Area	10
1.4	Aim	11
1.5	Research Question	11
1.6	Research Objective	12
1.7	Significance of Work	12
1.8	Scope and Limitation	14
1.9	Conclusion	16
CHAPTER 2 LITERATURE REVIEW		**17**
2.1	Introduction	17
2.2	Types of Fire	17
	2.2.1 Open Burning	17
	2.2.2 Wildfire	18
2.3	Factors Contributing to Fire Occurrence	20
	2.3.1 Human Factors	21
	2.3.2 Natural Factor	23
2.4	Methods to Detect Wildfires	25
	2.4.1 Direct Methods	25

2.4.2 Indirect Methods 27
2.5 Previous Studies on Wildfire Estimation Using Geospatial Techniques 29
2.5.1 Spectral Analysis 29
2.5.2 Spatial and Meteorological Analysis 31
2.6 Types of Spectral Indices Used in the Previous Study to Detect Wildfire 33
2.6.1 Land Surface Temperature (LST) 33
2.6.2 Normalized Difference Vegetation Index (NDVI) 35
2.6.3 Normalized Difference Moisture Index (NDMI) 36
2.6.4 Normalized Difference Water Index (NDWI) 37
2.6.5 Normalized Difference Drought Index (NDDI) 38
2.6.6 Normalized Burn Ratio (NBR) 38
2.7 Spatial Analysis Used in Previous Studies to Determine Wildfire Hazard Zones 39
2.7.1 Interpolation Technique to Identify Wildfire Hazard Zone 40
2.7.2 Kernel Density Estimation in Identifying Wildfire Occurrence Density 41
2.8 Effect of LST on Wildfire Occurrence 42
2.9 Statistical Analysis Using Multiple Linear Regression 44
2.10 Conclusion 45

CHAPTER 3 RESEARCH METHODOLOGY 46
3.1 Introduction 46
3.2 Research Methodology 46
3.3 Data Acquisition 50
3.3.1 Spatial Data 50
3.3.2 Non-Spatial Data 50
3.4 Data Pre-processing 51
3.4.1 Tabular Data 51
3.4.2 Remote Sensing and GIS Data 52
3.5 Evaluation of Wildfire Occurrence and LST Variation from the Year 2014 to 2024 53
3.5.1 Establishment of Spatiotemporal Pattern of Wildfire Occurrence from the Year 2014 to 2024 53
3.5.2 Derivation of LST from the Years 2014 to 2024 54
3.6 Correlation between Spectral Indices and LST for the Year 2024 56
3.6.1 Extraction of the Chosen Spectral Indices for the Year 2024 56
3.6.2 Execution of Statistical Analysis Using Linear Regression 58
3.7 Determination of the Wildfire Hazard Zone in Perlis 58

3.7.1 Determination of Wildfire Zoning Using Kernel Density Estimation (KDE) 59
3.7.2 Model Generation and Hazard Zone Mapping 59
3.8 Conclusion 61

CHAPTER 4 RESULTS AND DISCUSSION 62
4.1 Introduction 62
4.2 Analysis of Frequency of Wildfire Occurrence and LST from the Year 2014 to 2024 62
4.2.1 Wildfire Occurrence Density Mapping from the Year 2014 to 2024 62
4.2.2 Variation of LST from the Years 2014 to 2024 66
4.3 Relationship between Spectral Indices and LST 70
4.3.1 Map of the Chosen Spectral Indices 70
4.3.2 Statistical Correlation and Validation Using MLR 79
4.4 Assessment of Wildfire Hazard Zone in Perlis 82
4.4.1 Identification of Wildfire Hazard Zone for Perlis State Using KDE 82
4.4.2 Fire Hazard Index and Zoning Using MLR 86
4.5 Discussion 89
4.5.1 Interpreting the Wildfire Occurrence Frequency and Variation of LST 89
4.5.2 Describing the Correlation Between Spectral Indices and LST 91
4.5.3 Aligning the Fire Hazard Index in Predicting Wildfire Hazard Zones 93

CHAPTER 5 CONCLUSION 98
5.1 Introduction 98
5.2 Conclusion 98
5.3 Recommendations for Future Works 101

REFERENCES 102

APPENDICES 127

AUTHOR'S PROFILE 132

LIST OF TABLES

Tables	Title	Page
Table 1.1	Monthly Percentage Of Recorded Cases From The Year 2014 To The Year 2024	5
Table 1.2	Research Gap Of Previous Studies Conducted In Malaysia.	9
Table 3.1	Satellite Data And Fire Cases Acquisition	51
Table 3.2	Sample Of The Data Filtered From The Fire And Rescue Department	52
Table 3.3	Formulation Used To Derive LST	55
Table 4.1	The Mann-Kendall Test For Wildfire Cases From The Year 2014 To 2024 In Perlis	64
Table 4.2	The Accuracy Confusion Matrix Of LULC For The Year 2024	72
Table 4.3	Result Of The Overall Model	82
Table 4.4	Result Of MLR Of Model Parameter	82

LIST OF FIGURES

Figures	Title	Page
Figure 1.1	Post-Fire Incidents Near Bukit Lagi, Perlis	3
Figure 1.2	Study Area Of This Research Work	11
Figure 3.1	Overall Methodology Flowchart For The Study	49
Figure 3.2	Radiometric Correction Using Raster Calculator For Each Spectral Band	53
Figure 4.1	Number Of Wildfire Cases In March From The Year 2014 To The Year 2024 In Perlis	63
Figure 4.2	Comparison Of The Total Number Of Fire Cases From The Year 2014 To 2024 In Perlis	64
Figure 4.3	Spatial Distribution Of Wildfire Cases From The Year 2014 To 2024 In Perlis	65
Figure 4.4	LST Variation From The Years 2014 To 2017 In Perlis	67
Figure 4.5	Lst Variation From The Years 2018 To 2021 In Perlis	68
Figure 4.6	LST Variation From The Years 2018 To 2021 In Perlis	69
Figure 4.7	The LULC Map Of Perlis For The Year 2024	73
Figure 4.8	Map Of NDVI For March 2024 In Perlis	74
Figure 4.9	Map Of NDMI For March 2024 In Perlis	75
Figure 4.10	Map Of NDWI For March 2024 In Perlis	76
Figure 4.11	Map Of NDDI For March 2024 In Perlis	77
Figure 4.12	Map Of NBR For March 2024 In Perlis	78
Figure 4.13	The Relationship Between NDVI And LST For The Year 2024	79
Figure 4.14	The Relationship Between NDWI And LST For The Year 2024	80
Figure 4.15	The Relationship Between NDMI And LST For The Year 2024	80
Figure 4.16	The Relationship Between NDDI And LST For The Year 2024	81
Figure 4.17	The Relationship Between NBR And LST For The Year 2024	81

Figure 4.18	Hotspot Of Wildfire Incidents From The Year 2014 To 2024 In Perlis	84
Figure 4.19	Density Of Wildfire Occurrence By Year In Perlis	85
Figure 4.20	The Wildfire Hazard Zone Based On Fire Location In Perlis	87
Figure 4.21	The Wildfire Hazard Zone Based On Spectral Indices Values In Perlis	88
Figure 4.22	Post-Fire Image Taken On 28th January 2026 At Chuping, Perlis	96

LIST OF PLATES

Plates	Title	Page
Plate 1.1	The Heat Status Of Perlis (Metmalaysia Website Retrieved On 20th March 2024)	13

LIST OF ABBREVIATIONS

Abbreviations

AHP	Analytic Hierarchy Process
AMO	Atlantic Multidecadal Oscillation
AO	Arctic Oscillation
AVHRR	Advanced Very-High-Resolution Radiometer
CBI	Composite Burn Index
CO	Carbon Oxide
COPD	Chronic Obstructive Pulmonary Disease
DA	Dual-Angle algorithm
DEM	Digital Elevation Model
dNBR	Difference Normalized Burned Ratio
ENSO	El Niño Southern Oscillation
ENTLN	Earth Network Total Lightning Network
EP/NP	East Pacific/North Pacific
FMC	Fuel Moisture Content
FWI	Fire Weather Index
GEE	Google Earth Engine
GIS	Geographic Information System
GLM	Generalized Linear Model
GPS	Global Positioning System

GWR	Geographical Weighted Regression
IDW	Inverse Distance Weighting
IR	Infra-Red
KDE	Kernel Density Estimation
KML	Keyhole Markup Language
LST	Land Surface Temperature
LULC	Land Use Land Cover
MLR	Multiple Linear Regression
MODIS	Moderate Resolution Imaging Spectroradiometer
NASA	National Aeronautics and Space Administration
NBR	Normalized Burn Ratio
NDBI	Normalized Difference Built-up Index
NDDI	Normalized Difference Drought Index
NDMI	Normalized Difference Moisture Index
NDVI	Normalized Difference Vegetation Index
NDWI	Normalized Difference Water Index
NIR	Near Infrared
NLDN	National Lightning Detection Network
NOAA	National Oceanic and Atmospheric Administration
OLS	Ordinary Least Squares
OSM	Open Street Map
PM	Particulate Matter

QA	Quality Assessment
SAVI	Soil Adjusted Vegetation Index
SC	Single-Channel algorithm
SDG	Sustainable Development Goal
SEA	Southeast Asia
SRTM	Shuttle Radar Topography Mission
SW	Split-Window algorithm
SWIR	Short Wave Infra-Red
TIR	Thermal Infrared
UAV	Unmanned Aerial Vehicle
USGS	United State Geological Survey
VIIRS	Visible Infrared Imaging Radiometer Suite
WLLN	World Wide Lightning Location Network
WRI	Water Ratio Index

CHAPTER 1
INTRODUCTION

1.1 Research Background

Wildfires or forest fires are uncontrolled fires that rapidly propagate across vegetation and forested areas, which can adversely impact the economy, the environment, and society in several ways. Wildfires have various advantageous effects, including the suppression of insects and diseases, the enhancement of soil nutrient regimens, and the facilitation of forest regeneration (Chowdhury & Hassan, 2015). Despite the positive impacts of wildfires, the adverse consequences of the incident are extremely concerning. Several negative perceptions of the incidents include the loss of forestry revenues, the acceleration of global warming, the destruction of neighbourhoods, critical infrastructure, and biodiversity, and the increase in respiratory diseases (Abdollahi, Islam, Gupta, & Hassan, 2018). In recent decades, wildfires have become increasingly common and more vigorous due to both meteorological and human-induced factors.

Human-induced factors related to the direct and indirect presence of human activities during the ignition. Human-induced wildfires constitute 60–80% of the overall sum of fires from all ignition sources (Guo et al., 2016). Human factors that can ignite fires include arson, negligence, use of fire, population density, distance to settlements, and distance to roads. The increased of transportation facilities in forested regions also heightened outdoor recreational activities, especially during weekends and public holidays (Costafreda-Aumedes, Comas, & Vega-Garcia, 2017). However, since late 2019, climate change has significantly affected the occurrence of wildfires on a larger scale. Consequently, meteorological conditions are utilised globally to formulate indices that assess fire risk, as well as the intensity and rate of spread of a fire upon ignition (Trang, Andrew, Chu, & Enright, 2022).

Since the mid-20th century, climate change has presented a considerable threat to the worldwide environment. This phenomenon acted as an additional precursor for the heightened incidence of wildfires in Southeast Asia (SEA) regions (Khan et al., 2020). Chew, Ooi, Pang, & Lim (2023) assert that global climate change has led to increased temperatures and reduced precipitation, fostering extended dry and heated

conditions that facilitate the ignition and the proliferation of wildfires. The vulnerability of SEA to climate change is mostly due to its diverse monsoon and tropical rainforest climates, marked by high temperatures and significant precipitation (Dong et al., 2024). Alterations in the global climate have heightened the likelihood of wildfire incidents in the SEA countries due to extreme El Niño phenomena.

El Niño is a periodic phenomenon that transpires over the years, which can exacerbate the intensity of flames. The rise in temperatures, along with prolonged and intensified droughts during El Niño, is resulting in more extensive and frequent wildfires due to the enhanced desiccation and ignition of vegetative fuels (Chaparro, Vall-llossera, et al., 2016). It was noted that in 2015, this phenomenon contributed to the increased incidence of wildfires in the SEA countries (Khan et al., 2020). The drought induced by El Niño was also responsible for the exceptionally severe wildfires in 1997 and 2006 in Indonesia (Wee, Park, Alcantara, & Lee, 2024). El Niño typically elevates summer temperatures in several countries, thereby increasing the risk of wildfires (Cordero et al., 2024). Wildfires may initiate in a limited region but swiftly proliferate to cover vast areas, especially in hot, dry, and windy circumstances.

Over the past decades, uncontrollable and catastrophic wildfires have become expected annual events globally. Portugal has witnessed a significant rise in burned areas in recent decades (Nunes, 2012; Lourenco, Fernandes, Nunes, Bento-Goncalves, & Vieira, 2013). The General Directorate of Forestry in Turkey documented a total of 63,724 wildfires in the last twenty years (Çolak & Sunar, 2020). Meanwhile, in the United States, Canada has recorded an increase in frequency and intensity of wildfires that constitute around 25% of the global peatland area (Pelletier, Millard, & Darling, 2023). Additionally, in Asian countries with a tropical monsoon climate, the wildfire has become an annual event. In Vietnam, the General Statistics Office reported 4571 cases of wildfires from 2009 to 2018, destroying up to 22,000 ha of forest, peaking in 2010 with 6,723 ha destroyed (Nguyen & Tong, 2023). According to Rendana et al. (2023), in 2019, the total area burned in South Sumatra amounted to 52,716 hectares. Wildfires occurred 2341 times in Indonesia between 2018 and 2022, resulting in the permanent displacement of 156 individuals, the destruction of 38 houses, and 3 educational facilities (Aldiansyah & Madani, 2024). According to the data that has been presented, wildfires are a global problem that is becoming more frequent and intense.

Likewise, Malaysia also encountered the same issue of wildfire. As mentioned by Mat Deli (2023), historical data demonstrate that disturbed or open forest areas,

marked by dryness and an abundance of combustible debris, exhibit heightened susceptibility to wildfire. From 1992 to 1998, there were 1,232 fires reported involving forests in Peninsular Malaysia, Sabah, and Sarawak (Jamaruppin, Bayuaji, Ghani, & Rahman, 2016). Notably, during the El Niño event, this risk was elevated during the drought period, which occurs almost annually (Fisal, Litangah, & Ismanyah, 2017). Sabah and Sarawak have a higher incidence of wildfires than Peninsular Malaysia, as indicated by historical data, with approximately one million hectares of predominantly over-logged forests having vanished (Chew, Ooi, Pang, & Wong, 2022).

In Peninsular Malaysia, a total of 119 reports on wildfire outbreaks were recorded between 2010 and 2016, encompassing a total area of 5,347 ha of the Permanent Reserve Forest (Musri et al., 2020). Though the majority of occurrences were categorized as small-scale, encompassing areas under 100 hectares, the frequency of these incidents is increasing (Chew et al., 2023), especially during the El Niño season. Between January 15, 2024, and January 13, 2025, a total of 182 Visible Infrared Imaging Radiometer Suite (VIIRS) fire alarms were recorded, focusing solely on high-confidence signals (Global Forest Watch, 2025). Figure 1.1 illustrate post wildfire near Bukit Lagi in Perlis, Malaysia that occur in January 2026, the beginning of hot and dry season. The wildfire occur at the grasslands adjacent to Dewan 2020, located at approximately 6°24'58.87"N and 100°11'42.08"E.

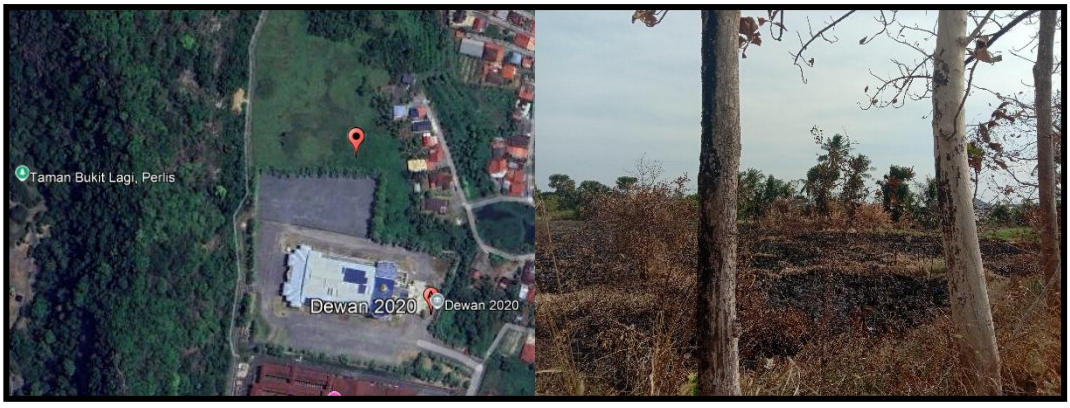

Figure 1.1 Post-Fire Incidents Near Bukit Lagi, Perlis

Previously, fire management agencies mainly used direct methods to assess fire occurrence. The fire risk assessment was based on expert judgment and a set of explanatory variables, including fuels, topography, and weather (Weinstein & Woodbury, 2010). The methods commonly utilized for fire detection are watch towers, optical smoke detection, and spotter planes (Alkhatib, 2014). These methods are not only expensive and inflexible but also incapable of encompassing extensive areas

(Allison, Johnston, Craig, & Jennings, 2016). In contrast, indirect methods using satellite surveillance, able to cover large areas, provide an expansive perspective of fire behaviour, and the data can last several decades (Mohapatra & Trinh, 2022; Thangavel et al., 2023). Hence, it is crucial to utilize the advancements in technology for early detection, monitoring, and management, such as Geographic Information Systems (GIS) and remote sensing.

GIS and remote sensing technology have been progressively employed in decision-making and the management of natural resources. The development of spatially specific GIS models has considerably improved this process by allowing authorities to map and study the factors affecting wildfire incidence over a broad geographic region (Setiawan, Mahmud, Mansor, Shariff, & Nuruddin, 2004). Remote sensing and GIS are essential methodologies for monitoring extensive occurrences in both spatial and temporal dimensions, especially in remote areas like forests (Gupta & Shukla, 2022). Satellite-derived data have been extensively utilized to monitor alterations on the Earth's surface and evaluate their environmental consequences (Zhang, Hu, & Ban, 2022). Wildfire analysis with remote sensing data is conducted using visible and infrared images, which are frequently employed to derive parameters related to wildfires (Gizatullin & Alekseenko, 2022).

Remote sensing technology is a valuable instrument for evaluating wildfires due to its particular benefits in terms of the availability of spatial, spectral, radiometric, and temporal data. Analysing spectral indices can yield insights for pinpointing high-risk areas and modelling the probability of future events based on spatial relationships with climate variables (Parvar, Saeidi, & Mirkarimi, 2024). The detection of wildfires can be aided by vegetation and climate data such as LST, NDVI, NDMI, and NDWI (Bhattacharya et al., 2025). These approaches provide a considerable advantage in terms of efficiency and dependability, especially in distant places with extreme weather conditions and extensive areas threatened by wildfires (Singh & Srivastava, 2025).

In conclusion, geospatial analysis is becoming important for assessing wildfires. The integration of remote sensing and GIS enables a comprehensive evaluation throughout all phases of the wildfire lifecycle, from pre-fire hazard mapping to post-fire recovery monitoring. Cloud-based platforms that are easily accessible and incorporate geographic data might enhance the accessibility of wildfire risk management for all entities. Sentinel-2 and 3, and Landsat OLI/TIRS 8 and 9 are among the most effective instruments for monitoring vegetation, detecting active wildfires, and

assessing the progression of burn severity over time. The integration of remote sensing and GIS facilitates the generation of comprehensive wildfire risk maps through geographical overlays, statistical analysis, and predictive modelling.

1.2 Problem Statement

In recent decades, wildfires have occurred with increased frequency and intensity due to human activity and climate change. Several regions, particularly those characterised by Mediterranean, semi-arid, or forested ecosystems, are increasingly susceptible to wildfires due to rising global temperatures and changes in rainfall patterns. Table 1.1 presents the monthly percentage of recorded cases in Perlis, and the data shows that wildfire occurrences in March and April account for 50% of overall incidents, which typically signify hot and dry weather. Wildfires are becoming increasingly unpredictable and larger, which has significant impacts on society, the economy, and the environment. These incidents devastate natural ecosystems, emit carbon, compromise infrastructure, cause public health concerns, and adversely affect soil and water systems over an extended duration. For this reason, it is imperative to have precise and timely methods of predicting the severity of wildfires to prevent them, devise a plan for suppression, and establish recovery planning after a fire.

Table 1.1
Monthly Percentage Of Recorded Cases From The Year 2014 To The Year 2024

Month	Total number of recorded cases	Percentage (%)
January	77	5
February	22	1
March	795	50
April	316	20
May	46	3
June	45	3
July	39	2
August	58	4
September	27	2
October	23	1
November	20	1
December	132	8

Source: (author, 2026)

Conventional approaches to evaluating burned areas from the ground only cover a limited area and can be costly and time-consuming. In contrast, geospatial technologies, particularly remote sensing and GIS, are highly advantageous for the rapid and comprehensive estimation of wildfires (Gupta & Shukla, 2022). Satellite imagery is preferable for evaluating the likelihood of wildfire occurrence, as this method is more

effective in acquiring timely data and is able to cover a larger extent. Spectral indices such as LST, NDVI, NDMI, and NBR are the most common indices utilized in many wildfire analysis studies. These indices are essential for assessing wildfires on both regional and global scales, and the information can enhance the understanding of the impact of climate change on fire patterns.

Over the past few decades, numerous studies have been conducted globally to investigate the impact of wildfires and the likelihood of their occurrence through the use of spectral indices. However, there are few references related to wildfire estimation, and limited studies utilize LST for assessing the likelihood of wildfire occurrence in Malaysia, despite the increasing threat posed by wildfires. LST is an important parameter to be explored as elevated temperatures might result in reduced moisture, increasing the likelihood of dryness and susceptibility to ignition (Parvar et al., 2024). There is a lack of studies examining the correlation between various remote sensing indices and the increase in surface temperature.

Yet, upon further examination, it becomes apparent that there are numerous methodological and conceptual issues that indicate the existence of research gaps. Jamaruppin et al. (2016) utilised LST to assess the fire hazards in Kuantan, Pahang. LST was determined using a split-window measurement algorithm, and the findings discovered that the temperature significantly increased during ignition, exceeding 34°C, and decreased to below 16°C after ignition. The study ignores vegetation factors that may alter fire danger, such as the health of vegetation or the moisture content of fuel sources. This makes the fire prediction model less comprehensive. The technique used is proper for temperature change monitoring between pre-fire and post-fire events, but not suitable for wildfire hazard assessment.

Junaidi et al. (2021) investigated the relationship between LST and NBR in Kuala Baram, Sarawak, using the Pearson correlation statistic. The findings indicate a strong negative relationship between LST and NBR, where unburned regions generally exhibit lower LST values, whereas burned forested areas are likely to have elevated surface temperatures. The study connects the thermal and spectral indices, though it primarily focuses on post-fire analysis rather than assessing wildfire risk. Therefore, the fire prediction model is insufficient to encompass other vegetation aspects due to the fact that it only employs LST and NBR. The method presented in the study may be suitable to assess the effect of fire severity on the surrounding LST.

Moreover, Ya'acob et al. (2022) investigated the influence of Land Use Land Cover (LULC), LST, and NDVI on regions affected by active fires within the Raja Musa Forest Reserve, Kuala Selangor, using the Analytical Hierarchy Process (AHP) method. From the findings, LULC is identified as the most critical factor, followed by LST and NDVI. The study presented anthropogenic, climatic, and environmental variables that may affect wildfire occurrence. However, the study failed to establish a definitive causal background and lacked sufficient clarity regarding the interactions among these variables. The results cannot be employed to assess wildfire hazard due to the absence of effective statistical methodologies capable of simulating the correlations between each index. Thus, the method is not suitable for wildfire hazard assessment.

Not only that, Chew et al. (2023) discussed how variables such as temperature, precipitation, and wind velocity may influence the frequency of wildfires in Pahang using Google Earth Engine (GEE). The results show that mean temperature and precipitation have a significant influence on wildfire ignition, and wind speed expedites the spread. This work enhances the understanding of the significant impact of weather on the initiation and propagation of flames. But it solely examines meteorological variables and does not directly associate LST and vegetation indices with fire incidence. This demonstrates a disparity between the assessment of thermal images and the real-time simulation of fire activity. The study also does not examine methods for integrating meteorological and geospatial data into a particular prediction model.

Ghazali et al. (2025) mainly employed the differenced Normalised Burn Ratio (dNBR) derived from the burn index formula to assess the severity of the fires in Dungun, Terengganu. The data revealed that the locations with the highest dNBR values experienced the most extensive burning, indicating that the index serves as an effective method for assessing the severity of damage post-fire. This strategy solely examines historical data and does not consider pre-fire factors that could aid in predicting the likelihood of a wildfire; excluding LST also neglects critical thermal dynamics essential for assessing the likelihood of ignition. Therefore, the technique employed is not relevant for wildfire hazard application.

Table 1.2 illustrates the research gap in wildfire studies conducted in Malaysia. Based on the table, it can be deduced that few studies in Malaysia have adopted geospatial indicators, such as LST and NDVI, to detect and monitor wildfires; however, the studies do not include the prediction of the wildfire hazard zone. All five studies analyse the application of spectral indicators, but each concentrates on a limited set of

indices. None of the studies provides a comprehensive and predictive model that integrates data from several spectral indices to assess wildfire occurrence. Although the studies generated a few wildfire severity map, yet, there are no maps of wildfire hazard zones produced. The deficiency of studies on wildfire hazard zones through geospatial analysis has opened a gap in wildfire applications in Malaysia.

The wildfire incidents in Perlis typically rose during March and April, since these months coincide with the late dry season, where prolonged low rainfall, high surrounding temperatures, and strong winds create ideal conditions for wildfires to ignite. Dry vegetation becomes highly flammable, while agricultural land-clearing activities further increase the risk of uncontrolled fires. Despite ongoing mitigation efforts such as public awareness campaigns by the Perlis state Environment Department and restrictions on open burning, the number and intensity of wildfires remain high during the hot and dry weather. These measures have been limited by weak enforcement, insufficient monitoring of high-risk areas, and extreme weather conditions that contribute to fire outbreaks. Current mitigation strategies may not have been sufficient to significantly reduce the frequency or severity of wildfires in Perlis during these critical months. Therefore, a robust model should be developed to monitor the high-hazard zone in Perlis during the hot and dry weather.

Table 1.2
Research Gap Of Previous Studies Conducted In Malaysia

No.	Author	Method	Results and analysis	Research gap
1.	Jamaruppin et al. (2016)	Split-window measurement algorithm	The classification of level fire hazard based on LST in Kuantan, Pahang, indicates a significant increase in temperature across extensive areas from pre-fire to during the fire, exceeding 34°C.	
2.	Junaidi et al., (2021)	Pearson correlation statistic	This study has demonstrated a significant negative correlation between LST and NBR values in Kuala Baram, Sarawak. The data suggest that unburned areas exhibit low surface temperatures, but forested regions impacted by fires display elevated temperatures.	Multispectral framework for the predictive modelling of wildfire hazard zones.
3.	Ya'Acob et al., (2022)	AHP method	The determination of active fire hotspots at Raja Musa Forest Reserve, Kuala Selangor, revealed that LULC has the most influence, followed by LST and NDVI.	
4.	Chew et al., (2023)	GEE JavaScript code editor	The investigation on the relationships of climatic factors and fire occurrences shows that mean temperature and rainfall significantly influence the occurrence of fires in Pahang.	
5.	Ghazali et al., (2025)	Burn index formula	The evaluation of forest fire severity in Dungun, Terengganu, using the dNBR index, indicates that most of the affected areas exhibit high-severity burn.	

Source: (author, 2026)

Although satellite data is becoming more prevalent and geospatial analysis techniques are becoming more sophisticated, it is still exceedingly challenging to accurately foresee the ignition of wildfires. There should be a definite technique that incorporates spectral indices into a reliable wildfire estimation model; this is because these indices can clarify the circumstances that are prone to ignite fires. LST is sometimes considered a fire danger indicator; however, it cannot independently predict flames without incorporating additional relevant factors such as NDMI and NDDI. The dearth of localised validation reduces the relevance of LST-based fire risk mapping in Malaysia. Addressing this gap is essential for enhancing the efficacy of early warning systems and implementing targeted mitigation measures. This is particularly relevant as climate change is exacerbating the frequency and intensity of droughts.

The occurrence of wildfires is generally caused by elevated temperatures that consistently reduce vegetation moisture. Therefore, the indices adopted for predicting wildfire occurrence shall be improved. The estimation of LST will aid in monitoring the relationship between temperature and wildfire incidents in Perlis, and the utilisation of vegetation indices can help in monitoring the vegetation condition in forested and agricultural regions during the dry season. Thus, this study tries to fill the gap by developing a multispectral indices framework for the predictive modelling of wildfire hazard zones through the investigation of the relationship between NDVI, NDWI, NDMI, NDDI, and NBR, with LST. This study presents a more comprehensive insight into wildfire hazard assessment compared to other studies conducted in Malaysia.

1.3 Study Area

The study covers the geographical area of Perlis, the smallest state located in the northernmost part of Malaysia. The study area includes the three political boundaries of Perlis that comprise all 22 mukims. Even though Perlis is relatively small, it has a variety of forest habitats, such as limestone hill forests, dipterocarp forests, and seasonal deciduous forests, especially within the Perlis State Park and nearby forest reserves. These habitats are susceptible to seasonal droughts, rendering them prone to ignition during the arid season. Moreover, the state experiences a tropical monsoon climate, typically from February to April, which increases susceptibility to wildfires due to prolonged low precipitation and elevated temperatures, with a historical maximum of 40°C observed during this period. Perlis is ideally suited for studies on wildfire

detection due to its manageable scale, which facilitates comprehensive monitoring and data collection. Figure 1.2 demonstrates the study area of this research work.

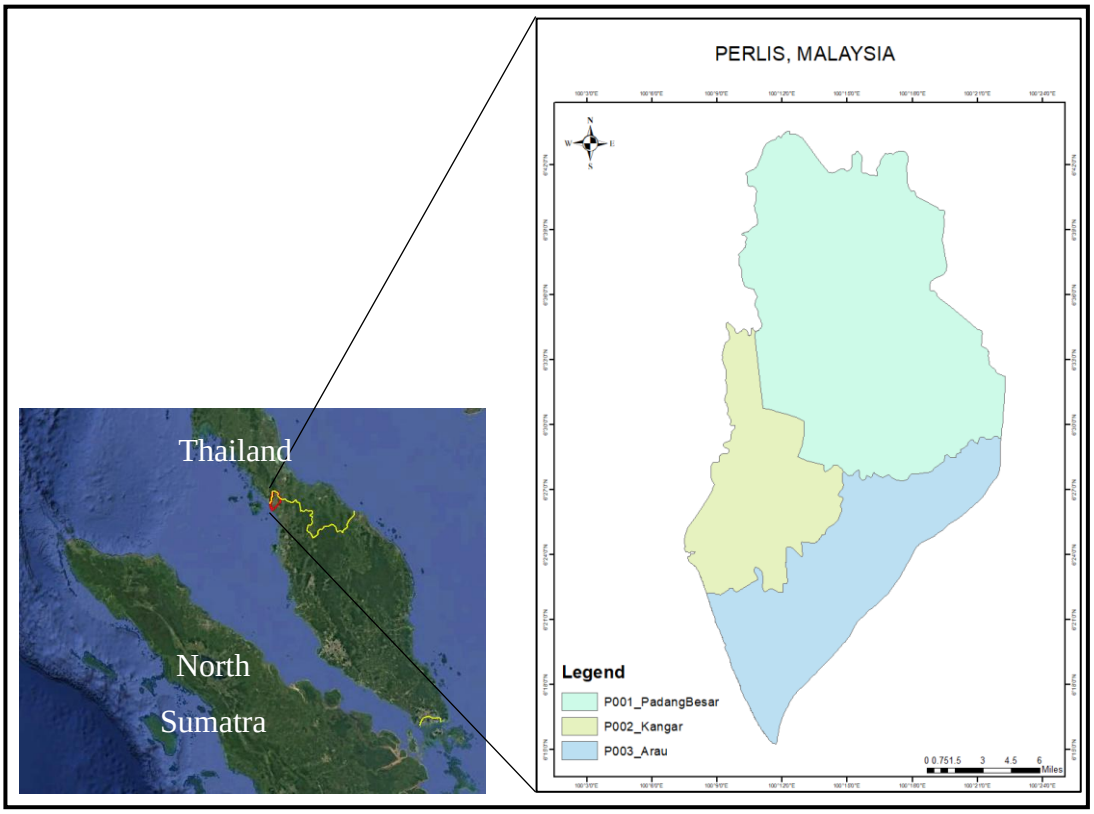

Figure 1.2 Study Area Of This Research Work

1.4 Aim

The study aims to develop a multispectral indices framework for the predictive modelling of the wildfire hazard zone in Perlis. Specifically, this study seeks to analyse the spatiotemporal pattern of LST and fire occurrences, particularly during the hot and dry season, which usually transpires in March. By evaluating the relationship of LST with other spectral indices, this study aims to enhance the understanding of various spectral indices as a predictive indicator of wildfire occurrence.

1.5 Research Question

i) What is the trend of LST and wildfire occurrence between the years 2014 and the year 2024?

ii) How significant are the LST, NDVI, NDMI, NBR, NDWI, and NDDI in influencing wildfire occurrence in 2024?

iii) Where is the most potential wildfire hazard zone within the state of Perlis?

1.6 Research Objective

i) To examine the changing trend of LST and wildfire occurrence from the year 2014 to the year 2024.
ii) To determine the correlation between LST and multispectral indices in relation to wildfire occurrences.
iii) To develop a model of wildfire hazard zone within the state of Perlis using the integration of multispectral indices and the Ordinary Least Squares (OLS) method.

1.7 Significance of Work

This study presents an estimation of the wildfire hazardous areas within the state of Perlis based on geospatial analysis using LST, NDVI, NDWI, NDMI, NDDI, and NBR. The main focus is to enhance the accuracy of fire predictions by utilising LST data, which includes vegetation stress, moisture availability, and surface heating. Spectral indices are crucial factors to consider while evaluating the possibility of wildfire incidence within a particular area. Hence, this study has the potential to enhance academic understanding of the risk factors of wildfires and geospatial estimation analysis in assessing the possibility of wildfire occurrence. Besides, this study pertains to the occurrences that transpired in the state of Hawaii. The wildfires that happened in Lahaina, Hawaii, were caused by uncontrolled fires in brush lands that eventually spread to nearby housing due to prolonged drought and strong winds during Hurricane Dora (Roy et al., 2024).

The state of Perlis is recognized as one of the regions in Malaysia that experiences high temperatures up to 40°c (Suhaimi, 2024) and is mostly made up of an expansive forest and agricultural region. Figure 1.2 demonstrates that the heat status of Perlis has ascended to stage 2 during the dry season in March 2024, compared to other states. Therefore, the assessment of wildfire risk is necessary to identify regions indicating the potential for wildfire incidents in Perlis, and the containment of wildfires holds significant importance in mitigating the extent of fire-related destruction. In line with Sustainable Development Goal (SDG) 13, which is to take immediate action to combat climate change and its effects, this study holds significant value for the authorities involved.

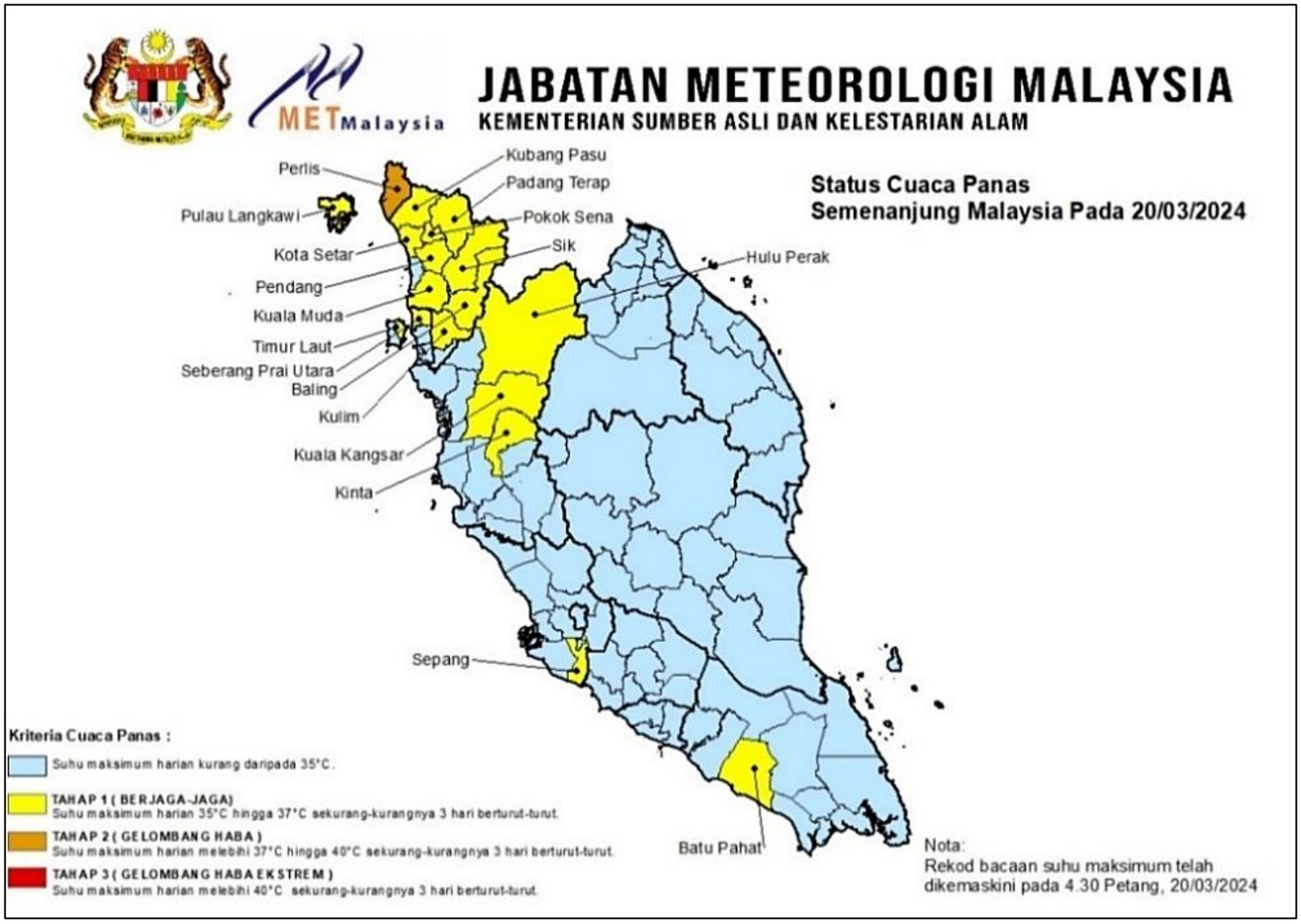

Plate 1.1 The Heat Status Of Perlis (Metmalaysia Website Retrieved On 20th March 2024)

Furthermore, this study presents a cost-effective and scalable method for monitoring wildfires. Ground-based fire detection systems may encounter limitations regarding their visibility range and response time. Conversely, satellite-derived indices provide high-resolution, near-real-time information over extensive, inaccessible regions. Consequently, they are highly advantageous in areas with limited terrestrial infrastructure. This study assists in decision-making for the assessments on the environmental policy by providing relevant data about high-risk regions and the temporal dynamics of fire propagation. These findings can aid in formulating tactics for fire suppression, coordinating controlled burns, and determining land management practices. It aids experts in understanding the interplay between climate and fire, particularly in the context of rising global temperatures.

Apart from that, studies on wildfire detection and hazard zone mapping applying GIS methods have broad potential for national policy, the economy, and society. From a societal standpoint, early identification and accurate mapping of wildfires improve community safety, therefore facilitating quick evacuations and lowering the death toll as well as property loss. Wildfires can seriously affect infrastructure, agricultural fields, and important timber supplies, therefore causing direct financial losses and long-term disturbance of livelihoods. By directing resource allocation for both post-fire rehabilitation and firefighting operations, an accurate fire estimate helps reduce any significant losses. Nationally, environmental preservation and climate policy depend much on the estimate of wildfires. This study affects legal frameworks meant to lower fire risks and safeguard environmental assets, land-use planning, and strategies of forest management.

1.8 Scope and Limitation

This study focuses on spectral indices data obtained from Landsat 8 OLI/TIRS to ascertain the frequency and locations of wildfires in Perlis. The objective of this study is to determine whether there is a correlation between elevated LST patterns and regions with a high incidence of wildfires and to ascertain the relationship of various spectral indices with LST. The goal is to identify the most hazardous areas for wildfire incidents in Perlis, which are renowned for their high temperature readings.

The scope of this study is the analysis of satellite-based LST data over ten years to identify patterns that may indicate wildfire occurrence. This study will particularly

estimate the incidence of wildfires in Perlis during the hot and dry season; hence, the Landsat data and statistics utilised are derived in March and do not reflect the entire month within that period. The study analyses the spatial variations of wildfire distributions utilising GIS and remote sensing technologies. Secondary data have been used to determine the relationship between spectral indices and wildfire occurrence within Perlis state; therefore, deficiencies in in situ data may influence the results of this study. Hence, the risk factors selected to estimate the occurrence of wildfires are fire-related indices, including LST, NDVI, NDWI, NDMI, NDDI, and NBR.

Despite the fact that the selected methodology has some advantages, the investigation exhibits several limitations. The cloud cover, haze, and other atmospheric disturbances can diminish the accuracy and continuity of spectral indices data, particularly during the monsoon season, complicating the determination of each index. There is also a limitation on the temporal resolution of the satellite images before and after a fire outbreak, which prevents the NBR from being adequately analyzed and can only reflect the simulation after a fire outbreak. The study also ignores social, economic, and human-made factors known to trigger wildfires in Perlis, such as illegal agricultural burning or negligent use of fire.

Limited availability of satellite images and ground-based data provided by the Fire and Rescue Department may influence the results of this study. The Landsat imagery has low temporal resolution, which inhibits the monitoring of wildfire extent and severity through NBR analysis. Not only that, cloud and haze interference can make it difficult to accurately map burned areas. Lack of information regarding the fire perimeter in the historical data can reduce model performance and make it harder to simulate how fires spread across landscapes. The consequences of these limitations can be reduced using geospatial methods, ensuring the reliability of the results presented in this study.

Geospatial analysis is an excellent method for assessing the likelihood and magnitude of wildfire occurrences, yet it possesses several limitations that diminish its efficacy and accuracy. A significant worry is that clouds and smoke can obstruct satellite visibility, complicating the identification and analysis of fires. This is particularly perilous when flames are present, and the timely collection of information is essential. Even though utilising LST data is an effective method for assessing wildfire risk, the study's findings must be interpreted considering the constraints of geographic resolution, data quality, and contextual significance. Future researchers may enhance

fire risk models for Malaysia by integrating high-resolution data, real-time fire detection technologies, and socio-environmental variables.

1.9 Conclusion

This chapter discusses the significance of forecasting wildfires and the increasing relevance of remote sensing in understanding and managing fire-related hazards. The primary objective was to identify and quantify the threat of wildfires by concentrating on the integration of various spectral indices. Wildfires are increasingly prevalent and hazardous globally, necessitating the development of methods for rapid and precise detection of thermal anomalies and forecasting potential ignition locations. The background of wildfire incidents, the challenges associated with conventional ground-based monitoring techniques, and the advantages of utilising satellite-derived indices to rapidly acquire information across a wide area were discussed. Though few studies have been conducted on estimating wildfire occurrence globally, there is a limited study that emphasizes predicting wildfire in Malaysia, especially Perlis. The chapter addressed the rationale for concentrating on spectral indices, as well as the scope and limitations of the study. This chapter establishes the fundamental literature review that will be covered in subsequent chapters by demonstrating the potential utility of spectral indices in wildfire monitoring. The next chapter will discuss the previous studies conducted related to wildfire prediction based on remote sensing indices.

CHAPTER 2
LITERATURE REVIEW

2.1 Introduction

Fire is one of the most destructive and significant phenomena in nature. The combination of heat, fuel, and oxygen initiates a chemical reaction known as combustion. Initially, it was used to maintain warmth, safety, and comfort, as well as to cook and eventually to construct factories, cultivate, and work with metal. Fire has historically represented life, energy, and transformation, but it may also pose significant hazards, resulting in extensive wildfires, property destruction, and fatalities.

2.2 Types of Fire

Bushfires, open burning, and wildfires are the types of fire incidents that are frequently reported involving forests and agricultural areas. Forests are intricate and natural ecosystems consisting of a diverse array of trees that sustain a vast array of living organisms, are the primary sources of carbon on our planet, and have a significant impact on the global carbon cycle (Asha'ari & Badrunsham, 2014).

2.2.1 Open Burning

Open burning refers to the act of burning undesired substances in the open air, resulting in the direct emission of smoke and harmful pollutants into the atmosphere. The open burning of plant debris in extensive peat regions, shifting agricultural practices, the harvesting of non-timber forest resources, and the absence of a cohesive water management strategy (Razali & Nuruddin, 2012). Open burning of residue from agriculture removes waste products, controls weeds, and releases nutrients for the next crop (Pasukphun, 2018). Though open burning may offer benefits to some people, it also poses a serious risk to the environment and the health sector. The open burning of mixed wastes is a notable contributor to air pollution, resulting in many detrimental impacts on the environment (Pathak et al., 2023), such as haze.

In SEA, open burning has been partially associated with the resurgence of haze, in addition to its detrimental health effects (Ariffin & Wan Yaacob, 2017). Air pollution resulting from open burning constitutes a significant issue in Thailand, threatening public health, damaging the ecosystem, and affecting the tourism sector (Pasukphun, 2018). The practice of open burning emits toxic compounds and greenhouse gases that are able to deteriorate air quality. The open incineration of municipal waste is a significant contributor to the substantial release of aerosols into the environment (Kumar, Ojha, & Singh, 2021). Particulate matter (PM), a hazardous substance resulting from open-air burning, is responsible for approximately 4.2 million premature deaths, accounting for 6.7% of all fatalities in 2016 (Nugraha, Mozasurya, Hidayat, & Saptoadi, 2023).

In Malaysia, from 2010 to 2012, open burning occurred mostly in woods, shrubs, farms, and plantations; however, since 2013, most open burning in the country has been garbage burning in residential areas and roadsides (Ariffin & Wan Yaacob, 2017). The government has enacted regulations that reduce the chances of open burning or render it illegal. The Environmental Quality Act 1974 is widely regarded as the most detailed legislation to address pollution control and environmental protection (Khairil, Jeganathan, Razman, Syed Zakaria, & Arifin, 2018). However, enforcement is frequently insufficient, particularly in low-income or rural regions lacking proper waste management facilities. Utilizing safer, more environmentally sustainable methods for waste management is crucial for the protection of both humanity and the world.

2.2.2 Wildfire

Wildfires are unplanned fires that occur in forests, grasslands, or other wildlands. For a wildfire to occur, three essential criteria must be met: the presence of fuel, oxygen, and a source of heat. A combination of dry weather, drought, and strong winds can create ideal conditions for a catastrophic event. Wildfires have garnered significant attention in recent years because of their overwhelming effects on ecological, economic, and diplomatic levels (Babu & Roy, 2019; Ya'acob et al., 2022). These incidents are generally seen as a threat because of the potential health risks created, the amount of carbon dioxide released into the atmosphere when vegetation is burned, and the potential for economic damage (Chowdhury & Hassan, 2015).

Wildfires can be profoundly detrimental to the environment, public health, the economy, and communities. Although certain fires serve a critical ecological function, they frequently lead to substantial losses in human life, infrastructure, and forest resources, particularly in regions where the risk of fire is on the rise as a result of human activity (Tran et al., 2024). This incident also contributes to the deterioration of forest ecosystems and their biological resources, as well as the loss of human lives and property (Talukdar et al., 2024). Wildfires also destroy rangeland species and forest trees, wildlife habitats, soil, degrade natural landscapes, reduce soil acidity, reduce nitrogen reserves, and spread inferior plant species (Velayati, Boloorani, Kiavarz, Samani, & Alavipanah, 2024).

Uncontrollable and calamitous wildfires have become an annual occurrence on a global scale in recent decades. The General Directorate of Forestry in Turkey recorded 63,724 wildfires over the past two decades (Çolak & Sunar, 2020). From 1992 to 2018, China saw an annual average of 6,323 wildfires that ravaged approximately 72,910 hectares of forest (Wu, 2021). In Canada, the heightened frequency and severity of wildfires account for around 25% of the global peatland area (Pelletier et al., 2023). Indonesia also encounters the same issue during the El Niño and the dry season. In 2019, the total area incinerated in South Sumatra was 52,716 hectares (Rendana et al., 2023). Between 2018 and 2022, Indonesia experienced 2,341 wildfires, leading to the displacement of 156 individuals, the loss of 38 residences, and 3 educational institutions (Aldiansyah & Madani, 2024).

Malaysia has encountered multiple catastrophic wildfires as a result of El Niño and the dry season, which had a significant influence on biogeochemical cycles and the vitality of the ecosystem. The escalating need for land, propelled by population expansion, urbanization, development, and economic prosperity, is resulting in a surge in wildfire occurrences (Asha'ari & Badrunsham, 2014). In a news article released by Idris (2020) through Utusan Malaysia, Selangor experienced a surge of over 11 percent in wildfires, with 247 incidents reported in the initial half of 2020, in contrast to 222 incidents during the corresponding period in the previous year. In the future, wildfires are anticipated to cause more substantial devastation globally as a result of climate change and further human development.

A bushfire is a type of wildfire that swiftly spreads and occurs in scrubland or grassland. The construction of residential or commercial buildings on rural-urban interfaces is experiencing significant growth due to heightened human activity in these

areas. Compared to structures erected in metropolitan areas, these buildings created in rural-urban interfaces are located closer to natural vegetation, thus facing an increased danger of bushfires. Bushfires are influenced by several biophysical and climatic variables of the Earth. One of the most significant factors that influences the size, intensity, speed, and predictability of bushfires is the weather (Sharma, Aryal, & Rajabifard, 2022).

During the past few decades, bushfires have caused substantial property losses and human casualties globally, especially in Australia. In 2012, a study estimated an annual average of 13 fatalities due to bushfires (Partheepan, Sanati, & Hassan, 2023). Between September 2019 and March 2020, 34 individuals perished, and 3,000 residences were destroyed due to bushfires in New South Wales (Bandara, Navaratnam, & Rajeev, 2023). During the 2020 Australian bushfire season, more than 17 million hectares of land were burned, resulting in the devastation of 3094 residential properties (Shi, Feng, Stewart, & Gao, 2024).

Apart from fatalities and economic loss, bushfires also have a significant impact on human health. The spread of bushfire smoke increases the likelihood of hospitalisation and emergency department visits for respiratory illnesses such as asthma, Chronic Obstructive Pulmonary Disease (COPD), and respiratory infections (Yu, Xu, Abramson, & Guo, 2020). More than 95% of Australian bushfire victims were reported to have experienced at least one physical health symptom, including eye discomfort, dry throat, or cough (Rodney et al., 2021). To sum up, bushfires have both short-term and long-term economic and health impacts, which mandate the implementation of an appropriate strategy to combat these incidents.

2.3 Factors Contributing to Fire Occurrence

Wildfires might occur due to several factors, including human-related factors and natural factors. In terms of natural causes, weather is the main element influencing the susceptibility of wildfire ignition. Alterations in land use, agricultural practices, negligence, and intentional arson are examples of human activities that significantly elevate the risk of fires. It is important to consider the causes of wildfires to evaluate wildfire occurrence across various landscapes and enable local authorities to identify the patterns of incidents.

2.3.1 Human Factors

Fire outbreaks in forested areas are generally triggered by human activities. Human factors are important in fire risk assessment, especially in Mediterranean nations where the ignition may be initiated by accident or arson (Vasilakos et al., 2009). A study by Lovreglio et al. (2010) demonstrates that a major contributor to negligence is the utilization of fire in agricultural practices, specifically the burning of stubble. According to Lourenco et al. (2013), approximately 40% of fire ignitions in Portugal were caused by arson and negligence. Similarly, Mundo, Wiegand, Kanagaraj, & Kitzberger (2013) also found that 65% of 855 fire cases in Naquen Province, Chile, were caused by human negligence and accidents. The socio-economic factors, such as poverty rates, level of education, and resource accessibility, substantially affect human negligence in the occurrence of wildfires (Daraz, Bojnec, & Khan, 2024). The careless use of fire, including unattended campfires, garbage burning, and slash-and-burn activities, is linked to a lack of awareness due to low educational levels. These actions are also supported by the availability of infrastructure in forested areas.

Not only that, the density of roads and availability of access to the forest, such as hiking trails, railroads, and forest roads, have increased the risk of fire occurrence. A study by Vasilakos et al. (2009) mentioned that the likelihood of fire ignition reduces as the distance from primary and minor roadways increases. The density of local roads was identified as a significant factor in the Linear Regression model, as these roads provide access to rural lands and forested areas (Oliveira et al., 2012). As noted by Narayanaraj & Wimberly (2012), the occurrences of ignitions due to human activities, such as fishing, hunting, and camping, were predominantly in areas with a high concentration of roads, as these activities may involve the use of fire in forested areas. A sensitivity analysis has been conducted to ascertain the impact of the key factors in fire ignition, and it revealed that the density of touristic infrastructures was identified as the most significant contributor (Arndt, Vacik, Koch, Arpaci, & Gossow, 2013). Guo et al. (2014) make a similar point that the occurrence of fire is relatively high in areas near railways. The availability of infrastructure in forests has eventually increased outdoor recreational activities like camping and picnicking, which will increase the probability of ignition.

Another human factor that triggers fire occurrence is population density. The population interaction map by Sadasivuni et al. (2013) illustrates that the density of populations heightens the distribution of wildfire ignition possibilities in Southern Mississippi. According to Guo et al. (2016), there is a lower probability of fire occurrence in low-populated areas compared to densely populated areas. In general, excessive population densities are associated with an increased frequency of wildfires (Costafreda-Aumedes et al., 2017). This is consistent with the data obtained by Adamek, Jankovska, Hadincova, Kula, & Wild (2018), where population density is a crucial factor that influences fire ignition. The Wuyi and Xuefeng mountains in China have a reduced fire risk due to their sparsely distributed population, despite the presence of highly populated forests, resulting in a comparatively low probability of human-induced wildfires (Yang, Jin, & Zhou, 2021). It is also reported that 11% of towns within the Atlantic region with high population density are subjected to a significant risk of wildfires (Chas-Amil et al., 2022). The incidence of arson, discarded cigarettes, and open burning is concentrated in regions with elevated population density.

Furthermore, agricultural practices and deforestation have also been contributing to the ignition of wildfires. According to Morton et al. (2008), 84% of high-frequency fires during the studied period resulted from active deforestation areas in Bolivia and the Brazilian states of Mato Grosso, Pará, and Rondônia. Elevated fire risk is also found in areas designated for agro-silvopastoral activities, intensive livestock farms, and agricultural fields (Devisscher et al., 2016). Likewise, a study by Adrianto et al. (2020) revealed that fires caused by plantations and agricultural practices occurred at a rate 17 times greater compared to main forests and more than twice the rate of secondary forests, primarily to eliminate vegetation in preparation for the next cultivation season. The study on deforestation and wildfire occurrence highlighted that countries exhibiting the highest deforestation rates had a greater frequency of wildfires compared to those with lower deforestation levels (Cardil et al., 2020). Deforestation was also predominantly observed in regions with elevated fire activity, demonstrating its significant impact on fire occurrence (Sim et al., 2023). This is because deforestation produces dry fuel, such as logging debris, dried leaves, and branches, making it more readily flammable.

Besides, another ignition source linked to extensive areas burned was fires caused by machinery, primarily situated near residential zones (Syphard & Keeley, 2015). It is reported that 14 incidents of wildfire arising in Australia were attributed to

the negligent usage of equipment or machinery in forested areas (Collins, Penman, & Price, 2016). Sparks generated during welding operations or melted solder drippings from pipe soldering have been identified as causes initiating fires within wooden structures in construction settings (Fernandez-Pello, 2017). Ignitions categorized as equipment-related sometimes originated from exhaust or sparks generated by power saws or other devices powered by gas or electric motors. The combined effects of severe drought, strong winds, and large fuel accumulation have generated an environment where a single spark can result in catastrophic effects for human lives, property, energy security, and ecosystems (Eagleston, Bester, Yusuf, Damodaran, & Reno, 2025).

2.3.2 Natural Factor

Since late 2019, climatic factors have been a dominant factor in the emergence of high-intensity wildfire behaviour (Sze, Jefferson, & Lee, 2019). The escalating frequency and extent of wildfires serve as a critical indicator of the rising threats associated with global warming (Diffenbaugh, Konings, & Field, 2021). Climate change elevates the duration of droughts, amplifies the occurrence of arid seasons, and hence prolongs the fire period (Pausas & Keeley, 2021). The consequences of global climate change have resulted in increased temperatures, creating an extended dry and warm phase that promotes the ignition and proliferation of wildfires (Chew et al., 2022a; Cimdins et al., 2022). Hot and arid conditions make the vegetation and soil lose moisture faster and increase the energy required for wildfire ignition. Significant strain from human activities on the Earth has resulted in global warming and climate change, causing substantial disturbances in forests worldwide due to increased incidences of fires (Mansoor et al., 2022). According to Trang et al. (2022), the majority of wildfires in northern Vietnam transpired during the dry season, which is between February and March, exhibiting a positive correlation with temperature. Heightened temperature expedites the evaporation rates of vegetation, hence making it more vulnerable to wildfire occurrence.

Other than that, precipitation is also a contributing factor to the occurrence of wildfires. The occurrence of wildfire appeared to be less significant in regions with high annual precipitation compared to those with lower precipitation levels (Collins, Bradstock, & Penman, 2014). Decreasing trends in summer precipitation significantly contribute to the observed increases in the area burned by wildfires in the western

United States during the past thirty years (Holden et al., 2018). Alterations in rainfall patterns are recognized as a potentially significant element influencing wildfires (Fasullo, Otto-Bliesner, & Stevenson, 2018). Fires are more likely to occur at a higher rate when the mean monthly rainfall in the preceding two months is reduced (Sze et al., 2019). Wildfires in Brunei are observed to escalate during periods of drought. Northern Brunei received the lowest annual rainfall; it is therefore the driest and most vulnerable area to fire ignition, in line with the wildfire hotspot zones (Shahriar et al., 2019; Zahran et al., 2020). The prevalence of fires in Northern Vietnam was associated with fuel moisture and precipitation, as low rainfall worsens the fuel dehydration conditions (Trang et al., 2022). The rate of fire ignition escalates rapidly with the combination of warm temperatures and low precipitation, especially during El Niño.

Another climatic factor that should be taken into consideration is wind speed. Wind speed can influence the rate and propagation of fire spread. A study by Nelson (2002) revealed that wind speed is shown to correspond with the spread rate data, indicating that wind influences the rate of fire spread within a region. Substantially elevated wind speeds were observed in regions with major fire incidents, and increased wind speeds also resulted in extended fire durations (Abatzoglou, Blach, Bradley, & Kolden, 2018). Although the correlation coefficients between wildfire ignition and maximal wind speed were significantly lower, this factor was observed to contribute to the wildfire's spread rate (Lu, Zhou, Li, & Wu, 2018). Wind amplifies evaporation potential, and with rising wind speed, the moisture content of forest fuels decreases; hence, there exists a positive correlation between wind speed and the probability of wildfires (Ma, Feng, Cheng, Chen, & Wang, 2020). The rapid spread of wildfires is further accelerated by elevated wind speeds. According to Lan et al. (2021), wind speed strongly impacts the frequency of fires in the northwest, southeast, and southwest regions in China. The intensity and risk of wildfires are exacerbated by the convergence of high temperatures, parched vegetation, and increased wind speed (Parvar et al., 2024). Intense winds can also desiccate vegetation, making it drier and more susceptible to ignition.

Apart from elevated temperatures and drought conditions, frequent lightning strikes also contribute to occasional episodes of heightened fire risk and wildfire occurrences (Mitchener & Parker, 2005). Wildfires ignited by lightning constituted 92% of the total acres destroyed in the mountain ranges of Central Washington (Narayanaraj & Wimberly, 2012). Lightning accounted for 57% of fire meteorological factors and

consistently elevated the probability of wildfire occurrence compared to other variables (Clarke et al., 2019). A possible reduction in the risk of lightning-induced wildfires was due to the reduced frequency of prolonged lightning activity, along with increased rainfall and humidity levels, as well as a decline in vapour pressure deficit (Pérez-Invernón et al., 2023). Wildfires are typically caused by cloud-to-ground lightning, which is mainly dry and has most of its moisture evaporated before it reaches the ground (Song, Xu, Li, & Oppong, 2024). Dry thunderstorms, characterized by lightning with minimal precipitation and a lack of the moisture necessary for precipitation, pose significant hazards as they can initiate wildfires (Rajendran & Vani, 2024). The spontaneous ignition of wildfires was triggered by an amount of heat that is higher than the minimum energy required for ignition induced by lightning when it struck dry vegetation or trees.

2.4 Methods to Detect Wildfires

Direct methods and indirect methods are the techniques employed to detect and control wildfire incidents. The direct method usually involves a straightforward monitoring and detection routine in forested areas. The indirect method typically involves remote sensing techniques and geospatial analysis in detecting wildfire events.

2.4.1 Direct Methods

Conventionally, the technique used to detect wildfires in the early years was by direct methods such as watchtowers, Unmanned Aerial Vehicle (UAV) surveillance, and optical cameras. Monitoring towers and forest patrols are included as one of the most frequently used methods by the authorities to detect wildfires (Alkhatib, 2014). Watchtowers must be strategically positioned to fulfill wildfire monitoring criteria, including extensive coverage, minimal expenditure, and reduced overlap (Bao, Xiao, Lai, Zhang, & Kim, 2015). As noted by Allison et al. (2016), watchtowers are fixed and need strategic placement to ensure visibility; hence, they are often employed to oversee high-risk situations. However, this method is less efficient as the coverage is not extensive in sparsely inhabited wilderness areas. Watchtowers only serve to monitor high-risk situations and are utilized for both detection and the verification and

localization of reported fires (Barmpoutis, Papaioannou, Dimitropoulus, & Grammalidis, 2020). Nevertheless, modern watchtowers are outfitted with high-definition digital video recorders, wireless connections, and solar power systems that minimize the operator's duties while simultaneously improving the accuracy and reliability of fire alarm issuance (Zhang et al., 2020). The conventional watchtowers used in the early years can be improved by installing a specialised camera that can maximise the functionality of the detection system.

Aerial surveillance using UAVs has also been employed as one of the techniques to detect wildfires. In Germany, the monitoring involves the use of a radiometer, gas and smoke detectors, and a thermal camera mounted on a blimp, then the acquired data are integrated with the blimp's Global Positioning System (GPS) data and a timestamp for viewing, thereafter input into detection algorithms to ascertain the necessity of executing an alarm (Krüll, Tobera, Willms, Essen, & Wahl, 2012). Compared to watchtowers, aircraft are capable of being manipulated, deployed, and are flexible, which enables them to be directed toward high-risk areas and repositioned as risky areas change (Allison et al., 2016). Due to their capacity to revisit frequently and the potential to detect accurate fire locations, they are well-suited for detection. UAVs integrated with GPS and ultra-high-resolution digital cameras are able to deliver high-definition aerial imagery with accurate locational data that is very helpful in early fire detection (Zhao, Ma, Li, & Zhang, 2018). Current drones are outfitted with high-resolution cameras that can capture better photographs, and the collected data can subsequently be used for diverse analyses and forecasts (Treneska & Stojkoska, 2021). UAVs are also distinguished by their adaptable flight trajectories, which enable them to respond to evolving fire patterns and survey various regions as necessary (Mohapatra & Trinh, 2022). A disadvantage of UAVs is that a single UAV is unable to provide sufficient coverage within an appropriate time frame if extensive regions require monitoring (Tzoumas et al., 2023).

Apart from that, infrared (IR) cameras, which often include heat and smoke sensors, have been adopted as a monitoring method in terrestrial systems. By drawing on the concept of an IR camera, Alkhatib (2014) explains that the processing unit monitors motion in images and assesses the number of pixels that exhibit smoke or fire illumination, thereafter transmitting the data to another algorithm to determine whether to alert the operator. At night, Short Wave IR (SWIR) cameras are capable of delivering improved footage that closely resembles daylight images captured by the same device

(Allison et al., 2016). To ensure the efficiency of IR cameras, the sensors should be able to detect even minimal smoke concentrations. These cameras should be able to readily detect smoke within the initial minutes of a fire from distances over 50 km, and when paired with optical zoom, they can observe much greater distances (Govil, Welch, Ball, & Pennypacker, 2020). Though the integration of smoke and flame detection from IR cameras has resulted in enhanced early fire detection technologies (Barmpoutis et al., 2020), the execution is still impractical as the initial expenditure of resources and labour to place the cameras may not be economically feasible in many extremely remote areas (Mohapatra & Trinh, 2022).

The automated lightning detection network has also been developed by numerous countries to identify lightning strikes in real time, and hence helps in locating the possible site of fire ignition. For instance, the Operational Lightning System (OLS) can only detect lightning when it occurs in the sensor's field of view (Bankert, Solbrig, Lee, & Miller, 2011). The lightning strike's orientation is crucial in determining the possibility of strikes and can be determined from the electric field sensed by the lightning detection network (Strelec et al., 2022). Records of lightning activity from the Worldwide Lightning Location Network (WLLN) can assist in identifying areas susceptible to lightning and forecasting the intensity of wildfires triggered by lightning occurrences (Rajendran & Vani, 2024). The National Lightning Detection Network (NLDN) and the Earth Networks Total Lightning Network (ENTLN) are effectively jointly detecting lightning at the scale of wildfire origins (Hatchett, Nauslar, & Brown, 2024).

2.4.2 Indirect Methods

Modern-day monitoring techniques mainly utilize satellite surveillance. Multiple algorithms have been created by analyzing data from Earth observation satellites in the last twenty years to find places that have been affected by fires (Rashkovetsky, Mauracher, Langer, & Schmitt, 2021). NASA and NOAA meteorological satellites are able to observe ocean currents, climatic variations, drought risks, and weather trends that offer a broader context of the biosphere and environmental processes (Mohapatra & Trinh, 2022). Satellite images are transmitted to the ground immediately upon the establishment of communication with the ground station network, and the images may be used to extract diverse types of actionable knowledge, including

wildfire (Thangavel et al., 2023). Compared to direct approaches, satellite surveillance is able to cover larger monitoring areas and extremely remote areas.

Ground sensors are useful in the early detection and prediction of wildfires as they are able to detect any environmental abnormalities. Employing ground-based sensor technology for environmental monitoring enables visibility through smoke and facilitates the identification of fire hotspots (Kadir, Irie, Rosa, & Othman, 2019). Any abnormalities sensed by the ground sensor network will trigger the fire monitoring system, and a UAV's mission will commence to the desired area (Afghah, Razi, Chakareski, & Ashdown, 2019). Sensors are strategically positioned around the area to monitor temperature, humidity level, solar radiation, and carbon monoxide (CO) levels (Dampage, Bandarayanake, Wanasinghe, Kottahachchi, & Jayasanka, 2022). The incorporation of such indices into prevalent fire hazard rating systems indicates the significance of environmental parameters in assessing wildfire risk (Krueger et al., 2022). A study revealed that the sensor exhibits a sufficiently quick response in detecting smoke emissions such as particulate matter (PM), Nitrous Oxide (N_2O), and CO (Findlay, Peaslee, Statter, Waller, & Smallridge, 2022). Ground sensors can also be utilized for environmental monitoring, including fuel moisture assessment, temperature, and air pressure detection, which aids in wildfire identification and control (Chan et al., 2024).

Fusion of remotely sensed indices has also been widely applied to indirectly detect and predict wildfire ignition. A study demonstrated the practicability of distinguishing between burned and unburned areas utilizing fire-related spectral indices (Amos, Petropoulos, & Felentinos, 2019). The accessibility of open-source imagery has facilitated accurate and efficient wildfire mapping through the application of spectral indices (Mpakairi, Ndaimani, & Kavhu, 2020). Vegetation predictors serve as an effective variable for fire occurrence in the affected area, considering the relationship between forest susceptibility, shown by NDVI values, and the likelihood of wildfire occurrence (Charizanos & Demirhan, 2023). The combination of fire-related indicators can yield valuable insights into fire susceptibility based on meteorological conditions and fuel characteristics, facilitating precise fire danger classification. Guiop-Servan et al. (2025) reviewed 192 papers and found that 42.19% utilized the NBR for fire prediction and mapping, while NDVI ranked second with 39.06%, and the composite burns index (CBI) ranked third with 18.23%.

2.5 Previous Studies on Wildfire Estimation Using Geospatial Techniques

The advancement in geospatial technology has made the studies on wildfire estimation more accurate and reliable. The available tools enable users to conduct various analyses, including spectral and non-spectral analyses. Spectral indices combined with meteorological variables help map the wildfire density and identify fire-prone areas.

2.5.1 Spectral Analysis

Publications that concentrate on wildfire estimation and mapping frequently adopt geospatial analysis that combines several spectral indices. In a study conducted by Çolak & Sunar (2020), the fire risk zones for the Menderes region, Turkey, were generated based on combined indices, including LST, NDWI, LULC, air temperature, and relative humidity. The LST, NDWI, and LULC were extracted from Landsat 8 satellite images, while air temperature and relative humidity were acquired from local meteorological data. The analysis showed that LST began rising a month before the fire, and most of the danger zones are above 25–30°C with relative humidity levels below 40% (Çolak & Sunar, 2020).

A study by Quan et al. (2021) assessed the wildfire danger for China using Fuel Moisture Content (FMC), FFL, and NDVI. The remotely sensed variables were extracted utilising MODIS data. The study expresses that there is a strong relationship between NDVI and FMC with wildfire danger assessment, where the wildfire is likely to occur in regions having low NDVI and FMC values (Quan et al., 2021). Low NDVI values may indicate unhealthy vegetation, and low FMC values may indicate dehydrated vegetation, which intensifies the risk for wildfire to occur.

By drawing on the concept of predicting wildfire occurrences in Russia, Gizatullin & Alekseenko (2022) applied raster algebra to determine vegetation indices and surface temperature. NDVI, Soil Adjusted Vegetation Index (SAVI), NDWI, and LST were extracted from MODIS data using QGIS software. The results demonstrate that a fire point may be identified at a particular location if the value of the indices is higher than its threshold value (Gizatullin & Alekseenko, 2022). A lower vegetation index value often indicates poorer living green vegetation, and higher surface

temperature may reduce vegetation moisture, which increases the likelihood of fire ignition.

Not only that, a study by Gupta & Shukla (2022) calculates several wildfire-related indices, including NDVI, NDMI, NBR, and LST, to investigate the temporal distribution of wildfires in the Mizoram district, India. The stated indices were calculated using Landsat 8 satellite images. The authors noted that the LST was increasing steadily while NDVI and NDMI values dropped dramatically during the dry season (Gupta & Shukla, 2022). The results imply that the probability of outbreaks during the dry season is higher due to the favourable conditions for a fire to ignite.

Besides, Sinha et al. (2023) have conducted a study analysing the impact of conditioning factors such as land cover types, slope, LST, NDWI, Water Ratio Index (WRI), and Normalised Difference Built-up Index (NDBI) on the incidence and propagation of wildfires in India. From the results and analysis, it can be seen that most of the fires occurred in Alpine scrub forest with LST above 30°C, lower WRI value, lower NDWI value, and lower positive NDBI value (Sinha et al., 2023). It can be concluded that increased LST causes the WRI and NDMI to decline; hence, the probability of fire occurrence is higher in the particular areas.

A study conducted in Golestan National Park, Iran, by Parvar et al. (2024) evaluated mean annual LST, NDVI, and LULC in developing a wildfire risk (FFR) map. The data were acquired from several sources, including the USGS website, Google Earth, Open Street Map (OSM), and the WorldClim website. The results illustrated that most of the fire happens in grasslands and densely forested areas with LST exceeding 25°C (Parvar et al., 2024). Wildfires showed an increasing trend correlated with elevated mean LST and the existence of drying vegetation.

Furthermore, Karurung et al. (2025) determined the factors that have a significant impact on wildfires in Kalimantan, Sumatra, and Papua during both rainy and drier seasons using LULC, NDVI, NDMI, precipitation, and LST. Landsat 8 OLI was utilised to get LULC, NDVI, and NDMI, whereas precipitation and LST were obtained by Google Earth Engine (GEE). The findings revealed that fires are most frequent during periods of low rainfall, lower NDMI values, lower NDVI values, and average LST above 20°C (Karurung et al., 2025). It can be concluded that fire occurrences increased with increasing LST and decreasing rainfall, diminishing soil moisture in the vegetation area.

In Malaysia, though there are limited studies conducted, the issues are still there. A study by Junaidi et al. (2021) on analysing wildfire incidents using NBR, NDVI, and LST was conducted for Kuala Baram, Sarawak. The indices were determined using Landsat 8 OLI images retrieved from the USGS website. The result shows that the LST was negatively correlated with NBR, with lower NBR values having higher LST and vice versa (Junaidi et al., 2021). From the results, it can be concluded that high-severity fires happened in areas with high temperatures and low NDVI values.

Another study by Ya'Acob et al. (2022) determined active fire hotspots using Landsat 8 at Raja Musa Forest Reserve, Selangor. The indices LULC, LST, road distance, and NDVI were weighted using the AHP method to develop a hotspot susceptibility map. The fuel type weighs 60% in affecting the susceptibility of peat swamp wildfire, while LST weightage is 20%, NDVI is 14%, and road distance is 6% through the AHP method (Ya'Acob et al., 2022). Thus, demonstrating that LULC, LST, and NDVI had a significant influence on fire hotspot determination.

To sum up, the LST, NDVI, NDWI, NDMI, and NBR

2.5.2 Spatial and Meteorological Analysis

The majority of the wildfires that occurred in France between the years 2001 and 2016 were due to climate change and human activities. A study was conducted by Barbero et al. (2019) to understand the relationship between wildfire occurrences and climatic factors. The study utilized MODIS data to identify wildfire events and meteorological data, including temperature, humidity, wind, and precipitation, and the relationship was modelled using a Generalized Linear Model (GLM). The findings highlight that climatic variability affects each region differently, where the majority of the wildfires that occur in the western region were influenced by prolonged drought, loss of moisture triggers wildfires in the Mediterranean region, and fuel moisture was the main factor of wildfire occurrence in the Northern region (Barbero et al., 2019). The results proved that weather variability and prolonged drought drive the occurrence of wildfires in a region.

Meanwhile, in Poland, most of the wildfires occurred due to human activities, such as arson, negligent use of fire, and accidentally igniting a fire. Kolanek, Szymanowski, & Raczyk (2021) conducted a study to measure the impact of human activities on wildfire occurrence. The study evaluated human factors related to wildfire

ignition, including distance from industrial or residential areas, distance from roads, population density, economic activities, and housing heating systems. Geographically Weighted Regression (GWR) was used to analyse the correlation, and the results demonstrated a strong relation between anthropogenic factors and wildfire occurrences, with distance to industrial or residential areas and distance to road being the most influential factors (Kolanek et al., 2021). It can be concluded that the proximity between roads, industrial areas, and residential areas to forested regions increases the possibility of wildfire due to human activities.

According to a study by Shi & Touge (2022), climatic phenomena impose a significant influence on major global wildfire incidents between the years 2001 and 2019. The study evaluates the relationship between major wildfire patterns and global climatic phenomena, such as El Niño Southern Oscillation (ENSO), Atlantic Multidecadal Oscillation (AMO), East Pacific/North Pacific Oscillation (EP/NP), and Arctic Oscillation (AO). The results emphasize that the wildfires that occurred in Ukraine and Kazakhstan were strongly influenced by AMO and EP/NP, while in Australia and Brazil, the wildfires were driven by ENSO and AO phenomena (Shi & Touge, 2022). From the findings, it can be deduced that wildfire occurrences were related to global climatic phenomena that happened regionally.

A study by Grillakis et al. (2022) focused on climatic factors, including relative humidity, temperature, precipitation, and wind, that impacted global burned areas. The study utilized MODIS imagery to extract burned area, and the climatic data were acquired from NASA's Global Fire Weather Database. Correlation analysis was conducted using linear regression, and the findings show that the variation in burned areas occurring in forested regions is most strongly associated with relative humidity as the climate variable, while the variation of burned areas occurring in non-forested regions exhibits a strong correlation between temperature and relative humidity (Grillakis et al., 2022). The study highlights the importance of climatic factors in assessing the severity of wildfires.

In China, extreme climate indices serve as a significant contributing factor to the widespread occurrence of wildfires. Xing et al. (2023) evaluated the relationship between annual and monthly extreme temperature and precipitation in China with wildfire occurrences. Wildfire data from 2005 to 2018 and data related to the extreme climate index were acquired and analysed. It was found that wildfires that occurred in China were mainly related to extreme temperature compared to the mean temperature

during the pre-monsoon and post-monsoon season, and in Southeast China, total precipitation helps in reducing wildfire cases compared to extreme precipitation (Xing et al., 2023). This proved that extreme climate, such as heatwaves and drought, amplifies wildfire risks, and the seasonal monsoon cycle has a significant influence on wildfire occurrence.

Chew et al. (2023) have conducted a study on the influences of temperature, precipitation, and wind speed on fire incidents in the districts of Rompin, Pekan, and Kuantan in Pahang, Malaysia. The results reveal that higher temperatures and lower precipitation are associated with increased fire susceptibility, while wind speed does not significantly affect the fire spread (Chew et al., 2023). The conditions were ideal for a fire to ignite as increased temperature and decreased rainfall diminished the soil moisture and dehydrated the vegetation.

Besides, a study by Van & Lee (2025) examines the impact of topographic variables, such as elevation, slope, and aspect, on wildfire propagation and severity over the United States from the years 1994 to 2017. The topographical data were derived from the SRTM Digital Elevation Model (DEM), and an analysis of spatial autocorrelation using Moran's I was performed to measure the wildfire severity for different terrain classes. It was found that topographical factors have a strong influence on wildfire propagation and severity, with the most severe wildfires occurring at low elevation, steep slope, and aspect that receive the most sunlight (Van & Lee, 2025). Though topographical variables do not directly influence wildfire ignition, they significantly influence the rate of fire spread and severity of the event.

2.6 Types of Spectral Indices Used in the Previous Study to Detect Wildfire

Mapping wildfires is essential for their management and disaster prevention, since it allows for the identification, tracking, and analysis of fire incidents. In recent decades, advancements in remote sensing and GIS have facilitated the mapping of wildfires with greater efficiency and speed.

2.6.1 Land Surface Temperature (LST)

Land Surface Temperature (LST) denotes the Earth's surface temperature and is a pivotal element affecting surface energy equilibrium, heat changes, energy transfers,

and regional climates. LST derived from thermal infrared (TIR) is becoming more applicable and preferred than ground station measurements over large-scale areas (NourEldeen et al., 2020). Several methods exist for the computation of LST, such as the Split-Window algorithm (SW), Dual-Angle algorithm (DA), and Single-Channel algorithm (SC) (Junaidi et al., 2021). Recent advances in remote sensing technology have enabled the determination of LST raster maps using a thermal band of satellites (Rendana et al., 2023).

The LST can be evaluated by the utilization of various satellite images. For instance, Landsat 8 imagery has been employed to examine the LST, specifically by utilizing band 10 and 11 images (Mohd Jaafar et al., 2020). The equation for the LST is presented in Equation 2.1, as specified by a widely used formula developed by the United States Geological Survey (USGS).

$$LST = \left[\frac{BT}{BT + (W \times BT/P \times ln\, e}\right] \quad (2.1)$$

Source: (Çolak & Sunar, 2020)

BT represents brightness temperature, e represents emissivity, and P is equal to 1.438×10−2 m K. LST was expected to have a significant correlation with wildfires, considering temperature is a primary factor influencing fuel moisture content, which is associated with fire ignition, propagation, and behaviour.

The fundamental idea enabling LST estimates is that all things with a temperature exceeding absolute zero radiate energy. Emissivity is the paramount parameter for ascertaining LST as it converts brightness temperature into land surface temperature (Çolak & Sunar, 2020). The regions affected by wildfires experience significantly higher temperatures, distinguishing them from the surrounding colder zones. Rising temperatures are often associated with arid conditions, which intensify evaporation and plant transpiration, hence diminishing soil moisture and heightening the vulnerability of vegetation to wildfires (Chew et al., 2023; Karurung et al., 2025). LST rises as a result of several natural and anthropogenic forces influencing the Earth's surface energy equilibrium. Climate change, induced by greenhouse gas emissions, results in global warming, elevating both atmospheric and surface temperatures. Urbanization is also one of the factors that affects the increase in surface temperature (Oad et al., 2023). Additional factors, including diminished soil moisture, extended droughts, and alterations in land use for agricultural or industrial purposes, can further enhance heat absorption.

2.6.2 Normalized Difference Vegetation Index (NDVI)

The use of NDVI in fire risk assessment has been widely adopted as it can categorize vegetation types or determine the ratio of living fuel (Liu et al., 2010; Karurung et al., 2025). NDVI is a visual indicator employed in remote sensing to assess the vitality of plants by analysing the transmission of visible and near-infrared light (Mohd Jaafar et al., 2020). The indicator is on the spongy layer located on the underside of leaves, which divides if the plant experiences malnutrition or stress and can differentiate between healthy and unhealthy plants, as well as separate plants from non-plant objects (Ya'acob et al., 2022; Moreno et al., 2023).

NDVI utilises the red and near-infrared (NIR) bands of satellite imaging to assess plant health. Healthy plants exhibit increased NIR reflectance and absorb greater amounts of red light, producing a high NDVI value compared to dry or unhealthy vegetation. Thus, this parameter can assist in identifying areas with a heightened susceptibility to ignition by monitoring vegetation condition and fuel availability. Most of the previous studies conducted demonstrate a significant drop in NDVI value during fire incidents (Gupta & Shukla, 2022; Mamgain et al., 2023). The mathematical equation to calculate NDVI is shown in Equation 2.2.

$$NDVI = \frac{NIR - RED}{NIR + RED} \tag{2.2}$$

Source: (Ya'acob et al., 2022)

The variable NIR represents the reflectance of the near-infrared band, which is equivalent to band 5, and RED represents the reflectance of the red band, which is equivalent to band 4 in the Landsat 8 spectral band. The NDVI calculation is significant since its value and distribution can characterise vegetation cover and density; an NDVI value approaching 1 signifies increasing vegetation density in the area, while an NDVI approaching -1 signifies the site exhibits non-vegetative characteristics (Artikanur et al., 2022). The likelihood of a fire is strongly correlated with the density of vegetation, whereby the higher the density of vegetation, the more fuel would be accessible, increasing the likelihood of a fire (Li et al., 2024; Bhattacharya et al., 2025).

When investigating fire incidents, the NDVI is a useful index since an increase in LST will increase the evaporation rate and deteriorate vegetation health (Sun & Kafatos, 2007; Gorgani et al., 2013). The utilisation of NDVI not only serves as an effective proxy for assessing fuel conditions, but is also frequently used in evaluating

vegetation recovery post-fire (Vlassova et al., 2014). NDVI can assess the temporal variations within the research area to illustrate the fluctuations in temperature over time (Anbazhagan & Paramasivam, 2016). The NDVI can be employed to detect the changes in plant phenology that occur in response to minimal fire severity (Emang et al., 2019; Ullah et al., 2023). This formula enables the consistent quantification of vegetation changes by normalising the difference in vegetation reflectance before and after a fire (Anucharan et al., 2025; Ghaderpour et al., 2025).

2.6.3 Normalized Difference Moisture Index (NDMI)

Normalized Difference Moisture Index (NDMI) provides an evaluation of soil moisture content across all features of the Earth's surface using the ratio of the SWIR band values to the NIR values. Changes in the water content of the tree canopies are associated with the SWIR reflectance (Rajan & Shanmugam, 2018). The NDMI, in conjunction with LST and NDVI, is a specialized index used to assess soil moisture levels (Rendana et al., 2023). The formula used to calculate NDMI is presented in Equation 2.3.

$$NDMI = \frac{NIR - SWIR}{NIR + SWIR} \tag{2.3}$$

Source: (Rendana et al., 2023)

Similar to NDVI, the variable NIR represents the reflectance of the near-infrared band, which is equivalent to band 5, while SWIR represents the reflectance of the short-wave infrared band, which is equivalent to band 6 in the Landsat 8 spectral band. The NDMI measures soil moisture across the Earth's surface features, making it an effective indicator of drought conditions. This index has a substantial capacity to identify the water content of more than eight leaf layers, compared to NIR-RED-based vegetation indices (Mohamed, 2022). Values ranging from 0 to 0.4 signify low water content, and values from 0.4 to 1 indicate high water content (Peña-molina et al., 2024). Vegetation and soil moisture were diminished as temperature increased, making the regions more vulnerable to sudden fire ignition.

The NDMI is frequently utilised to predict the likelihood of wildfire occurrence, as it assists in assessing the moisture content in vegetation and soil. In general, the NDMI and LST will reveal a negative relation because high temperatures will reduce the soil and vegetation moisture (Nejad & Zoratipour, 2019; Morshed et al., 2020; Tan

et al., 2020; Taripanah & Ranjbar, 2021). Dry soil is a factor to be taken into account, as vegetation is inherently flammable at high temperatures if the soil is dry, and also increases the intensity and duration of fires (Karurung et al., 2025). Regions with lower moisture levels would serve as more suitable fuel for wildfires than locations with higher moisture content (Bhattacharya et al., 2025; Dapke et al., 2025). This is crucial for assessing their likelihood of occurrence and monitoring the extent of wildfires.

2.6.4 Normalized Difference Water Index (NDWI)

Normalized Difference Water Index (NDWI) has proven effective in estimating vegetation moisture and fire risk when combined with other vegetation indices (Gray et al., 2018). The NDWI values range from -1 to 1. An NDWI value exceeding 0 indicates the presence of a water surface in the area (Artikanur et al., 2022). NDWI was applied to detect the existence of open water surfaces by analysing the green band, which is band 3, and the NIR band, which is band 5 (Moisa et al., 2023). The NDWI is calculated as shown in Equation 2.4.

$$NDWI = \frac{GREEN - NIR}{GREEN + NIR} \tag{2.4}$$

Source: (Moisa et al., 2023)

NDWI was initially developed as a supplemental vegetation index to NDVI to detect vegetation liquid water content, but it now closely correlates with total water content per pixel and negatively correlates with LST (Bala et al., 2018; Gray et al., 2018). In relation to wildfire occurrence and LST, NDWI exhibits a lower value during a higher temperature season (Guha et al., 2020; Abdalkadhum et al., 2021; Jothimani et al., 2021). Water bodies like lakes and rivers reflect a lower LST value since the features act as a cooling mechanism to thermal radiation (Morsy & Hadi, 2022). In addition to serving as a barrier to prevent the spread of fire, the open water bodies also provide areas with low fire potential (Bhattacharya et al., 2025). Consequently, regions with open water bodies are categorised as low fire susceptibility areas, while, conversely, regions without such waters are classified as high fire susceptibility areas.

2.6.5 Normalized Difference Drought Index (NDDI)

The NDDI is a metric that integrates data on vegetation health (NDVI) and water content (NDWI). It has been widely used in various research studies to assess drought conditions and is a suitable indicator for measuring dryness in specific regions (Burapapol & Nagasawa, 2016). The NDDI index was categorized into three classes: "non-drought" for NDDI values less than 0.1, "drought-moderate" for NDDI values ranging from 0.1 to 0.3, and "drought-severe" for NDDI values greater than 0.3 (Trinh & Vu, 2019). NDDI provides estimations of soil and vegetation dryness and the equilibrium of surface water (Aldiansyah & Madani, 2024). The formula to calculate the NDDI is shown in Equation 2.5 (Patil et al., 2024).

$$NDDI = \frac{NDVI - NDWI}{NDVI + NDWI} \tag{2.5}$$

Source: (Patil et al., 2024)

The NDDI is an instrument that enables individuals to predict the occurrence of wildfires by assessing plant health and atmospheric moisture levels. This indicates favourable conditions for dry weather, which may result in increased fire activity. The combination of information about both vegetation (NDVI) and water (NDWI) conditions can be used to determine vegetation drought conditions (Burapapol & Nagasawa, 2016; Yang et al., 2017). These indices also reacted to the fluctuations in LST values, as lower NDVI and NDWI are usually associated with high LST, thus reflecting high NDDI values (Du et al., 2018; Orimoloye et al., 2019). Increased NDVI values and elevated NDWI values were associated with lower NDDI values, indicating reduced drought severity (Artikanur et al., 2022). Drought in urban areas can exacerbate the urban heat island effect, hindering nature's capacity to deliver many social-environmental advantages, as well as to facilitate climate change adaptation and mitigation (Arif & Susena, 2024; Patel & Patel, 2024). NDDI is particularly effective for monitoring extended dry conditions, during which vegetation is more susceptible to ignition.

2.6.6 Normalized Burn Ratio (NBR)

The Normalized Burn Ratio (NBR) index is frequently employed to identify the extent of burned areas. The burn intensity is categorized into five levels: unburned, low

severity, moderate-low severity, moderate-high severity, and high severity (Junaidi et al., 2021). Wildfire events are indicated by the low NBR values due to low NIR reflectance and high SWIR reflectance owing to the reduction of vegetation after the fire (Kurnaz et al., 2020; Gupta & Shukla, 2022; Bitek et al., 2024). NBR values are expressed in the range of -1 to +1, with values near -1 suggesting burned vegetation and values near +1 suggesting unburned vegetation (Öncü & Çorumluoğlu, 2023; Anucharan et al., 2025). The formula used to determine NBR is as shown in Equation 2.6.

$$NBR = \frac{NIR - SWIR}{NIR + SWIR} \tag{2.6}$$

Source: (Anucharan et al., 2025)

NBR serves as an effective metric for assessing the extent and intensity of fires. However, areas of low fire severity may undergo continual growth post-fire, since grasses and shrubs obscure the burned ground, making damage harder to detect (Emang et al., 2019). The NBR is employed to identify the damaged vegetation areas and is responsive to changes in the forest after a fire (Fernández-Manso et al., 2020; Ghazali et al., 2025). The severity of burn, defined by the extent of change within a burned region relative to pre-fire conditions, is significantly influenced by the magnitude of the fire (Alexander, 2020; Junaidi et al., 2021). A high reflectance in the NIR band is indicative of healthy vegetation, whereas a very low reflectance is indicative of burned vegetation (Ezzaher et al., 2024; Bhattacharya et al., 2025) was used to examine the burnt intensity in the affected region. The NBR was crucial in assessing circumstances post-fire, and mapping the regional distribution of fire severity offers important knowledge into the ecological impacts of fires.

2.7 Spatial Analysis Used in Previous Studies to Determine Wildfire Hazard Zones

The interpolation of wildfire hazard zones can be conducted using several techniques, such as kriging, inverse distance weighting (IDW), hotspot analysis, and kernel density estimation (KDE). Each of the interpolation techniques may depict different results according to the suitability of the application and study area.

2.7.1 Interpolation Technique to Identify Wildfire Hazard Zone

Geospatial tools offer a variety of interpolation methods that can be used to map the wildfire susceptibility zone. Kriging is a type of generalized linear regression that serves as an ideal estimator in the context of minimizing mean square error, considering the interdependence of proximate samples while permitting a degree of independence among the sample locations (Dai, Liu, Kim, & Gu, 2003). It is a widely recognized interpolation method for obtaining fire propagation maps at an average resolution scale (Veraverbeke et al., 2014). The advantage of employing Kriging is its status as an accurate interpolator, signifying that interpolated values correspond precisely to observed values at sampled locations (Jain & Flannigan, 2017). A study by Heidari & Arfania (2022) used kriging interpolation to generate mean annual precipitation and temperature maps to evaluate wildfire susceptibility for the Andika region. This interpolation method was employed to estimate the possibility of forest wildfire recurrence in Central Yunnan Province (Y. Lan et al., 2023). The same method was also applied by Gharakhanlou & Perez (2025) to interpolate Fire Weather Index (FWI) values into continuous raster layers.

Apart from kriging, Inverse Distance Weighted (IDW) is also an interpolation technique offered by geospatial tools. IDW calculates the cell values by a linear-weighted combination of sampling points, with the weight assigned being a function of the distance between the input point and the output cell position (Childs, 2004). A primary assumption of this method is that as the distance from the known value increases, the similarity diminishes, since nearest points exert a more significant influence on a specific location than those situated at a wider distance (Simpson & Wu, 2014). In a study by Abdo, Almohamad, Al-Dughairi, & Al-Mutiry (2022), the IDW method was employed to determine the local pattern of rainfall, temperature, and wind speed data in assessing forest fire susceptibility in the Al-Draikich region. A similar method was also used by Salavati, Saniei, Ghaderpour, & Hassan (2022) to assess the fire risk in Kurdistan Province by generating the temperature and rainfall maps. The IDW interpolation provides acceptable results but does not surpass the optimal kriging method (Granville, Woolford, Dean, Boychuk, & McFayden, 2023).

Another interpolation technique used in wildfire susceptibility mapping is the Hot Spot Analysis method. The Getis-Ord Gi* statistic calculates z-scores and P-values to determine whether to approve or decline the null hypothesis of total spatial

randomization among the features (Rossi & Becker, 2019). This method has been widely applied in the estimation of spatial patterns of wildfire occurrence. The hot spot analysis is employed for analyzing the trend of forest and land fires (Arisanty et al., 2021). The density of wildfire occurrence and hot and cold spot zones within the Masito-Ugalla Ecosystem were identified utilizing the Hot Spot Getis-Ord Gi* tools in ArcGIS (Naftal et al., 2022). A study by Ma et al. (2022) employed the hot spot analysis of wildfire incidents to identify locations of statistically significant clustering, as it helps reduce uncertainty in mapping. Besides, Lanorte, Nole, & Cillis (2024) enhanced the categorization of burned area identification produced using spectral indices by deriving the maps from the Getis-Ord Gi*. However, this method should be applied together with IDW interpolation to create a continuous density surface from varying Gi* values (Kim, Kim, Lee, & Im, 2025).

2.7.2 Kernel Density Estimation in Identifying Wildfire Occurrence Density

Among other interpolation techniques, Kernel Density Estimation (KDE) seems suitable to be applied in this study. The KDE approach is a non-parametric technique that employs density estimation to assess the local likelihood of incidence and the level of vulnerability in a given area (Manepalli, Bham, & Kandada, 2011). This method computes density across a circular radius that covers the studied area (Mohaymany, Shahri, & Mirbagheri, 2013). According to Yu & Ai (2014), the standard representation of a kernel density estimator was described in Equation 2.7.

$$f(s) = \sum_{i=1}^{n} \frac{1}{h^2} k\left(\frac{d(s, c_i)}{h}\right) \tag{2.7}$$

In this context, *f(s)* represents the density assessed at position *s*, *h* denotes the search radius of the KDE, c_i signifies the observed event point, and *k( )* indicates the weight of event ci at the distance $d(s, c_i)$ from location *s*. A variety of kernel functions is available, including normal, uniform, quartic, and triangular (Thakali, Kwon, & Fu, 2015). The foundation of KDE is to generate better visual representations of different quantitative groups, based on the concept of a heat map distribution between central areas and adjacent regions (Bonnier, Finne, & Weiberg, 2019).

The KDE frequently employed technique for transforming historical fire data into a continuous surface. A study by Kuter, Yenilmez, & Kuter (2011) applied the KDE

to identify the high fire incident region on the Middle East Technical University (METU) campus in Ankara, Turkey. Similarly, Koutsias, Kalatsos, & Kalabokidis (2014) developed a map of fire-prone zones based on historical wildland fire ignition data at the national level in Greece, utilizing the KDE method. This interpolation technique has also been used to examine hotspot zones of all wildfires, including natural and anthropogenic fires, in California from 2000 to 2019 (Li & Banerjee, 2021). Moreover, this method can effectively illustrate the spatial distribution of fire occurrences and mitigate the impact of imprecise locations in historical records presented in point form (Shuo et al., 2021). The locations with high fire occurrences in the Provinces of China were identified by applying the coordinates of fire events to the kernel density analysis (Li et al., 2024). According to Baykal (2025), KDE produced significant results for a smaller studied area in contrast to the alternative methods.

2.8 Effect of LST on Wildfire Occurrence

The utilization of remote sensing and LST analysis is a valuable opportunity to effectively estimate, map, and evaluate the danger of wildfires. This approach offers a cost-effective and time-efficient means of achieving accurate results, both on a local and large scale. The increasing trends in LST suggest a progressive rise in environmental temperatures over time, which might potentially result in higher rates of evaporation, the drying out of vegetation, and lower soil moisture levels (Stoyanova et al., 2022; Chew et al., 2023; Parvar et al., 2024), thus contributing to the occurrence of fire incidents. A 1 ◦ C rise in temperature during the dry season could result in a 30% increase in the frequency of wildfires (Parvar et al., 2024). Higher temperatures and decreased soil moisture increase the susceptibility of forests to ignition and the spread of fires (Bostani & Pourebrahim, 2025; Rafaqat et al., 2025)

The effect of the burning was detected to be more severe if the LST increases because the elevated temperature causes vegetation and soil to dehydrate faster (Vlassova et al., 2014; Chaparro, Piles, Vall-Losera, & Camps, 2016). According to analysis by Çolak & Sunar (2020), temperature significantly impacts fire behavior, with LST being the second most significant parameter, and 41% of significant forest fires occur around midday, when temperatures reach their peak. A study by Rendana et al. (2023) described that the high fire risk region was located in high LST value zones, and there was a notable increase in the future LST value with a 6% increment as compared

with the current period. Another study by Kuduyu (2023) found that LST was the third most significant factor in predicting wildfires, with a variable importance score of 634.35, where the strong performance of LST can be attributed to the correlation between increasing temperatures in the spring and summer seasons and the occurrence of fires, coinciding with generally dry vegetation. Agricultural regions are the primary fire-prone areas, significantly impacted by high land surface temperatures, particularly above 45°C, with most documented fires exceeding 35°C during the summer (Moreno et al., 2023).

Continuous increased LST has a positive impact on the possible fire environment, as the sustained high temperatures might cause water scarcity and dryness in vegetation (Liu et al., 2010). The probability of wildfire ignition increases as the LST increases, especially during the dry season that usually transpires from February to March (Kamal, Ash'ari, & Abdullah, 2019; Aik, Ismail, & Muharam, 2020). Another study also noted that the average LST readings are higher than 27°C in March and April (Tajudin, Ya'acob, Ali, & Adnan, 2021). A study by Parajuli et al. (2020) shows that the mean temperature of March and May was above 30°C in the Teari Arc Landscape, which occupies 74% of the fire. Moreover, the same pattern of LST readings was also observed in Peninsular Malaysia, where the value will increase from February to April and will decline from August to October (Muhammad et al., 2024; Munawar et al., 2024). Apart from India and Malaysia, Thailand has also been observed to have a similar pattern of LST (Phantanaikasem et al., 2024; Talukdar et al., 2024)

Besides, from the year 1997 to 2008, states located in East Malaysia, such as Kelantan and Terengganu, experienced depletion of precipitation due to the southwest wind, leading to increased surface temperature and fire activity (Asha'ari & Badrunsham, 2014). Likewise, a study conducted in Kuantan, Pahang, by Jamaruppin et al. (2016) illustrated that approximately 65% of the high temperatures in the southern study region experienced an increase from lower to higher temperatures before the fire occurred. Another study denotes that the highest LST value was 31.2˚C before a wildfire incident, while it was 36.7˚C after the event, and the highest temperatures were found in urban areas with a lack of greenery, while the lowest temperatures were found in vegetation areas (Junaidi et al., 2021). This demonstrates that LST exerts a significant impact on the incidence of wildfires. A study by Chew et al. (2023) points out the notable presence of the highest maximum temperature at an average of 33°C and MODIS fire hotspots during the months of March and April. It is justifiable to

hypothesize that the climatic factor of maximum temperature exerts a substantial influence on the majority of wildfires within the designated research region.

2.9 Statistical Analysis Using Multiple Linear Regression

Wildfires are among the most destructive natural catastrophes because they cause damage to ecosystems, human populations, and the carbon cycle on a global scale. The interaction of natural, climatic, and anthropogenic factors needs to be investigated to gain an understanding of the severity and frequency of wildfires. A statistical technique known as Multiple Linear Regression (MLR) has been widely utilized to model the interaction of various conditions, such as sales forecasting, occupational risk, and fire prediction. According to Herawati et al. (2015), multiple regression analysis was employed to examine the effects of climate change and other variables on the historical occurrence of fires in the United States from 1961 to 1990. Regression analysis estimates the interaction between multiple parameters and demonstrates how independent variables affect the dependent variable (Shrestha, 2020).

MLR is an effective metric for assessing the relative influence of multiple factors on the final output. According to Liu & Zhang (2015), by calculating the regression coefficients, the MLR equation for forecasting fire rating can be shown as Equation 2.8.

$$\hat{y} = -5.066 - 0.0643x_1 + 0.1446x_2 + 0.0871x_3 + 1.2271x_4 \quad (2.8)$$

Where $\hat{y}$ is the fire danger rating and $x_1, x_2, x_3,$ and x_4 are the selected variables. In a previous study on statistical modelling of fire risk assessment, multiple regression analysis was found to be able to accurately predict the burned area and use it in fire hazard mapping, while the Analytical Hierarchy Process (AHP) was unable to include the burned area (Darvishi et al., 2020). A study by Neto et al. (2022) revealed that MLR exhibits a higher specificity percentage of 94% in categorizing burned areas, in contrast to the AHP, which achieves 85%.

Frequently, when multiple factors require prediction, a linear regression that simply relates the dependent variable to each of the predictor variables appears to be unreliable. When numerous predictor variables are analyzed, MLR analysis becomes more powerful in assessing relations between pairs of variables (Hoyt et al., 2006). Another advantage of MLR is that it arranges variables by their relative contribution to the model, identifying common characteristics and highlighting their importance in

explaining fire density distribution (Oliveira et al., 2012). Consequently, it is imperative to employ multiple regression analysis to derive conclusions with greater precision (Sun et al., 2023).

2.10 Conclusion

This chapter has explained the previous study conducted on wildfire estimation and monitoring. From the literature reviewed, there seem to be limited studies on the relationship between LST and wildfire occurrence in Malaysia, specifically in Perlis. Most of the studies for wildfire estimation and monitoring in Malaysia were conducted for the east coast states, such as Pahang and Kelantan; however, Perlis is known as the state with the highest temperature during the dry weather. Thus, the next chapter will describe the methodology to conduct the study.

CHAPTER 3
RESEARCH METHODOLOGY

3.1 Introduction

This chapter outlines the methodology employed to establish the correlation between environmental variables and LST, in addition to utilizing geospatial analysis to derive the Fire Hazard Index (FHI) and identify wildfire hazard zones in the state of Perlis. The approach integrates remote sensing, meteorological data, fire case records, and the spatial analysis capabilities of ArcGIS software. The process encompasses data acquisition, data pre-processing, and calculation of each index, correlation analysis between NDVI, NDMI, NDWI, NDDI, and NBR with LST, and hotspot identification by Kernel Density Analysis.

3.2 Research Methodology

This study attempts to analyze the relationship between several spectral indices, LST, and assess wildfire hazard zones using geospatial tools in ArcGIS software, specifically focusing on the state of Perlis. The approach integrates spatial and non-spatial data and spatial analytical techniques. The conceptual diagram is illustrated in Figure 3.1. The proposed structure was divided into four (4) phases, which are: i) preliminary study, ii) data acquisition, iii) data processing, and iv) results and analysis.

The first phase involves the study of the literature review of previous work, selection of the study area, and determination of the software used. The study area selected for this study is Perlis, Malaysia. Meanwhile, the software chosen to process the Landsat-8 satellite images is ArcGIS Desktop (ArcMap) and Google Earth Pro. The second phase will involve data acquisition. Records of fire incidents and Landsat satellite images were the primary sources of data. The data to be used are existing available data retrieved from accessible open-source databases such as USGS Explorer, and we also acquired data from agencies in Malaysia, such as the Fire and Rescue Department.

The third phase involves data processing. In the step-by-step procedure, the process will start with locating the fire incidents within Perlis state, referring to the fire incident data, and obtaining the coordinates using Google Earth Pro. The Google Earth Pro software will save the location in KML format and then convert it into a shapefile in ArcMap. Preprocessing Landsat 8 OLI images by eliminating unwanted cloud-covered pixels through cloud masking. This ensured the subsequent analyses were precise. Utilizing satellite imagery without cloud cover, spectral indices indicative of different environmental conditions were determined. The radiometric correction was applied to the satellite images using the Raster Calculator tool to convert digital numbers to reflectance values and to correct for sun angle. Then, geometric correction was conducted using the Projection Transformation tool to ensure all images are in the correct projection. To ensure the accuracy of the results, the quality of the satellite images was assessed using Quality Assessment (QA) Bands tools in ArcMap.

The distribution of wildfire occurrence in Perlis was mapped using data acquired from the Perlis state Fire and Rescue Department. The statistical data were filtered and geolocated in Google Earth Pro software. The point data were imported into ArcMap software, and the spatial density of the cases from the year 2014 to 2024 was analysed using the KDE tool. The temporal pattern of wildfire occurrence from the year 2014 to 2024 was evaluated using MS Excel software, and the number of wildfire cases was presented in the form of monthly and annual graphs. The Mann-Kendall test was performed for the annual data using the XLStat plug-in to test whether the temporal pattern was significant or not.

The LST was used to quantify the temperature of the ground and act as the main index, as it directly influences wildfire occurrence in the studied area. As the temperature of the surface increases, the rate of moisture loss also increases; hence, the possibility of wildfire igniting will also increase (Chew et al., 2023). However, using only LST was not sufficient in estimating wildfire occurrence since wildfires are influenced by multiple factors (Kong, 2024). Therefore, other spectral indices such as NDVI, NDMI, NDWI, NDDI, and NBR were evaluated in this study. These indices provide insights into plant health, atmospheric moisture levels, drought conditions, and surface temperature, all of which are crucial for assessing wildfire risk. These

computations were conducted using raster operations in ArcMap, which ensured that all layers were spatially consistent.

An analysis of statistical correlation was carried out between the computed indices and LST to determine the influence of several environmental factors on the potential for wildfires. Scatter plot graphs were created to assess the direction of the relationships, either positive or negative. Correlation analysis through MLR was performed to measure whether the relationship between each spectral index and LST is significant or not. Additionally, to identify regions with frequent wildfire occurrences, Kernel Density Analysis in ArcMap was employed to generate a continuous surface that illustrated the number of fires that occurred in the study area. These hotspots were employed to delineate areas with an elevated likelihood of ignition, hence indicating regions of heightened fire hazard.

The fourth phase will include the data visualization and analysis of the results achieved through the previous step in the methodology. The results for the evaluation of wildfire occurrence and wildfire hazard zones were visualized in the form of a hotspot map showing the potential wildfire occurrence area and graphs of the factors of wildfire correlation. The symbology of the wildfire density was altered to suit the theme of the maps properly. Whereas the relationship between spectral indices and LST will be presented in graphs and table form. The trendline was included in the graphs to better visualize the direction of the relationship, revealing how LST influenced the spectral indices' behavior. Finally, the results were analysed, and a discussion was made to evaluate the consistency of the findings.

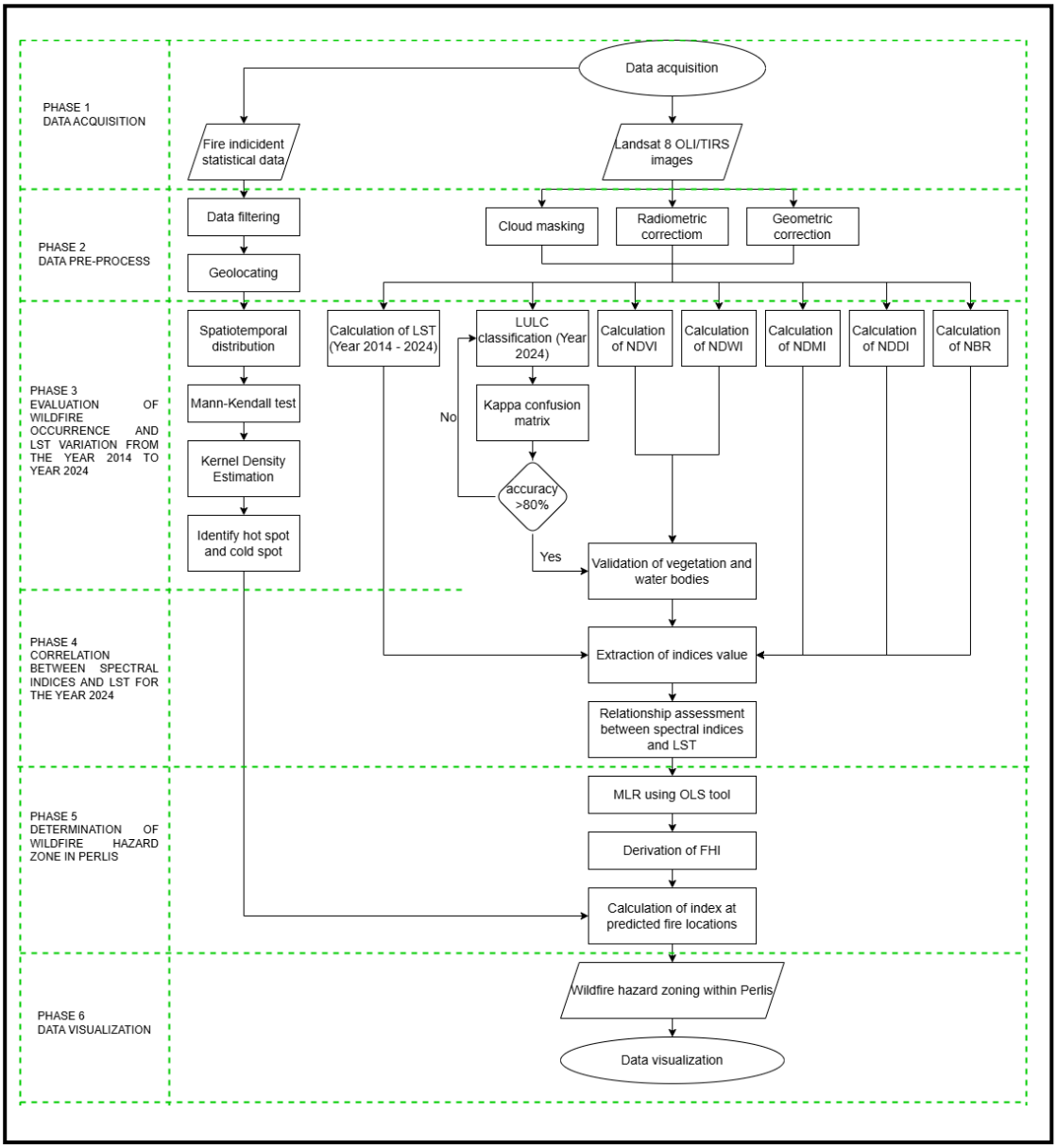

Figure 3.1 Overall Methodology Flowchart For The Study

3.3 Data Acquisition

Innovations in remote sensing, data analytics, and sensor technology have fostered the creation of new approaches for the early detection and prediction of wildfire in recent years (Kadir et al., 2023). The accuracy of the analysis is directly influenced by the selection of the appropriate satellite data and the related datasets.

3.3.1 Spatial Data

This study focuses on the acquisition and compilation of satellite-derived thermal data and vegetation indices that provide environmental context for the detection of wildfires in Malaysia. The thermal infrared data were primarily sourced from the Landsat 8 OLI–TIRS. These two sensors have a spatial resolution of 30 meters (reflective bands) and 100 meters (thermal bands) that offer seasonal coverage of the global landmass (Honary et al., 2025). The Landsat data were obtained from the USGS EarthExplorer platform. To ensure consistency in radiometric and positional quality, Tier-1 surface reflectance and surface temperature products were utilized. The datasets include metadata files with radiometric rescaling coefficients, thermal constants, and Quality Assessment (QA) bands. All of these elements are essential for computing LST and the cloud masking process. Malaysia's tropical climate experiences distinct monsoon and dry seasons, which significantly influence the behavior of fires. Images were collected from 2014 to 2024, including multiple dry seasons, to ensure temporal consistency. Utilizing data from several periods enables the comparison of years and distinguishes between everlasting heat sources and temporary fire-related anomalies. The Perlis state boundary was extracted from Malaysia’s administrative boundary downloaded from open-source software.

3.3.2 Non-Spatial Data

Other than satellite datasets, ground truth data and meteorological data from local agencies are also required in order to compare with the detected fire-prone region and to support correlation analyses between atmospheric conditions and wildfire occurrence. The fire incident reports were obtained from the Fire and Rescue Department to identify the frequency and location of wildfire incidents. The statistical

data obtained were presented in Excel format. The data included are file number, date of incidents, administrative unit, category of fire, address, distance from fire station, and response time. To ensure temporal consistency, the fire cases were classified according to months in a year, and only cases reported in March were analysed. The summarisation of data acquired is presented in Table 3.1

Table 3.1
Satellite Data And Fire Cases Acquisition

Data	Date	Data format	Data source
Landsat 8 OLI/TIRS	March 2014 March 2015 March 2016 March 3017 March 2018 March 2019 March 2020 March 2021 March 2022 March 2023 March 2024	Raster	https://earthexplorer.usgs.gov/
Fire cases	2014 – 2024	Statistic	Perlis Fire and Rescue Department

Source: (author, 2026)

3.4 Data Pre-processing

The statistical data and satellite imagery were pre-processed accordingly before continuing with further analysis to remove any blunders and to ensure the accuracy of the data. The tabular data was pre-processed using MS Excel software and Google Earth Pro software, while satellite imagery was pre-processed using ArcGIS software.

3.4.1 Tabular Data

Statistical data obtained from the Fire and Rescue Department were filtered according to research objectives. Fire cases related to forested regions, grasslands, and shrublands from the year 2014 to 2024 were extracted, and since this study focuses on investigating fire occurrence during the dry season, fire cases that occurred in March were specifically utilised. To ensure accuracy and consistency, the dataset was thoroughly filtered and organized before performing geolocation using Google Earth Pro software. The procedure involved identifying and eliminating records with identical dates, locations, and file numbers, and the dates were standardized into a uniform format, and partial location names were verified using gazetteers. The sample of the data that has been sorted is shown in Table 3.2.

Table 3.2
Sample Of The Data Filtered From The Fire And Rescue Department

No.	Date/file no.	Fire station involved	Reported incident	Address
1.	31/8/2024 323/20240831/23653	BBP Arau	Bush/weed fire	Jalan Pauh, Taman Pekan Arau, Arau
2.	17/8/2024 323/20240817/41129	BBP Arau	Bush/weed fire	No. 59, Jln Padang Nyu, Kg. Kubang Batu, Arau
3.	17/8/2024 75/20240818/91368	BBP Kangar	Bush/weed fire	Jalan Tasik Melati, Kangar
4.	17/8/2024 75/20240818/69113	BBP Kangar	Bush/weed fire	Kg.Bukit Kerang, Beseri, Kangar
5.	16/8/2024 322/20240816/79565	BBP Padang Besar	Bush/weed fire	Jalan Kesinai 2 Batu 10, Bukit Manik, Jalan Padang Besar(U)

Sources: (author, 2026)

3.4.2 Remote Sensing and GIS Data

Radiometric correction, including conversion of digital numbers to reflectance values, haze removal, and sun angle correction, was performed on the Landsat 8 images using the Raster Calculator tool in ArcGIS software, as shown in Figure 3.2. Before clipping to the research area boundary, all datasets were projected to a global unified coordinate reference system, which is WGS84, and resampled to a consistent spatial resolution using the Projection tool. Then, the satellite images retrieved from the USGS website were pre-processed using the Quality Assessment (QA) bands tool in the ArcMap software to ensure the quality of each band of the satellite images. Malaysia's administrative boundary shapefile was also reprojected to a global unified coordinate reference system, which is WGS84 UTM Zone 47, using the Projection and Transformation Tool. The Perlis state boundary was then clipped and separated according to its political zone, which are P001 Padang Besar, P002 Kangar, and P003 Arau.

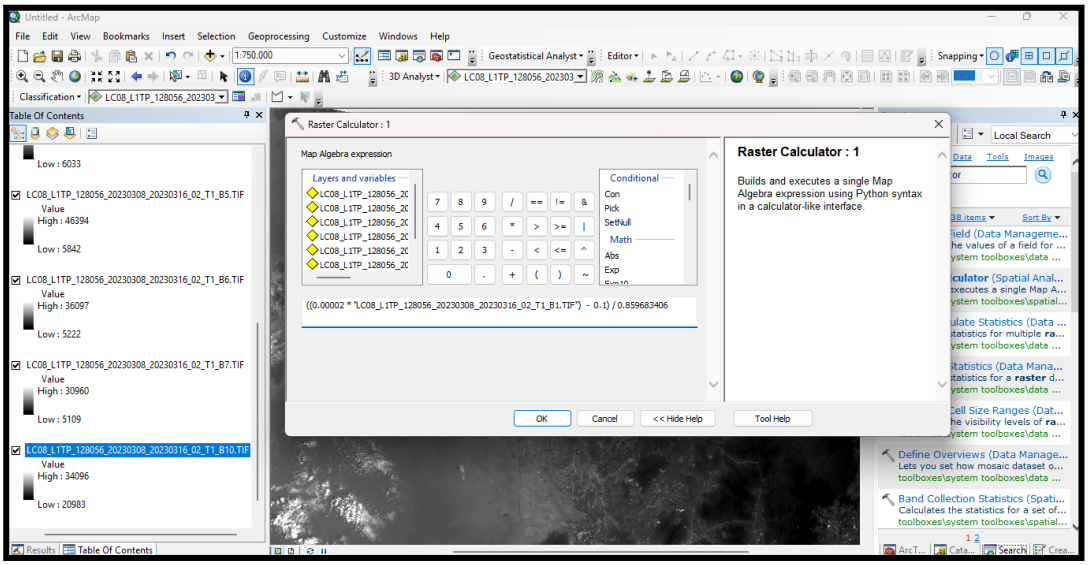

Figure 3.2 Radiometric Correction Using Raster Calculator For Each Spectral Band

3.5 Evaluation of Wildfire Occurrence and LST Variation from the Year 2014 to 2024

The study examined the temporal relationship between wildfire occurrence and variations in LST. Fire points recorded between the years 2014 and 2024 were used to examine the temporal distribution of wildfire occurrence. The research utilizes remotely sensed datasets, primarily derived from Landsat 8 OLI/TIRS at a spatial resolution of 30 m to obtain LST data, alongside statistical data obtained from the Fire and Rescue Department for the detection of active fires. The satellite images collected were particularly in March of each studied duration, with cloud cover less than 20%.

3.5.1 Establishment of Spatiotemporal Pattern of Wildfire Occurrence from the Year 2014 to 2024

The location of fire incidents from the filtered data was geolocated using Google Earth Pro software. The objective was to convert non-spatial datasets, which were presented in tabular form, into georeferenced spatial layers suited to perform analysis inside a GIS environment. The location of fire cases that occurred from the year 2014 to 2024 was pinpointed according to the address provided in the tabular data. The KML files of each year were imported into the ArcMap software, and point features were generated. Each point represents an individual fire incident, and the generated layer includes an attribute table that provides descriptive information about each point. The point features were exported to a shapefile and stored in a separate geodatabase

designated for this study. The geolocated fire locations were confirmed to be in the correct region of interest by cross-referencing them with the administrative maps of Perlis state. The shapefile of Perlis state's administrative and political boundaries was clipped from Malaysia's administrative boundary retrieved from an open-source website. The point features of fire cases were overlaid with the Perlis state boundary shapefile, and fire case distribution maps in March for each year were produced. Statistical graphs presenting the number of cases that occurred for each year were also produced and analysed using MS Excel software. Monthly and annual trend graphs demonstrating the number of cases that occurred from the year 2014 to 2024 were produced, and the Mann-Kendall test was performed for the annual number of cases to measure whether the trend is significant or not.

3.5.2 Derivation of LST from the Years 2014 to 2024

The data processing continues with the extraction of LST from Landsat 8 OLI/TIRS images. Spectral bands 4, 5, and 10 were downloaded in GeoTIFF format in accordance with the study conducted by Moisa et al. (2023). The LST was calculated sequentially following the steps suggested by Bhattacharya et al. (2025) using the Raster Calculator tool in ArcMap software. The six steps involved in the determination of LST using Landsat 8 are the conversion of digital numbers into radiance, the determination of brightness temperature using top-of-atmosphere radiance, the determination of NDVI, the determination of proportional vegetation using NDVI, the determination of land surface emissivity using proportional vegetation, and the determination of LST using brightness temperature and emissivity. The summarisation of the formula used to derive LST is presented in Table 3.2. The LST values obtained from satellite images were verified using temperature data from meteorological stations. This facilitated the assessment of the accuracy and reliability of the remotely obtained LST estimates. The results from LST processing were presented in the form of a heat map for each year.

Table 3.3
Formulation Used To Derive LST

Steps	Formulation	Description
i.	The conversion of a digital number into radiance. $L_\lambda = M_L \times Q_{cal} + A_L$	Lλ is the Top of Atmosphere (ToA) radiance. ML is the radiance multiplicative band. Qcal is a quantized calibrated pixel value (band 10). AL is the radiance additive band.
ii.	The determination of brightness temperature using ToA radiance. $BT = \frac{K2}{\ln\left(\frac{K1}{L_\lambda} + 1\right)} - 273.15$	BT is brightness temperature in degrees Celsius. K2 is the K2 band 10 thermal conversion constant. K1 is the K1 band 10 thermal conversion constant.
iii.	The determination of NDVI $NDVI = \frac{NIR - red}{NIR + red}$	NDVI is the Normalized Difference Vegetation Index. NIR corresponds to Band 5. Red corresponds to Band 4.
iv.	The determination of proportional vegetation using NDVI $P_v = \left(\frac{NDVI - NDVI_{min}}{NDVI_{max} - NDVI_{min}}\right)^2$	P_v is proportional to vegetation. $NDVI_{min}$ is the minimum value of NDVI. $NDVI_{max}$ is the maximum value of NDVI.
v.	The determination of land surface emissivity using P_v $\varepsilon = 0.004 \times P_v + 0.986$	ε is land surface emissivity.
Vi	The determination of LST $LST = \frac{BT}{1 + \left(\frac{\lambda \times BT}{\rho}\right) \times \ln(\varepsilon)}$	LST is Land Surface Temperature. λ is the central band wavelength constant. ρ is Planck's constant.

Source: (author, 2026)

3.6 Correlation between Spectral Indices and LST for the Year 2024

The relationship between spectral indices and LST was processed to achieve objective two, which is to determine the correlation between NDVI, NDMI, NDWI, NDDI, NBR, and LST for the year 2024 in relation to wildfire occurrence. The spectral indices used in this study are NDVI, NDMI, NDWI, NDDI, and NBR. All of the indices were determined using Landsat 8 OLI/TIRS Tier 1 images retrieved from the USGS website. The criteria for selecting satellite imagery were an acquisition date in March 2024, with cloud cover less than 20%, and the path and row covering the whole studied area. The satellite imagery acquired in March was used because the probability of fire igniting during the dry season is higher compared to months with a higher precipitation rate.

3.6.1 Extraction of the Chosen Spectral Indices for the Year 2024

The Clip tool was employed to cut the images according to the studied region. The formulation used to calculate each spectral index is presented accordingly in Table 3.3. Raster Calculator in ArcMap's Spatial Analysis tools was used to calculate the indices. All generated raster images were projected to a common coordinate system, which is WGS84. Following that, sample points were established to facilitate the extraction of values. Using the Create Fishnet tool, a uniformly distributed sample of points around the study region was created. The distribution of sample points was determined by the number of rows and columns defined by the users. An increased number of defined rows and columns results in a greater quantity of sample points generated. In this study, the number of rows and columns used is 50, which is sufficient to cover the whole geographical area of the studied region. The pixel values for NDVI, NBR, NDWI, NDMI, NDDI, and LST were assigned to each sample point utilizing the Extract Multi Values to Points tool. Statistical analysis was performed using the index values found in the produced attribute table. The attribute table was exported as a CSV file for further statistical analysis using MS Excel software. The outputs were stored in the project's database created earlier, accompanied by relevant details describing the data's origin, projection methods, and processing techniques.

Table 3.4
Formulation Used To Derive Spectral Indices

No.	Formulation	Description
i.	$NDVI = \frac{NIR - RED}{NIR + RED}$	NIR is the near-infrared band (band 5) RED is band 4
ii.	$NDMI = \frac{NIR - SWIR}{NIR + SWIR}$	NIR is band 5 SWIR is band 6
iii.	$NDWI = \frac{GREEN - NIR}{GREEN + NIR}$	GREEN is band 3 NIR is band 4
iv.	$NDDI = \frac{NDVI - NDWI}{NDVI + NDWI}$	
v.	$NBR = \frac{NIR - SWIR}{NIR + SWIR}$	NIR is band 5 SWIR is band 7

Source: (author, 2026)

The derivation of NDVI and NDWI was validated using the LULC maps. To determine the land cover for 2024, a supervised classification method was used. The LULC was classified into five (5) classes, which are built-up areas, forests, paddy fields, vegetation and grasslands, and water bodies. To extract the pixel information associated with the land cover classes, the multiple training sample polygons for each class were created using the Training Sample Manager tool. The sampling method used to extract the LULC is Stratified Random Sampling, where the samples are distributed randomly across different areas within each subgroup. Approximately a total of 400 samples were collected to classify five (5) classes, with 80 validation samples for each class. The samples taken were cross-validated with the Google Earth Pro software. Create a signature file and save the file. Then, the Maximum Likelihood Classification tool was used for the classification process. In the processing window, specify the input signature file and the output location. Change the symbology and state the class name to properly visualize the LULC map. To verify the classification's accuracy, the Kappa coefficients were computed using the Compute Confusion Matrix tool. An accuracy range of 0.8 to 1 denotes a high degree of agreement between the classification and the ground truth data (Ya'acob et al., 2022).

3.6.2 Execution of Statistical Analysis Using Linear Regression

The relationship between LST and each spectral index was modelled in the form of a scatter plot using MS Excel software, and a trend line showing a positive or negative relationship was drawn on the scatter plot. Linear regression facilitates predictive modelling through the utilization of several parameters (Guan, 2023), hence emphasizing the applicability of this method with the objectives of this study. In this study, the statistical analysis was conducted using the XLStat plug-in in MS Excel software. LST was selected as the independent variable, whereas the other spectral indices were selected as dependent variables. The output was presented in a correlation table.

3.7 Determination of the Wildfire Hazard Zone in Perlis

This study employed ArcMap's Kernel Density Estimation (KDE) tool, as referred to by Li et al. (2024), to identify areas with a high incidence of previous wildfires to assess wildfire hazard zones in Perlis. The data utilized is a point shapefile generated from geolocated fire incidents using Google Earth Pro software. The KDE method was applied to historical wildfire incident data to identify spatial clustering patterns and to assess the relative likelihood of fire occurrence within the study area. According to a previous study, this method is not suitable for regions with a large geographical area (Baykal, 2025), thus making it appropriate to be applied to Perlis state, since Perlis is known as one of the smallest states in Malaysia.

KDE has been widely used in identifying spatial patterns of fire occurrence. According to Manepalli et al. (2011), the Kernel estimator for a specified collection of observations from an unidentified probability density function can be expressed as:

$$f(x) = \frac{1}{nh}\sum_{i=1}^{n} K\left(\frac{x - x_i}{h}\right) \tag{3.1}$$

Source: (Manepalli et al., 2011)

Where *f(x)* represents the estimator of the probability density. *n* is the number of samples, *h* is referred to as the smoothing parameter, *K* is known as the kernel, *x* is the point at which the density is computed, and x_i is the independent sample. This method was employed in spatial analysis using ArcGIS software to analyse fire occurrence locations, therefore revealing regions with elevated wildfire occurrence density (Li & Banerjee, 2021). KDE proposes that clustered fire points correlate with increased

intensity but reduce as the distance increases, and the theory aligns with the mechanisms of fire propagation, where proximity to active fires influences the likelihood of igniting a new fire (Li et al., 2024).

3.7.1 Determination of Wildfire Zoning Using Kernel Density Estimation (KDE)

The first step was merging fire incident point data of historical wildfires that occurred within the research area from 2014 to 2024. The Kernel Density dialog box required the wildfire point layer as input and the frequency of fire occurrences as a population field. The search radius was determined by the spatial distribution of the data. The output cell size was chosen to achieve the required spatial resolution for analysis, typically 30 meters. The KDE output produced a raster surface indicating regions with a high frequency of fire incidents and areas with minimal occurrences. By using the Reclassify tool, the raster surface was categorized into wildfire hazard zones. A high hazard of wildfires is indicated by high kernel values, which indicate places where fires occur frequently or in clusters. The classification employed natural breaks (Jenks), depending on the distribution of the data. The results were presented in the form of a density map. According to Kim et al. (2025), the reclassification of fire occurrence density was categorized as presented in Table 3.4.

Table 3.5
Category Of Fire Occurrence Density

Category	Raster Value	Hazard level	Description
1	0.01 0.062	Very low	Negligible fire occurrence
2	0.063 – 0.125	Low	Infrequent fire occurrence
3	0.126 – 0.187	Moderate	Occasional fire occurrence
4	0.188 – 0.250	High	Frequent fire occurrence
5	0.251 – 0.312	Very high	Persistent fire occurrence

Source: Kim et al. (2025)

3.7.2 Model Generation and Hazard Zone Mapping

As suggested by Oliveira et al. (2012), Multiple Linear Regression (MLR) was performed to measure the strength of influence between the spectral indices and LST. The formulation of independent variables and the dependent variable to demonstrate the linear relationship can be calculated using Equation 3.1 by Liu & Zhang (2015):

$$Y = \beta_0 + \beta_1 X_1 + \cdots + \beta_n X_n + E \quad (3.2)$$

Source: (Liu & Zhang, 2015)

Where Y is the dependent variable, β is the estimated parameter, X is the independent variable, and E is the constant. MLR has the capacity to determine how multiple predictor variables may affect the specified value and can identify any outliers (Alauddin et al., 2018). A study by Neto et al. (2022) highlights that MLR exhibited more consistency in relation to the percentage of burned area compared to AHP.

The generation of the Fire Hazard Index for Perlis state, based on the chosen spectral indices, begins with acquiring the coefficient value for each index using the Ordinary Least Squares (OLS) tool as suggested by Wee et al. (2024). Raster data of each index and point data of fire cases were imported into the software. The point data of fire cases were analyzed for cluster patterns using the Integrate tool. The tool analyzes the features that fall within a specified distance was assumed to represent the same location and were clustered together. In this study, the XY tolerance specified was 500 meters, where we assumed that fire cases that fall within a 500-meter buffer zone represent the same locality. Then, the Collect Event tool was used to convert the integrated fire point data into weighted point data. The geometry of the output of Collect Event was joined with fire point data using the Join tool, and a new feature layer was created. The values of the spectral indices corresponding to each point data were extracted using the Extract Multi Value tool.

Open the attribute table and identify the appropriate dependent and explanatory variables. Open the OLS tool, specify the parameter required, and run the tool. In this study, the dependent variable selected was the count of fire cases, and the explanatory variables were LST, NDVI, NDMI, NDWI, NDDI, and NBR. The processing report was generated, and the coefficient for each spectral index was produced. The processing report that was generated from the OLS tool was observed, and the coefficient values for each spectral index were identified. By using the Raster Calculator tool, the calculation for the Fire Hazard Index was performed based on the MLR equation. A new raster layer of wildfire hazard zone for Perlis state was produced. The raster layer was reclassified into five classes: “Very Low Hazard”, “Low Hazard”, “Moderate Hazard”, High Hazard”, and “Very High Hazard”. A hazard zone map was generated and presented accordingly.

3.8 Conclusion

This chapter established the methodological framework for assessing the impact of LST on wildfire occurrences in Perlis. The acquired data was corrected accordingly using appropriate tools in the ArcGIS software. The data processing method successfully transformed tabular wildfire information into geographical datasets appropriate for GIS analyses. The spatiotemporal pattern of LST and wildfire occurrence in Perlis was visualized and analysed; hence, the linkage between wildfire occurrence and LST pattern during the hot and dry season can be ascertained. The correlation between multispectral indices and LST was examined, and the coefficient values of each index were determined to derive the Fire Hazard Index (FHI). The dataset derived from this study provided the spatial framework necessary to examine in greater detail the mechanisms of wildfire occurrence, various spectral indices, and their correlation with LST. The integration of GIS and statistical methodologies enables a comprehensive analysis of the geographical and temporal alterations induced by wildfires on temperature.

CHAPTER 4
RESULTS AND DISCUSSION

4.1 Introduction

This chapter will describe the processing results for objective one, objective two, and objective three. This chapter begins with an analysis of the processing results for objective one, which is to examine the changing trend of LST and wildfire occurrence from the year 2014 to 2024. The debate continues with the description of the processing result for objective two, which examines the relationship between spatial indices and LST. This chapter will also include a discussion of the processing result for objective three, the proposal of the most potential wildfire occurrence within the state of Perlis.

4.2 Analysis of Frequency of Wildfire Occurrence and LST from the Year 2014 to 2024

The frequency analysis was conducted to examine the trend of wildfire occurrence and LST from the year 2014 to 2024 in Perlis. The findings of the spatiotemporal pattern of wildfire occurrence from the years 2014 to 2024 were illustrated in Figures 4.1 to 4.3, showing the total number of wildfire cases in March, the comparison of the number of cases for each month, and the spatial distribution of wildfire cases. Figures 4.4 to 4.6 present the results of the LST pattern from the years 2014 to 2024.

4.2.1 Wildfire Occurrence Density Mapping from the Year 2014 to 2024

The results of wildfire incidents reported in Perlis from the year 2014 to the year 2024 are illustrated in Figures 4.1 to 4.3. Local fire incident data indicate that there were 1,600 wildfires recorded from January 2014 to August 2024, with an average of approximately 140 cases, which is equivalent to approximately 47% each year. Figure 4.1 presents the number of fire cases in March during the studied period in Perlis. Comparing the values, it can be seen that the trend line indicates an increasing pattern, with the number of cases increasing by approximately 60% between the years 2014 and

2024. The similarity between each year is that the number of cases generally peaks in March and starts to decline in April. The results indicate that elevated LST will accelerate the loss of soil and vegetation moisture, thus increasing the probability of ignition.

Figure 4.2 illustrates the total number of fire cases according to months in each of the studied years. From the graphs, it can be seen that the rate at which fires occurred from the year 2014 to 2024 differed. However, there is a distinct similarity between all the findings shown, which is that the highest number of cases reported each year is in March, corresponding to the monsoon season, which is typically dry. The years 2019 and 2022 demonstrated a different pattern, where the number of cases peaked in December and January, respectively. Statistics indicate that in 2019, the number of cases began to rise in late December, along with the increase in temperature during that period, as reported by The Global Historical Weather and Climate Data.

The Mann-Kendall test was carried out to detect a significant trend in wildfire occurrences from the year 2014 to 2024 in Perlis. The parameters that should be taken into consideration when interpreting the result of the Mann-Kendall test are p-value, Kendall's Tau, and z-score. The results of the Mann-Kendall test are summarised in Table 4.1. It can be seen that there is a significant trend of wildfire occurrence from the year 2014 to 2024 in Perlis, as the p-value is 0.005 (p-value < 0.05). The Kendall's Tau value of +0.978 and the z-score of 4.333 (z-score > 0) indicate an increasing trend. The overall trend summarisation was that there is a trend in the series (Hypothesis = Ha) as the computed p-value is lower than the significance level alpha=0.05.

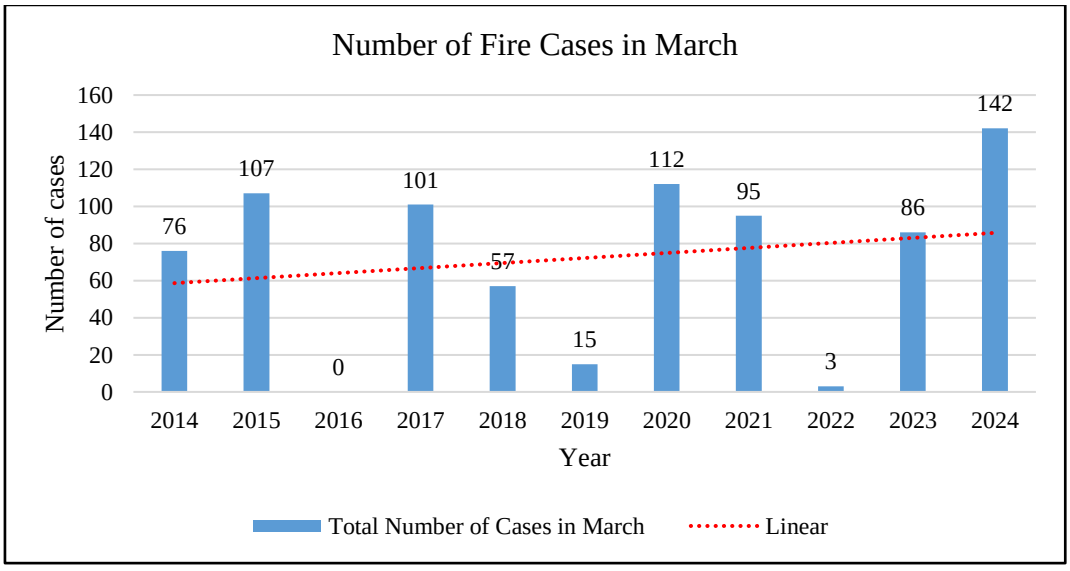

Figure 4.1 Number Of Wildfire Cases In March From The Year 2014 To The Year 2024 In Perlis

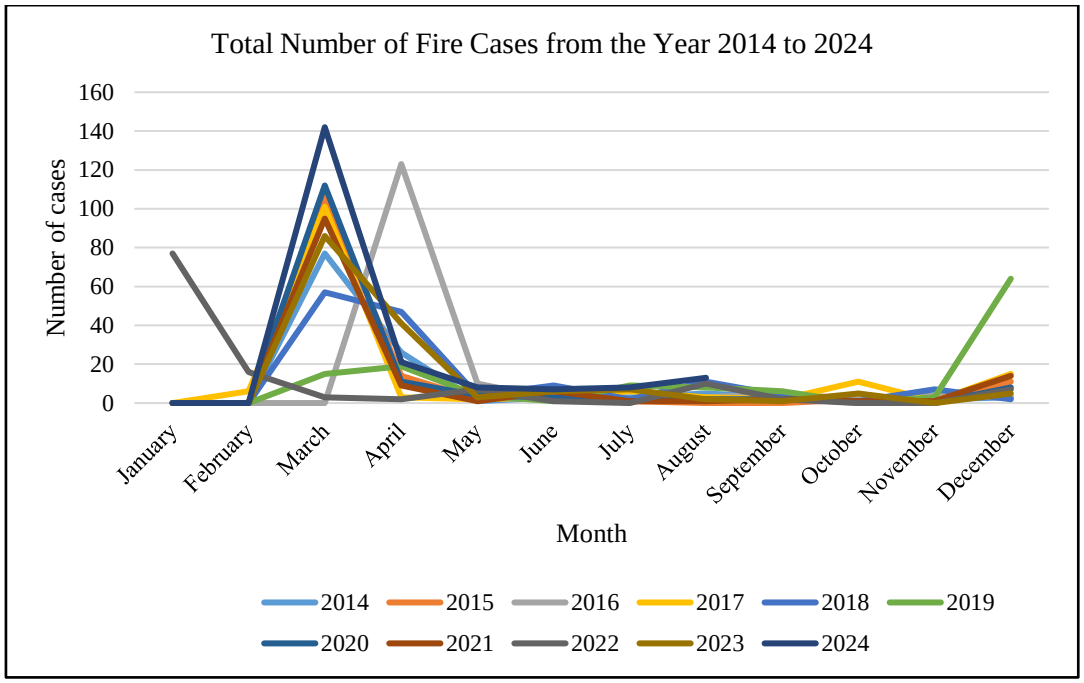

Figure 4.2 Comparison Of The Total Number Of Fire Cases From The Year 2014 To 2024 In Perlis

Table 4.1
The Mann-Kendall Test For Wildfire Cases From The Year 2014 To 2024 In Perlis

Variable	S statistics	Kendall's Tau	p-value	z-score	Trend direction
Number of cases	43	0.978	0.005	4.333	Increasing

Figure 4.3 illustrates the spatial distribution of wildfire occurrence from the year 2014 to 2024 in Perlis. The state was divided according to its political zone for better analysis of the spatial pattern of wildfire occurrence. In this figure, the light blue denotes the Padang Besar political zone (P001), light purple represents the Kangar political zone (P002), and light green represents the Arau political zone (P003). As demonstrated by the figure, wildfire occurrence was most concentrated in the Kangar political zone, followed by Padang Besar, and the least concentrated in Arau. A similar pattern of case recurrence between the studied years was seen to be concentrated in the Kangar area, followed by the Padang Besar area.

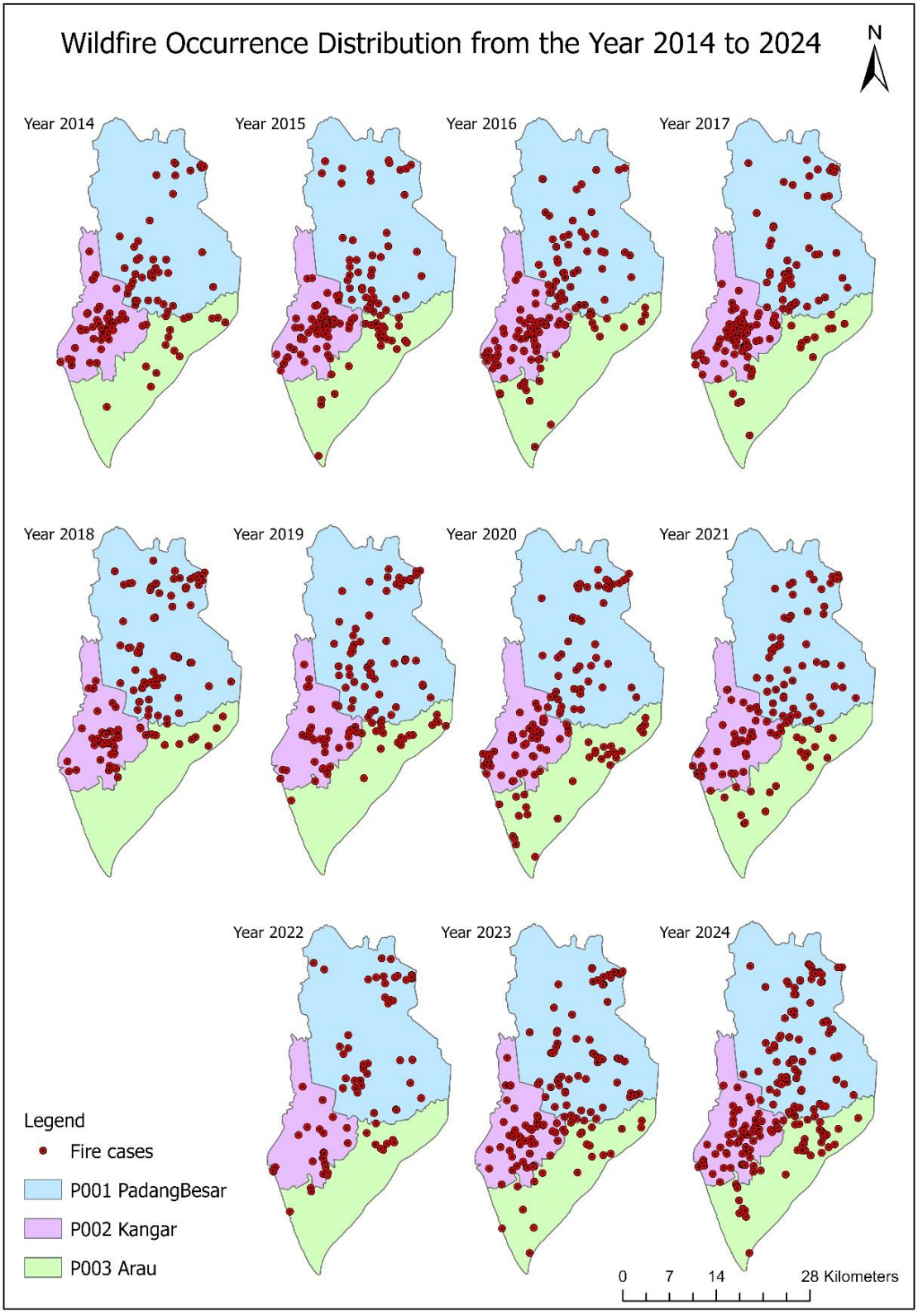

Figure 4.3 Spatial Distribution Of Wildfire Cases From The Year 2014 To 2024 In Perlis

4.2.2 Variation of LST from the Years 2014 to 2024

Land Surface Temperature (LST), derived from satellite data, indicates the temperature of the Earth's surface. Assessing climatic conditions is crucial for determining their feasibility for wildfire occurrence. The calculation of LST was accomplished using Landsat satellite imagery acquired in March of each year. Figures 4.4 to 4.6 present the changes in LST from the year 2014 to the year 2024. The results obtained reveal significant variations across the studied period. The findings showed that the high LST value exceeded 30°C in March for each studied year. The highest LST measured was in the year 2023 with approximately 39.6°C, as illustrated in Figure 4.6. The lowest surface temperature was measured in the year 2018 with approximately 13°C, as presented in Figure 4.8. It can be seen from the data that there is a fluctuation in the warming trend from the year 2014 to 2024.

From the results, it is apparent that the southern and central regions generally exhibited consistently elevated LST values, corresponding to areas characterized by sparse vegetation and urbanized areas. The reading of LST for both areas reached a maximum of approximately 38°C. It is also apparent that the region with a high LST value is observed in the paddy field region due to the agricultural cycle, which is a non-vegetated phase. Compared to other surfaces with high canopy density, a surface with lower canopy density, like paddy fields, may absorb more solar radiation, resulting in slightly higher LST. Except for the year 2022, when the region with a high LST value was observed at the built-up area, which is the Kangar town, as shown in Figure 4.7. Conversely, lower LST values were detected at water bodies, forested areas, and high-altitude regions with a mean temperature as low as 17°C. These results may be due to the cooling effect offered by water bodies and dense forests with high canopy density that provide full shade to the surface.

Land Surface Temperature Variation from the Year 2014 to 2017

Year 2014

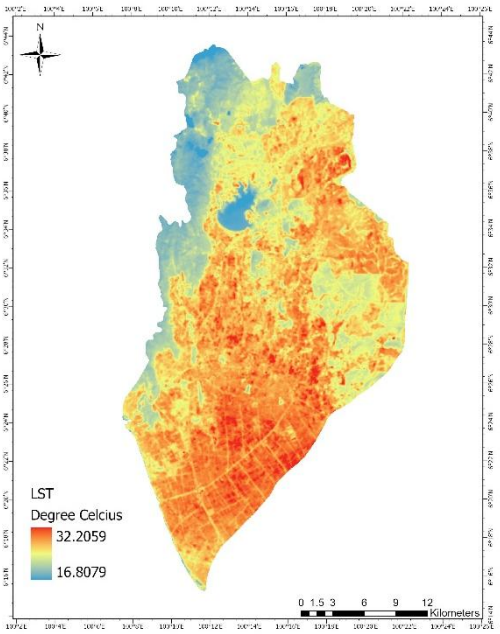

Year 2015

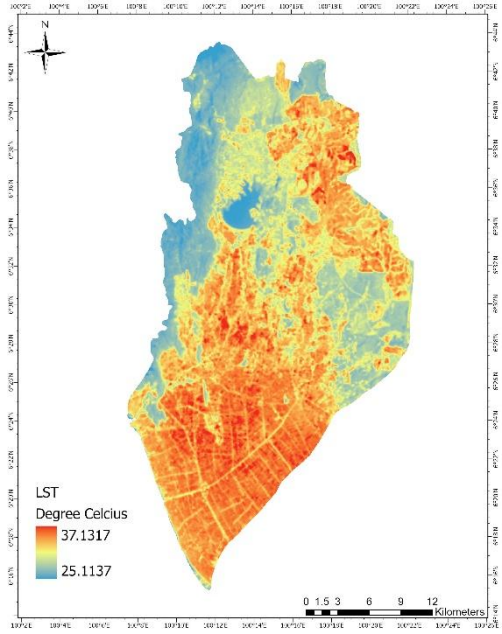

Year 2016

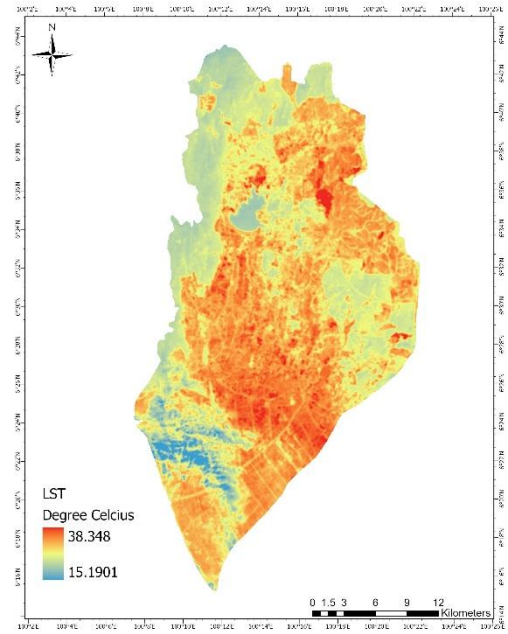

Year 2017

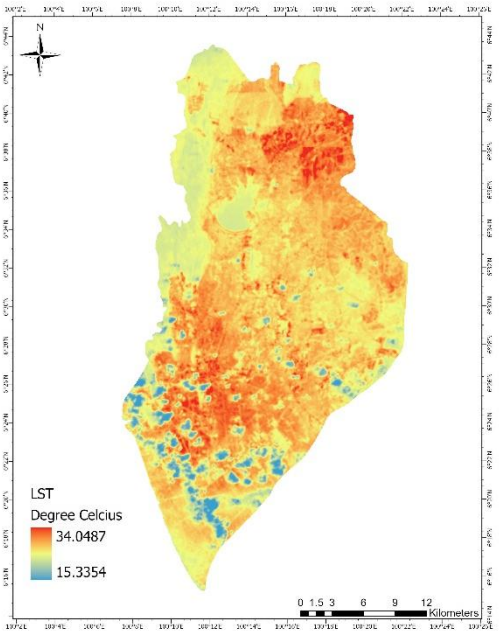

Figure 4.4 LST Variation From The Years 2014 To 2017 In Perlis

Land Surface Temperature Variation from the Year 2018 to 2021

Year 2018

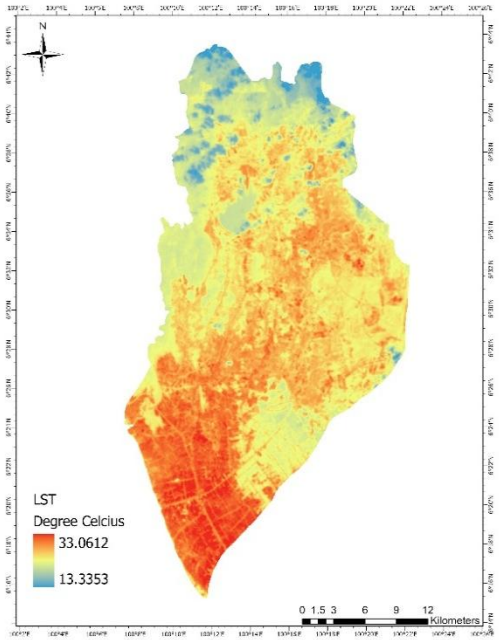

Year 2019

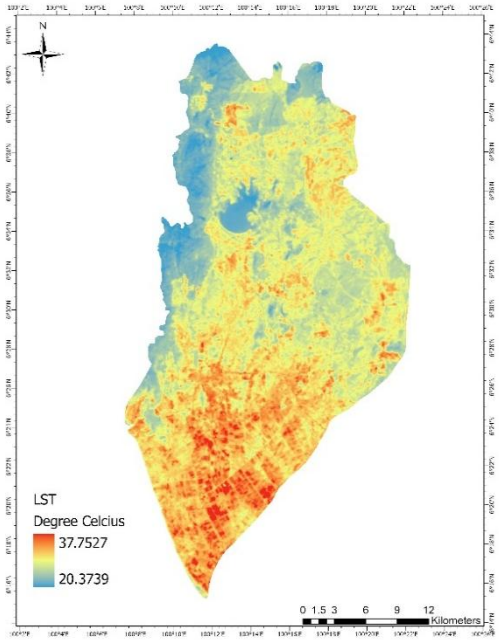

Year 2020

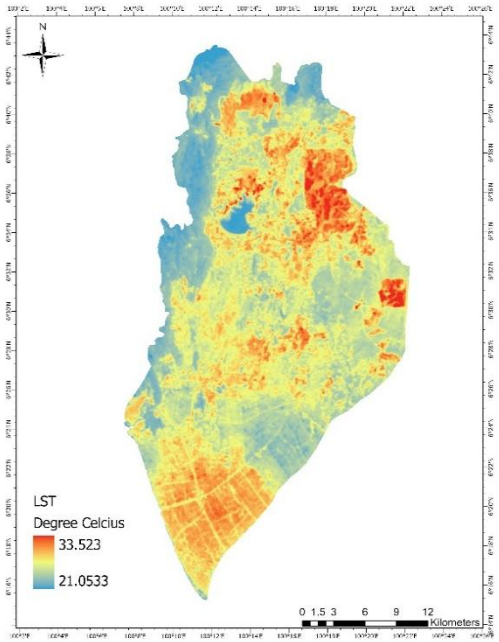

Year 2021

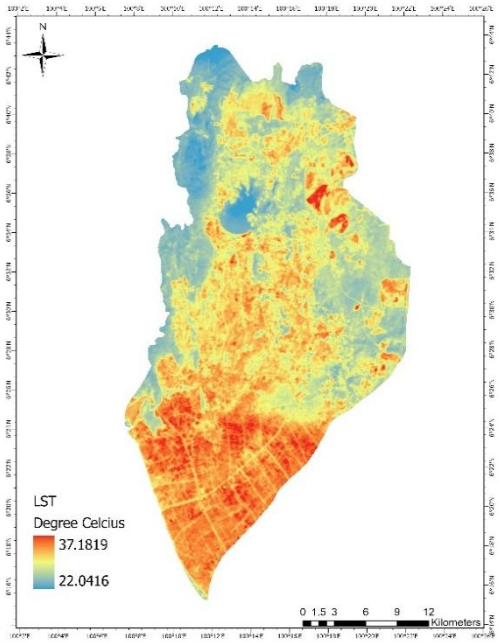

Figure 4.5 Lst Variation From The Years 2018 To 2021 In Perlis

Land Surface Temperature Variation from the Year 2022 to 2024

Year 2022

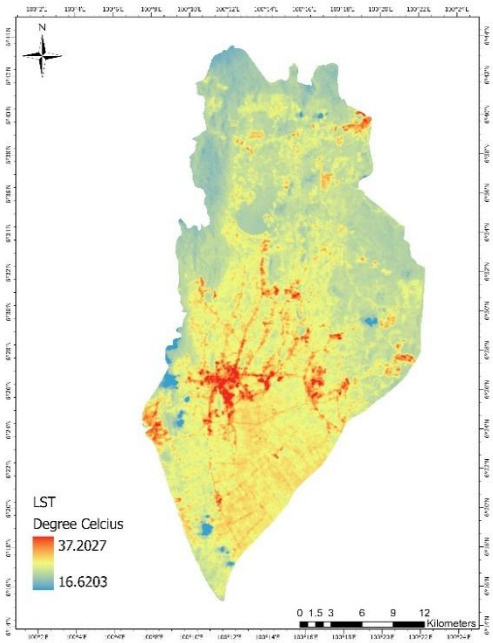

Year 2023

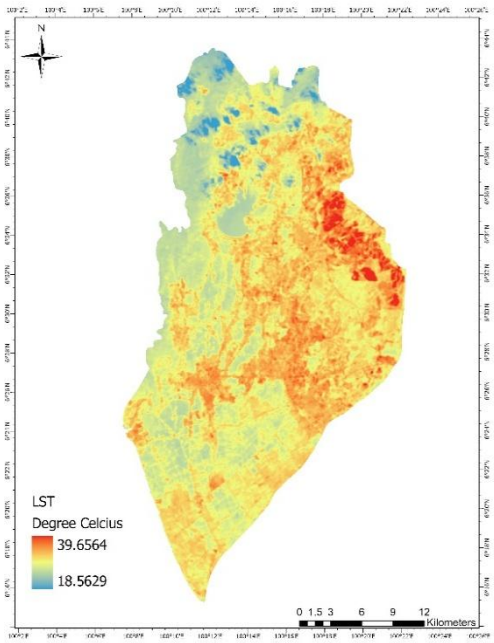

Year 2024

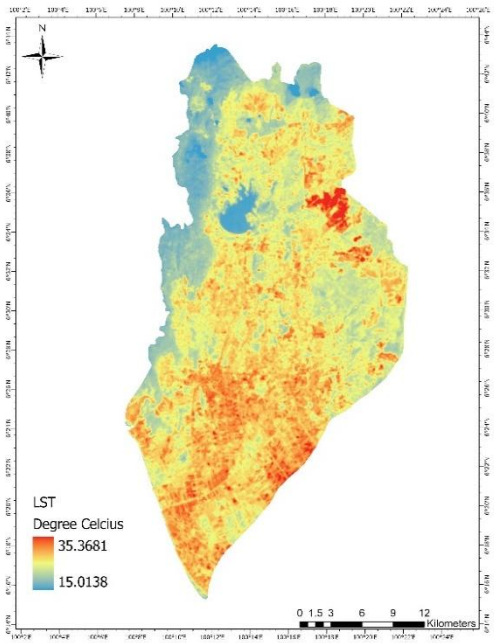

Figure 4.6 LST Variation From The Years 2018 To 2021 In Perlis

4.3 Relationship between Spectral Indices and LST

Figures 4.7 to 4.11 illustrate the thematic map of the chosen spectral indices derived from Landsat data for March 2024 in Perlis. Since the dry season in Perlis usually peaks in March, this study particularly investigates the abnormality of the spectral indices that leads to a high wildfire occurrence in March. Figures 4.12 to 4.16 present the relationship between each spectral indices with LST, and Table 4.1 demonstrates the result for correlation analysis between each spectral indices with LST using MLR.

4.3.1 Map of the Chosen Spectral Indices

The spectral indices that are frequently paired with LST are NDVI, NDMI, NDWI, NDDI, and NBR, has been derived from Landsat images using specified spectral bands as mentioned in Table 3.3. Figure 4.7 illustrates the LULC map of Perlis state. The land cover was categorized into five classes, which are developed area, forest, paddy field, vegetation and grassland, and water bodies. The developed areas were depicted in red color, the forested areas were indicated in dark green color, the paddy fields were in yellow, the vegetation and grasslands were depicted in light green, and water bodies were indicated by dark blue color. From the figure, it can be seen that the areas with NDVI values in Figure 4.8 were coincident with the forested areas, and the water bodies in Figure 4.10 were coincident with the water bodies indicated in the LULC map. Table 4.2 displays the outcome of the LULC classification validation process using the Kappa confusion matrix. As can be seen, the Kappa coefficient value for 2024 was 0.88, meaning that there was 88% consistency between the ground truth data and the categorized data.

The NDVI map in Figure 4.8 was illustrated using a dark green to red color ramp, where dark green to light green denotes a high NDVI value, yellow indicates a moderate value, and orange to red indicates a low NDVI value. The map shows that the resultant highest and lowest NDVI values were 0.847 and -0.202, respectively. The NDVI value closer to +1 indicates that the vegetation was in good health condition, and in the figure, the high NDVI value was observed at the Nakawan Range, which includes Perlis State Park and Bukit Ayer Ecoforest Park. Whereas the NDVI values closer to -1 are usually related to vegetation with poor health conditions (Artikanur et al., 2022).

In this figure, the paddy fields at Arau and the grasslands at Chuping were represented in orange color, signifying lower NDVI values, and the Timah Tasoh Lake was represented in red color, indicating no vegetation. This condition shows that the paddy fields are experiencing dehydration due to dry weather.

Figure 4.9 demonstrates the NDMI map for March 2024 in Perlis. The map was explained using a dark blue to red color ramp, where dark blue to light green indicates a high moisture level, yellow indicates a moderate moisture level, and orange to red indicates low moisture. According to Rendana et al. (2023), the NDMI value ranges from -1 to +1, with values greater than 0 representing a high moisture level and values lower than 0 representing a low moisture level. From the figure, it can be seen that the maximum and minimum moisture levels for March 2024 were 0.403 and -0.710, respectively. The forested area at Perlis State Park and Bukit Ayer Ecoforest Park showed high moisture levels, while the paddy fields in the Arau and Kangar region, as well as a few grasslands at Chuping, were experiencing water deficits due to dry weather, as shown in Figure 4.9. The NDMI map shows that paddy fields and grasslands are facing water stress during the drought season.

The NDWI was typically used to detect water bodies or flooded areas. Even though it is less suitable to measure internal vegetation moisture, this index was useful to distinguish water features from other land use features. The NDWI map for Perlis state in March 2024 is shown in Figure 4.10 and was represented using the same color ramp as NDMI. From the figure, the Timah Tasoh Lake was clearly delineated with a high index value of 0.938; non-water features showed low NDWI, with the lowest value being -0.674. The NDWI map is important to detect water resources for drought mitigation planning.

Figure 4.11 presents the map of NDDI for March 2024 in Perlis. The map shows the severity of drought in March 2024, obtained from Landsat 8 data. The value for NDDI usually ranges from -1 to +1, where -1 signifies a minor drought level or wet condition, while +1 signifies more severe drought (Patil et al., 2024). The Figure shows five different classes of drought severity, which are indicated by the purple color, indicating very low severity; light blue, indicating low severity; green, signifying moderate severity; yellow, signifying high severity; and red color denoting very high severity. As highlighted in this figure, most of the very high drought severity was found at the Padang Besar area, while the Kangar and Arau areas had moderate to very high severity index. The forested area at Nakawan Range shows moderate to low drought

severity, and the very low drought severity was found at Timah Tasoh Lake. The result suggests that Perlis experienced severe drought during the pre-monsoon season, which usually transpires in March.

The NBR map is shown in Figure 4.12, presenting the severity of burned areas. According to Öncü & Çorumluoğlu (2023), the value for NBR ranges from -1 to +1, where negative values indicate burned areas and +1 indicates unburned areas. In the Figure, the index was presented in a white-to-black color ramp, where positive values are indicated by white color, while negative values are indicated by black color, highlighting the burned area. It can be seen that the lowest value of NBR was -0.744, implying a high burned severity, and the majority of the burned areas were found at paddy fields in the Arau area and grasslands in the Padang Besar area. The unburned area with the highest positive value of 0.570 was found at the forested area along Nakawan Range, and a few at the palm oil plantation in the Arau area.

Table 4.2
The Accuracy Confusion Matrix Of LULC For The Year 2024

Classes	Water bodies	Built-up areas	Forest	Vegetations and grasslands	Paddy Fields	User's accuracy
Water bodies	10	0	0	0	0	10
Built-up areas	0	8	0	1	1	10
Forest	0	0	10	0	1	11
Vegetations and grasslands	0	0	0	16	2	18
Paddy Fields	0	1	0	0	13	14
Total	10	9	10	17	17	63
Producer's accuracy	1	0.89	1	0.94	0.76	0
Kappa = 0.88						

Source: (author, 2026)

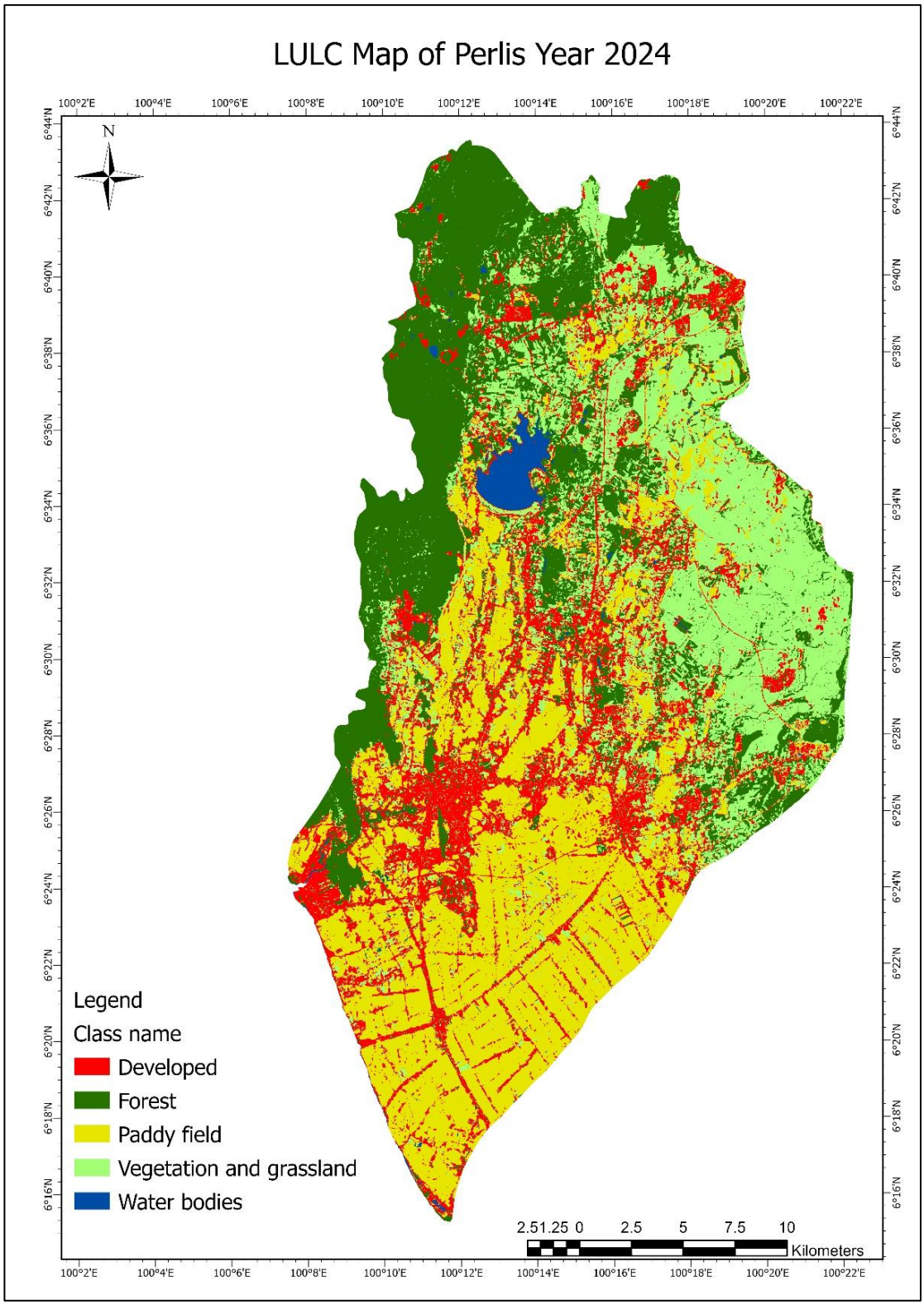

Figure 4.7 The LULC Map Of Perlis For The Year 2024

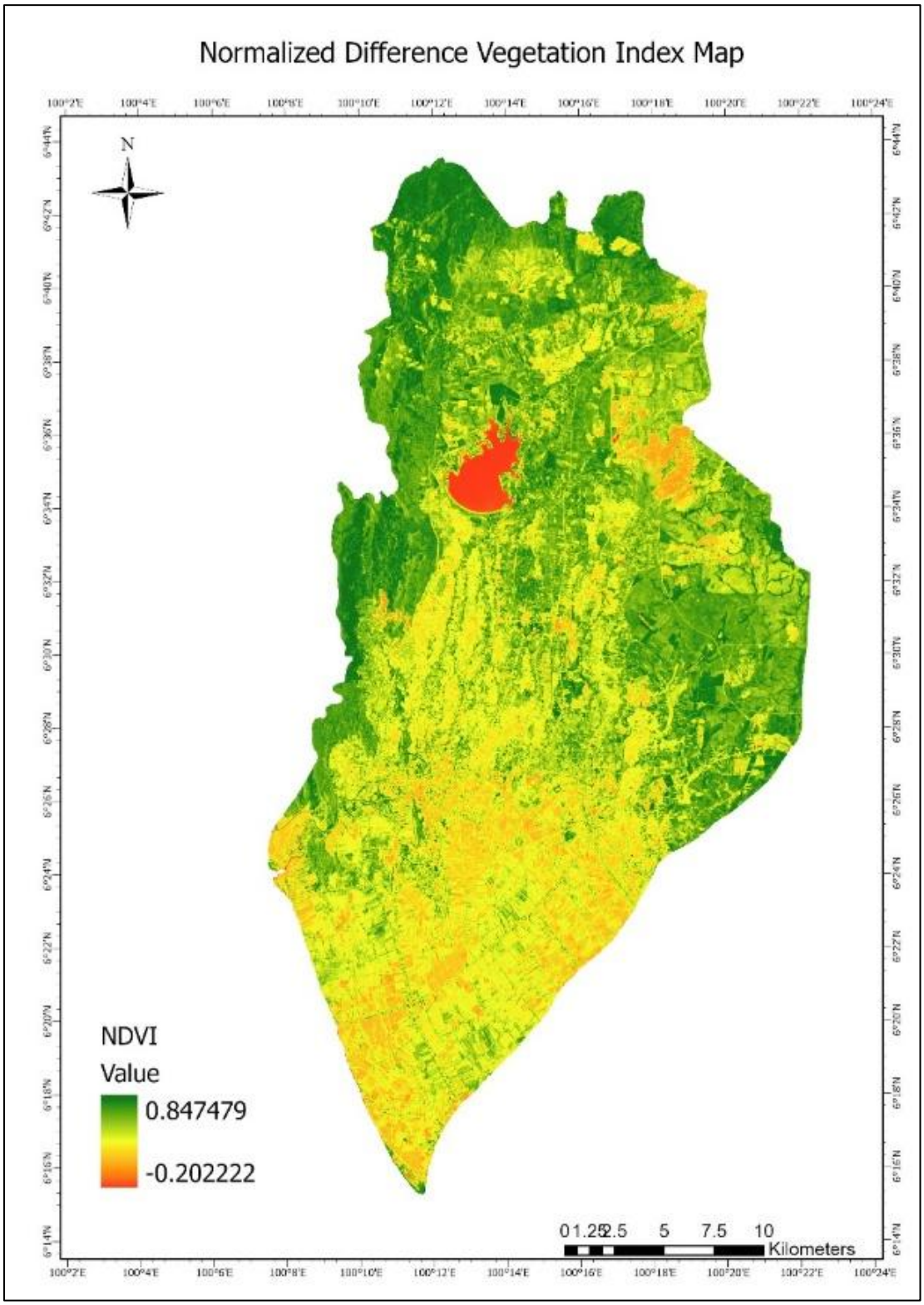

Figure 4.8 Map Of NDVI For March 2024 In Perlis

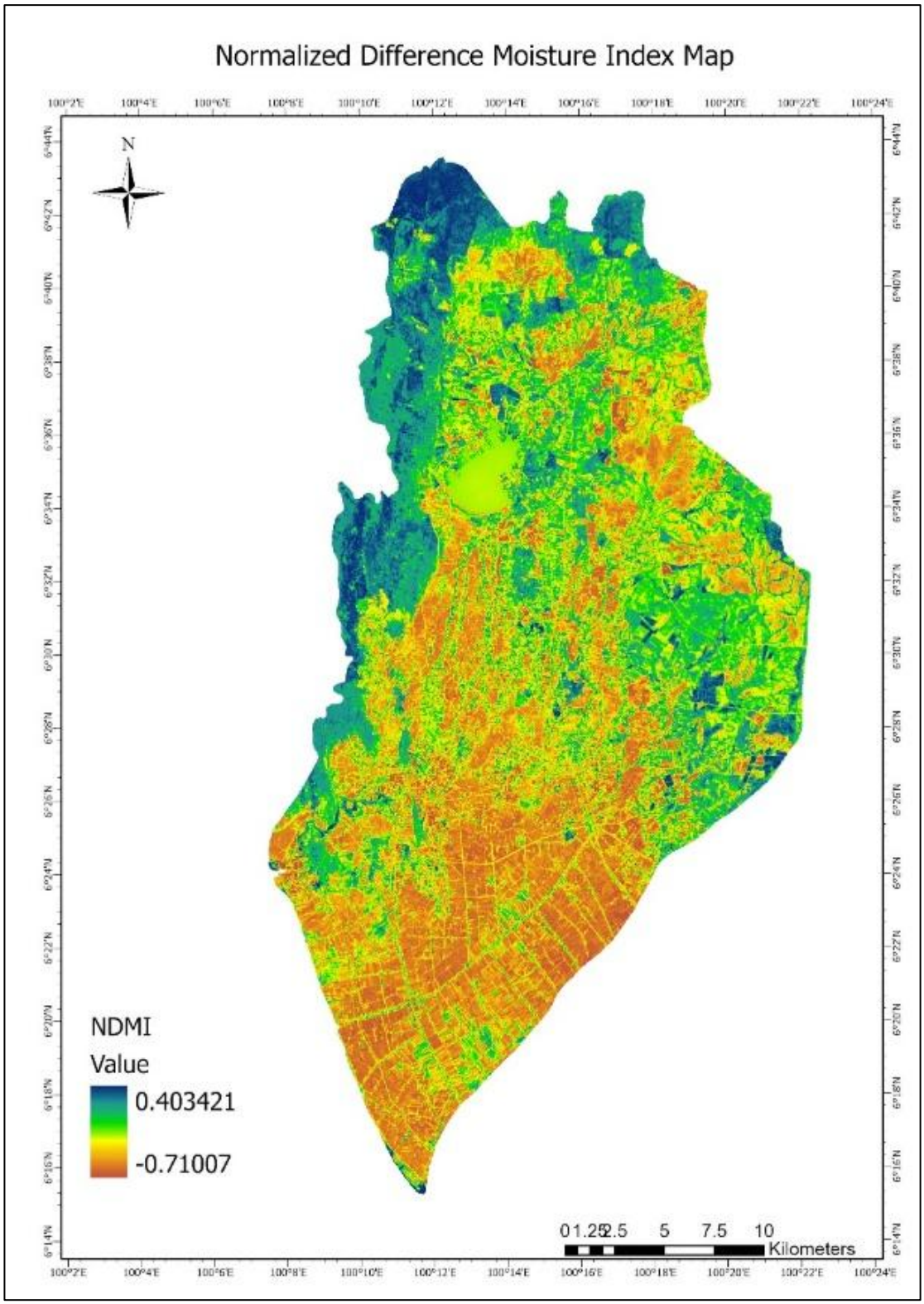

Figure 4.9 Map Of NDMI For March 2024 In Perlis

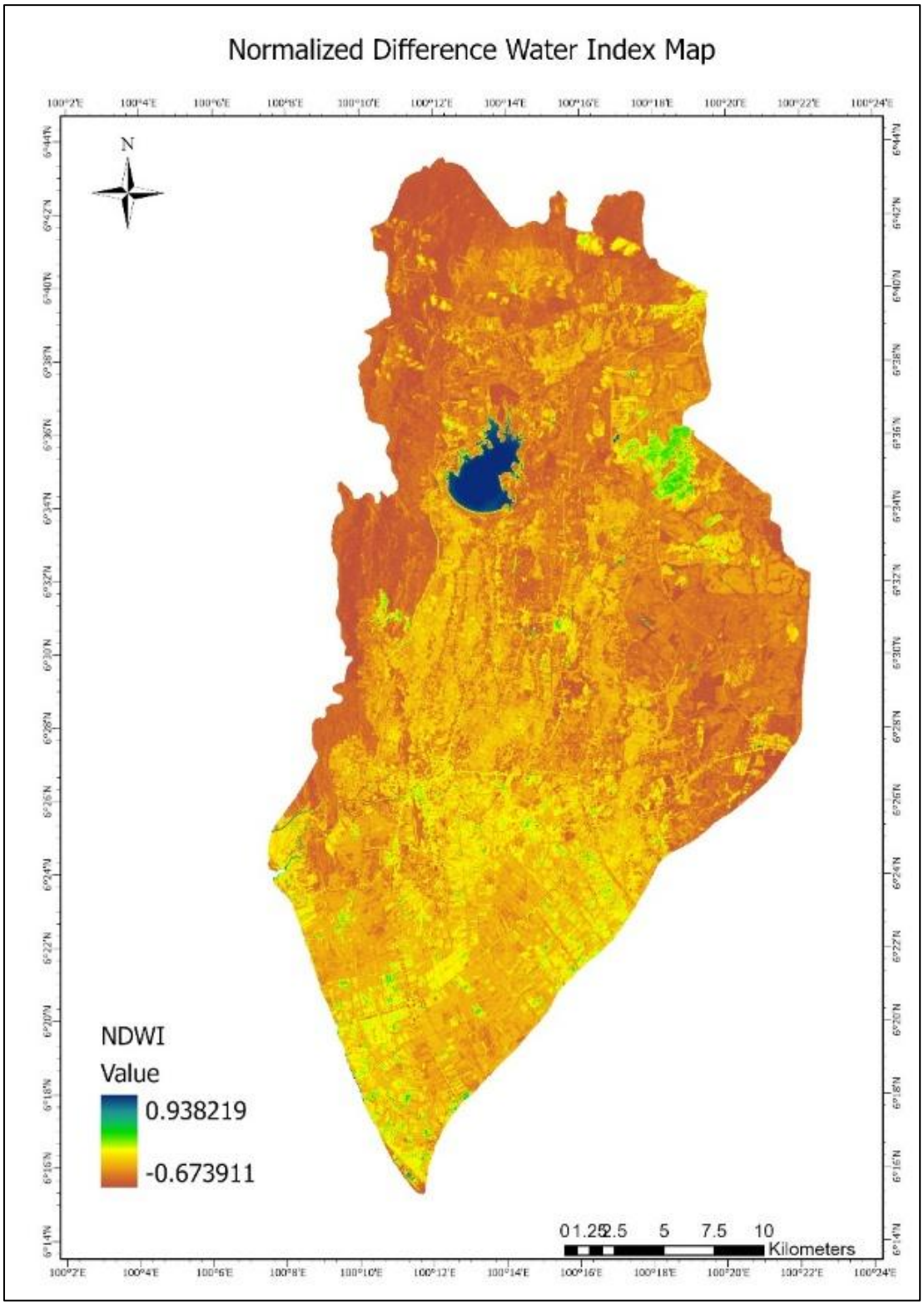

Figure 4.10 Map Of NDWI For March 2024 In Perlis

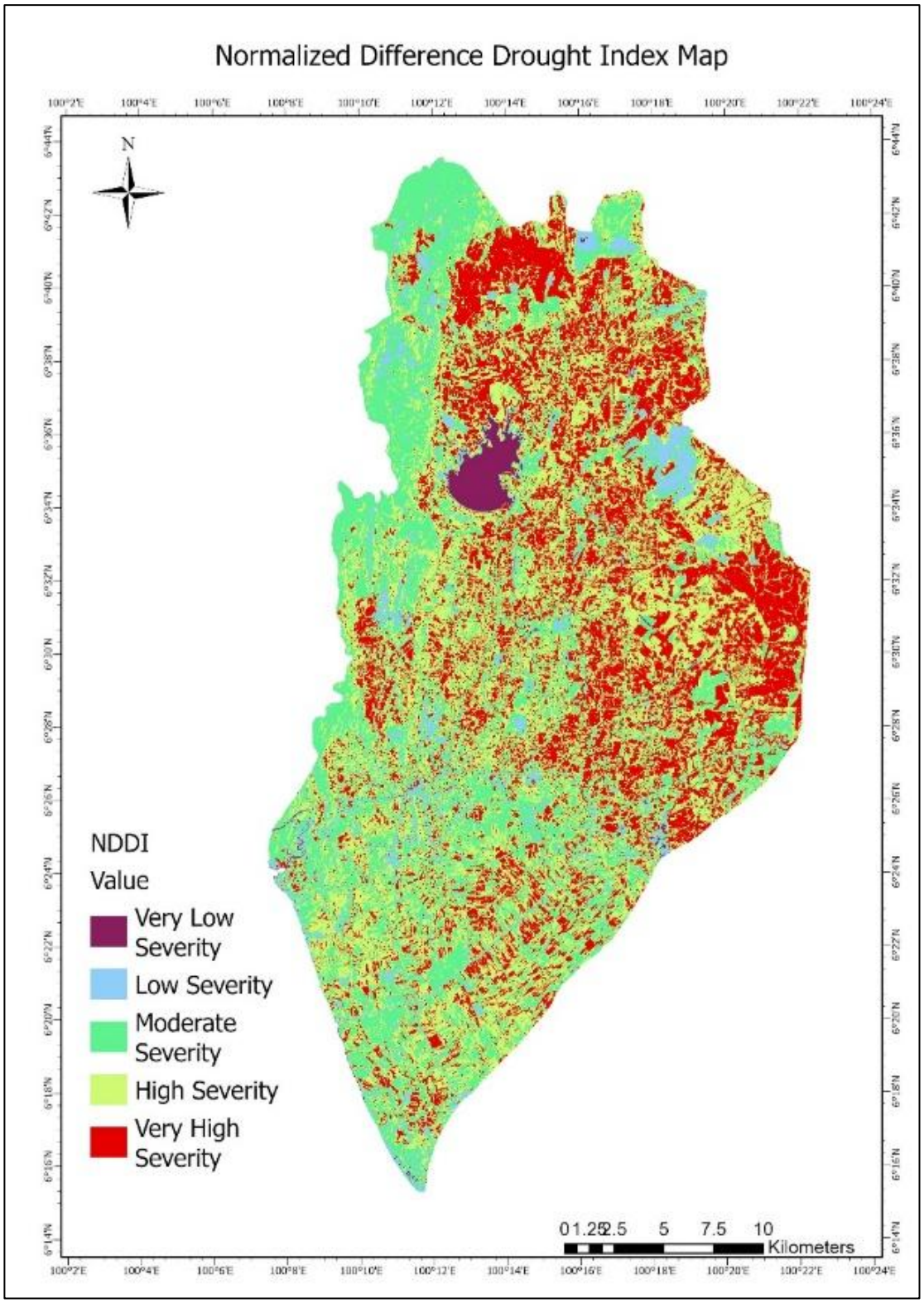

Figure 4.11 Map Of NDDI For March 2024 In Perlis



Figure 4.12 Map Of NBR For March 2024 In Perlis

4.3.2 Statistical Correlation and Validation Using MLR

The rising wildfire incidences have necessitated the development of more accurate wildfire prediction methods to prevent fire damage, which has ecological, social, and economic effects. Figures 4.13 to 4.17 demonstrate a distinct and complex relationship between LST and the selected spectral indices: NDVI, NDWI, NDMI, NBR, and NDDI. These indices each represent a distinct biophysical characteristic of the terrain. Figure 4.13 presents the relationship between NDVI and LST, and it exhibits a notably strong negative correlation with LST, with an R^2 value of 0.607. Areas exhibiting elevated NDVI values of 0.86, indicating dense and healthy vegetation, demonstrated a consistent inverse correlation with surface temperatures. This trend may be associated with vegetation's natural cooling processes, where evapotranspiration eliminates heat, while canopy cover reduces the amount of heat absorbed by the soil. Consequently, regions with green vegetation function as localized cool zones, thereby mitigating the overall intensity of heat over the landscape.

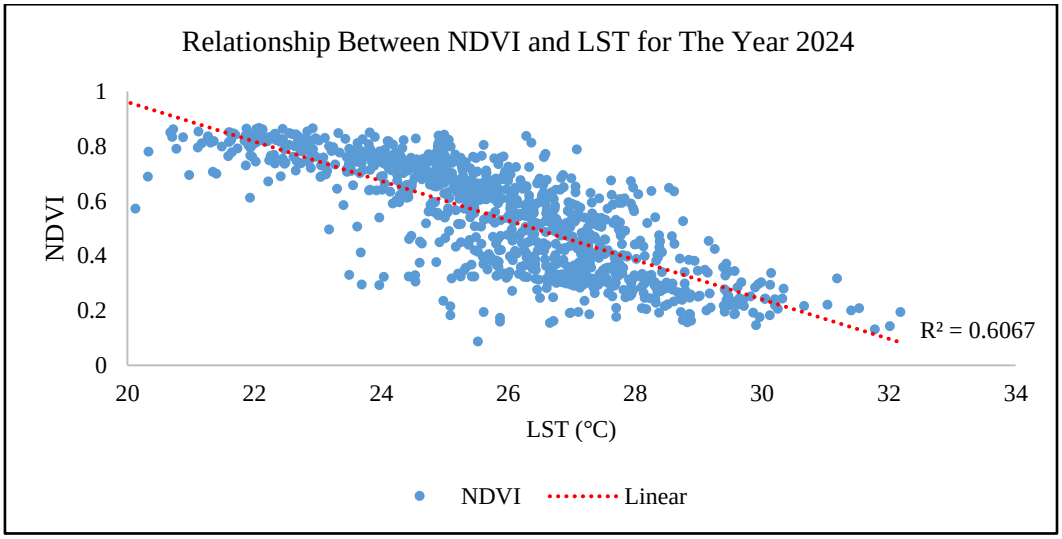

Figure 4.13 The Relationship Between NDVI And LST For The Year 2024

Figure 4.14 illustrates the relationship between NDWI and LST. It is anticipated that the relation between NDWI and LST is negative, as increased water level generally correlates with lower temperatures. The result of this study agrees with the hypothesis made, as it demonstrates a negative relationship. However, the relation is moderately strong, with an R^2 value of 0.476. This condition may be due to surfaces with high water content acting as a cooling agent, hence keeping the LST at a lower reading. Whereas surfaces with low or no water content absorb more solar radiation, leading to a higher LST reading. Meanwhile, the negative relation between NDMI and LST can be seen in

Figure 4.15. Similar to NDWI, the relation is moderately strong, with an R^2 value of 0.429. Areas with high NDMI values showed lower LST, suggesting that vegetation with higher moisture levels helps in regulating surface temperatures. Increasing NDMI values, indicative of increased surface moisture, were associated with decreasing temperatures. Moist surfaces effectively resist high thermal stress due to their slower heat absorption and more rapid cooling facilitated by evaporation.

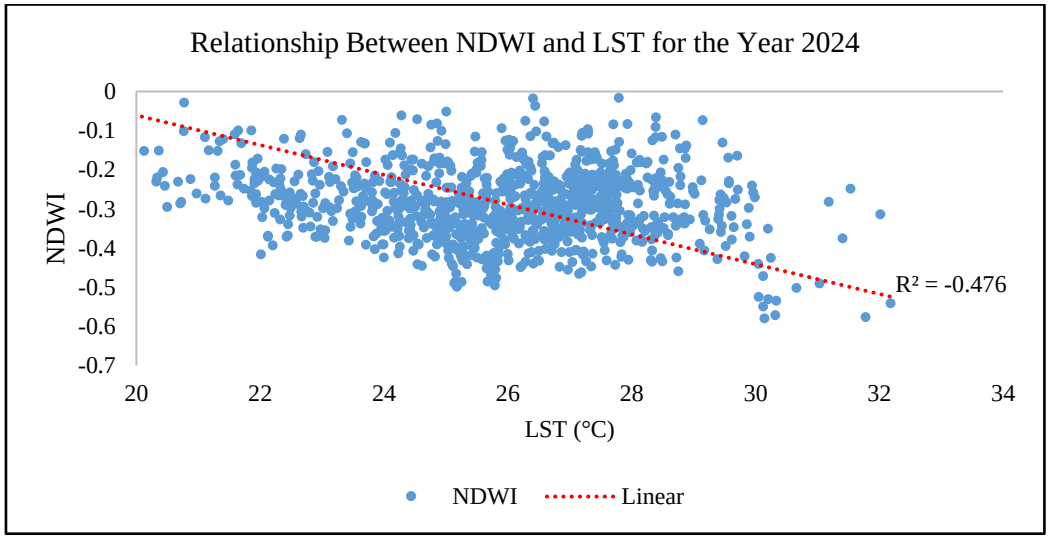

Figure 4.14 The Relationship Between NDWI And LST For The Year 2024

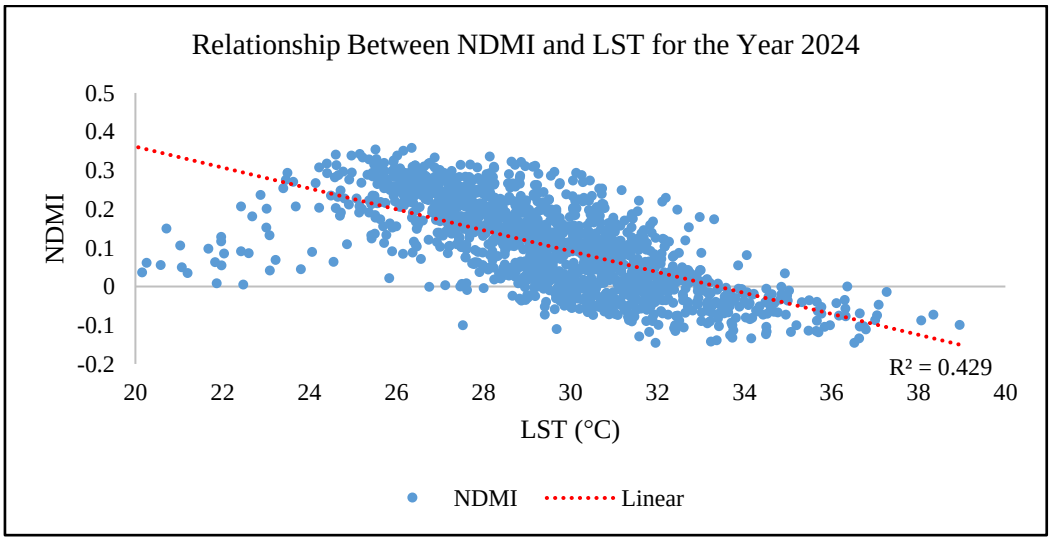

Figure 4.15 The Relationship Between NDMI And LST For The Year 2024

The NDDI exhibited a slight positive correlation with LST with an R^2 value of 0.425, as shown in Figure 4.16. Elevated NDDI levels, indicative of drought and reduced moisture in vegetation, were strongly correlated with increased surface temperatures. Dehydrated soils and vegetation lack sufficient water for evaporative cooling, resulting in increased heat absorption and preservation. This correlation indicates that areas susceptible to drought or moisture deficiency tend to exhibit

elevated temperatures, potentially resulting in thermal hotspots within the landscape. Meanwhile, the NBR, frequently employed to identify areas of vegetation that have been burned or destroyed by fire, and its relation with LST can be seen in Figure 4.17. The graph shows that NBR is negatively related to LST with an R^2 value of 0.627. Elevated NBR readings, indicative of healthy and unburned plants, paralleled reduced LST values. Conversely, areas with decreased NBR generally displayed elevated surface temperatures. This aligns with our understanding that the area affected by wildfire may exhibit higher LST compared to the area that is not burnt.

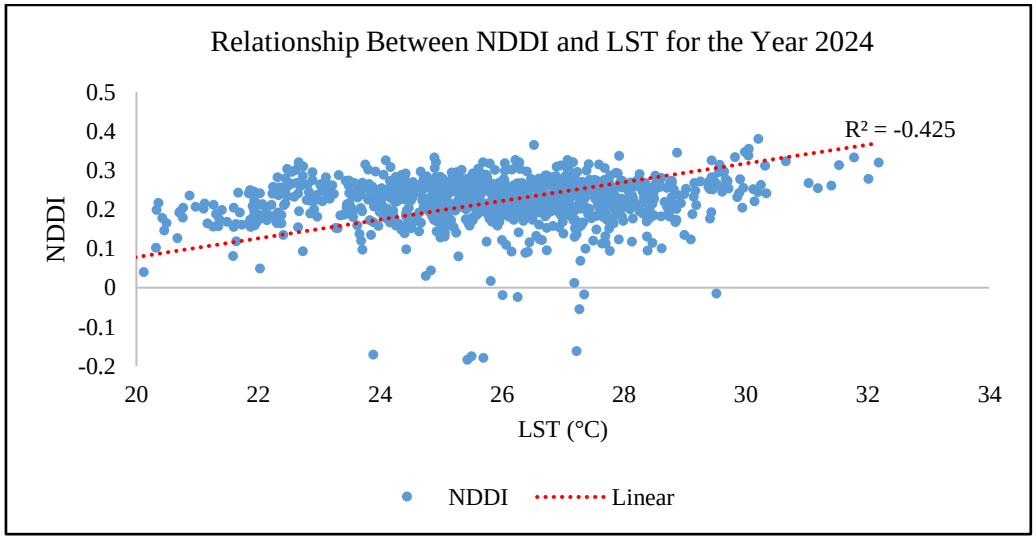

Figure 4.16 The Relationship Between NDDI And LST For The Year 2024

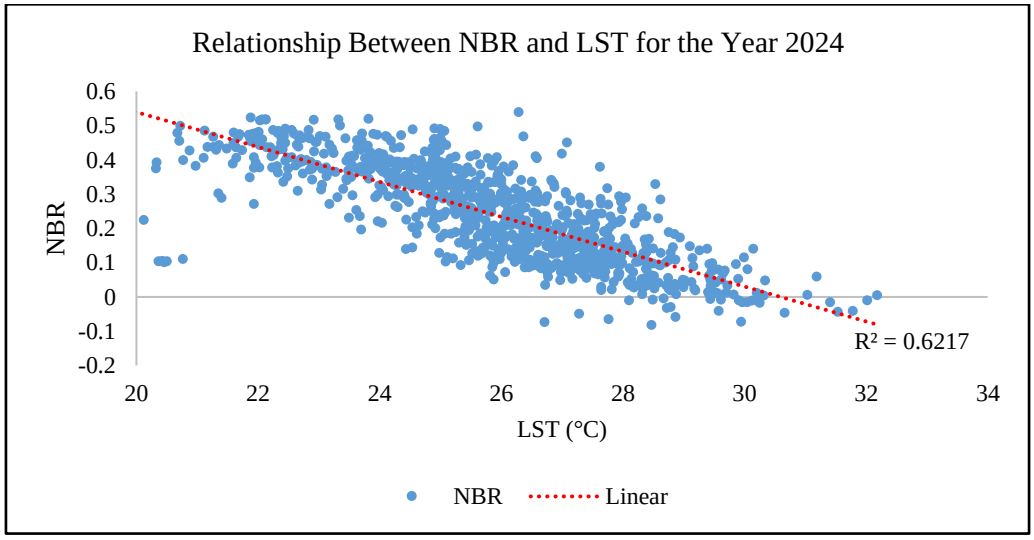

Figure 4.17 The Relationship Between NBR And LST For The Year 2024

The result obtained from the MLR analysis using the XLStat Plug-in in the MS Excel software was presented in Table 4.3. The model estimates the correlation of six indices with wildfire occurrence for the year 2024 in Perlis. From the table, it can be

seen that the model was statistically significant with a higher significance F value and explained 72% of the variance (R^2 = 0.717), suggesting that the model is suitable to be applied for Perlis state. Table 4.3 shows the correlation coefficients calculated with OLS tools in ArcMap software. The table demonstrates that the chosen indices were significant predictors of wildfire occurrence since the p-value of all indices was below 0.05, except for NDMI and NDWI with p-values of 0.054 and 0.088, respectively. The most significant predictors were NBR with the highest coefficient value of 19.113, followed by NDDI (coefficient value = 13.876).

Table 4.3
Result Of The Overall Model

Variable	R^2	Std error	p-value	significance F
FHI	0.717	1.094	0.0001	103.267

Source: (author, 2026)

Table 4.4
Result Of MLR Of Model Parameter

Indices	Coefficient	Std error	p-value	t-value	Pr > |t|
(Intercept)	-9.461	5.990	0.0001	-2.620	0.010
LST	0.366	0.196	0.096	4.074	0.0001
NDVI	4.946	10.151	0.023	0.047	0.023
NDWI	- 8.331	17.308	0.088	1.713	0.060
NDMI	-1.219	23.831	0.054	1.241	0.054
NDDI	13.876	25.626	0.004	0.482	0.033
NBR	19.113	11.135	0.002	-3.561	0.0000

Source: (author, 2026)

4.4 Assessment of Wildfire Hazard Zone in Perlis

The mapping results for objective three, which is to interpolate the potential wildfire occurrences within the state of Perlis, were presented in Figures 4.17 to 4.20. The identification of the hazard zone was divided into two categories: the hazard zone based on case density and the hazard zone based on spectral indices.

4.4.1 Identification of Wildfire Hazard Zone for Perlis State Using KDE

The spatial study of wildfire occurrences was performed with the KDE approach. The hotspot of wildfire occurrence from the year 2014 to 2024 in Perlis is demonstrated in Figure 4.17. The symbology of the cold spot was represented by a

gradient of blue colors where darker blue signifies a 99% confidence level, lighter blue indicates a 95% confidence level, and greenish blue indicates a 90% confidence level. Whereas the symbology of hotspots was illustrated by shades of red, which denote a 99% confidence level, orange indicates a 95% confidence level, and yellow indicates a 90% confidence level. The hotspot analysis indicates a significant trend in the spatial distribution and intensity of these occurrences throughout the state. The results indicate that wildfires predominantly occur in the central region, where statistically significant hotspots encompass the majority of the area. This central region exhibits the highest concentration of fire incidents, indicating a recurrent pattern of wildfires during the past decade.

The presence of multiple overlapping high-confidence hotspot zones in this region indicates a higher frequency of wildfires compared to the other parts of Perlis. This is likely due to a combination of land-use practices, vegetation types, and environmental conditions that facilitate the ignition and propagation of fires. Figure 4.17 also illustrates that a transitional zone of cold spot areas surrounds the main hotspot. This area serves as a barrier between high-temperature zones and cooler zones. Cold spots are predominantly located in the northern, eastern, and southern areas of Perlis. These areas exhibit confidence levels of 90%, 95%, and 99% in being classified as statistically low-frequency fire zones. This indicates that wildfires are not frequent despite a decade of observation. The clustering of cold spots indicates that these areas may possess distinct land characteristics, such as increased moisture, reduced human activity, or land cover types that are less susceptible to ignition.

The map that depicts the geographical distribution of wildfire incidents in Perlis from the year 2014 to 2024 is illustrated in Figure 4.18. The Figure illustrates the distribution of fire incidents in each political boundary. The color gradients employed are white for “very low density”, light blue for “low density”, pale yellow for “moderate density”, orange for “high density”, and red for “very high density”. The spatial study revealed that wildfires manifest in multiple areas of Perlis, with distinct clusters in particular administrative regions. This figure illustrates that the majority of wildfires occur in the central and southern regions of Perlis. The Kangar area exhibits the highest prevalence of fire occurrence densities categorized as “moderate to very high density”. The pattern remains uniform across each analyzed time. The Arau region displays “moderate to very low density” annually, while Padang Besar shows “moderate to very low density” from the year 2014 to 2017. However, in the following years, Padang

Besar has predominantly encountered fire occurrence densities categorized as "moderate to very high density". Since 2014, the high-density fire outbreaks have been predominantly concentrated in central Kangar. Nonetheless, alterations in fire patterns commenced in the year 2019, when the "moderate to very high density" was uniformly distributed throughout the state.

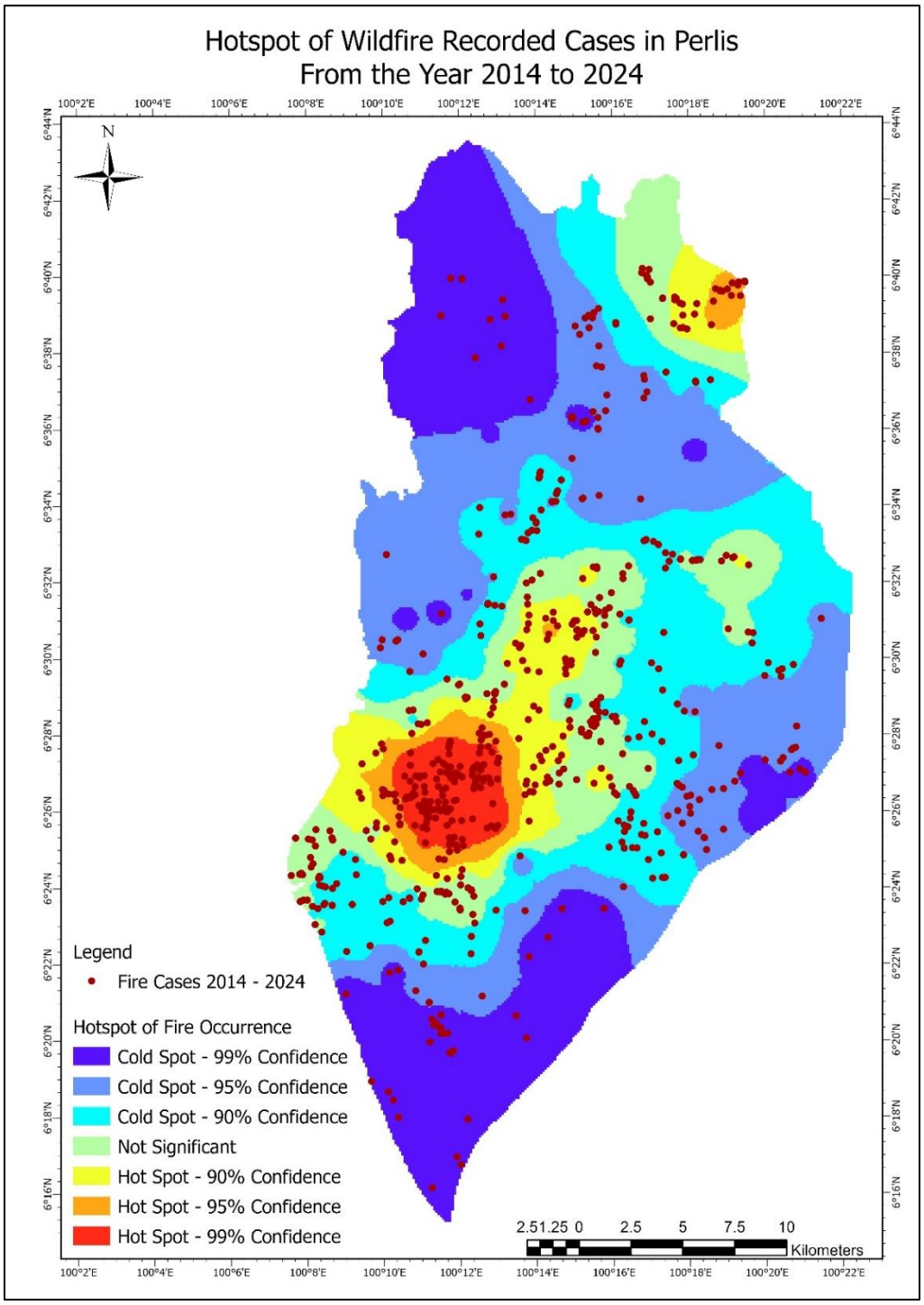

Figure 4.18 Hotspot Of Wildfire Incidents From The Year 2014 To 2024 In Perlis

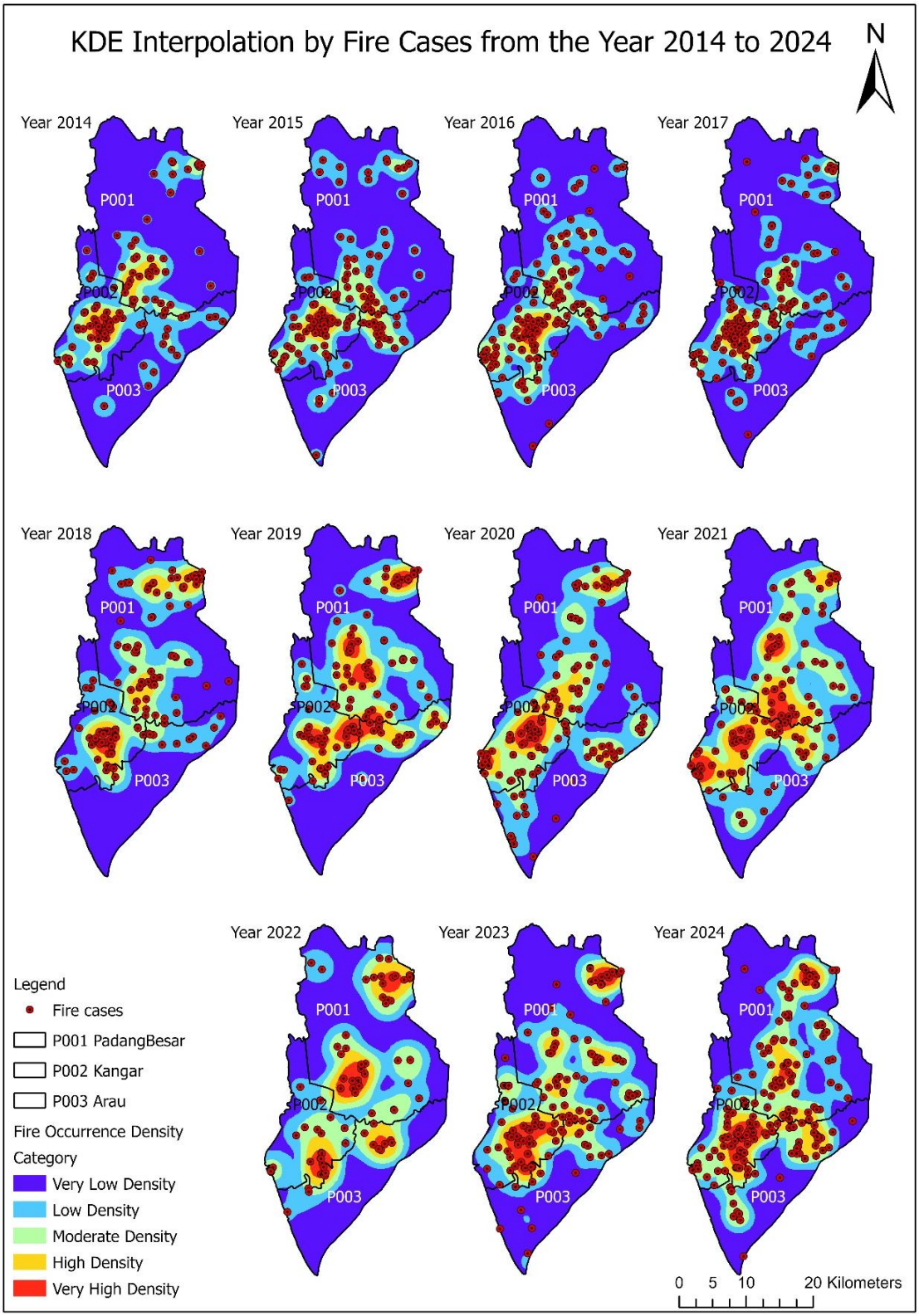

Figure 4.19 Density Of Wildfire Occurrence By Year In Perlis

4.4.2 Fire Hazard Index and Zoning Using MLR

The interpolation of the wildfire hazard zone based on the Fire Hazard Index (FHI) established using the MLR equation was illustrated in Figures 4.19 and 4.20. As mentioned before, the identification of hazard zones in Perlis was divided into two types, which are the interpolation of hazard zones based on fire locations and the interpolation of hazard zones based on the overall value of the spectral indices. The coefficients for each index used to generate the FHI were derived from the OLS tool in ArcMap software and are detailed in Table 4.3. Thus, the resultant FHI for Perlis state using the MLR equation was shown in Equation 4.1.

$$FHI = -9.460 + 0.367x_1 - 1.218x_2 + 4.946x_3 - 8.330x_4 + 13.876x_5 + 19.112x_6 \quad (4.1)$$

Source: (author, 2026)

Where x_1 is LST, x_2 is NDWI, x_3 is NDVI, x_4 is NDMI, x_5 is NDDI, and x_6 is NBR.

The generated index was applied for two conditions, which are using spectral index values at each corresponding fire location, and using spectral index values for the overall studied region. Figure 4.20 demonstrates the interpolation of the wildfire hazard zone based on fire location. The zone was classified into five categories ranging from "very low hazard" to "very high hazard". From the figure, it can be seen that the majority of the very high zone was found in the central region of the Kangar area and the northern region of Padang Besar. The critical zone is predominantly covered by built-up areas, paddy fields, and grasslands. The condition of points in the very high zones was detected as having a high LST value between 31°C and 33°C, a low NDVI value around -0.25, a low NDMI value around -0.06, and a moderate NDDI value of 0.45. Meanwhile, the majority of the very low zone was found in the reserved forest area along the Nakawan Range, reflecting a low LST value, a high NDVI value, and a high NDMI value.

Figure 4.21 illustrates the interpolation of the hazard zone based on spectral index values. The zone was classified into five categories and was presented using a dark blue to red color ramp. The dark blue indicates a "very low hazard" zone, light blue indicates a "low hazard" zone, light green denotes a "moderate hazard" zone, orange signifies a "high hazard" zone, and red signifies a "very high hazard" zone. As shown in the figure, the very high zone was mostly found in the southern area of Arau, and a few were found in the northern area of Padang Besar. The zone was mainly

covered by paddy fields and grasslands. The LST in the very high zone varied but showed a high reading, ranging from 28°C to 34°C. The NDVI, NDMI, and NDWI values were relatively low, approximately -0.35, -0.25, and -0.44, respectively. Similar to Figure 4.22, the very low zone was found at the reserved forest area along Nakawan Range.

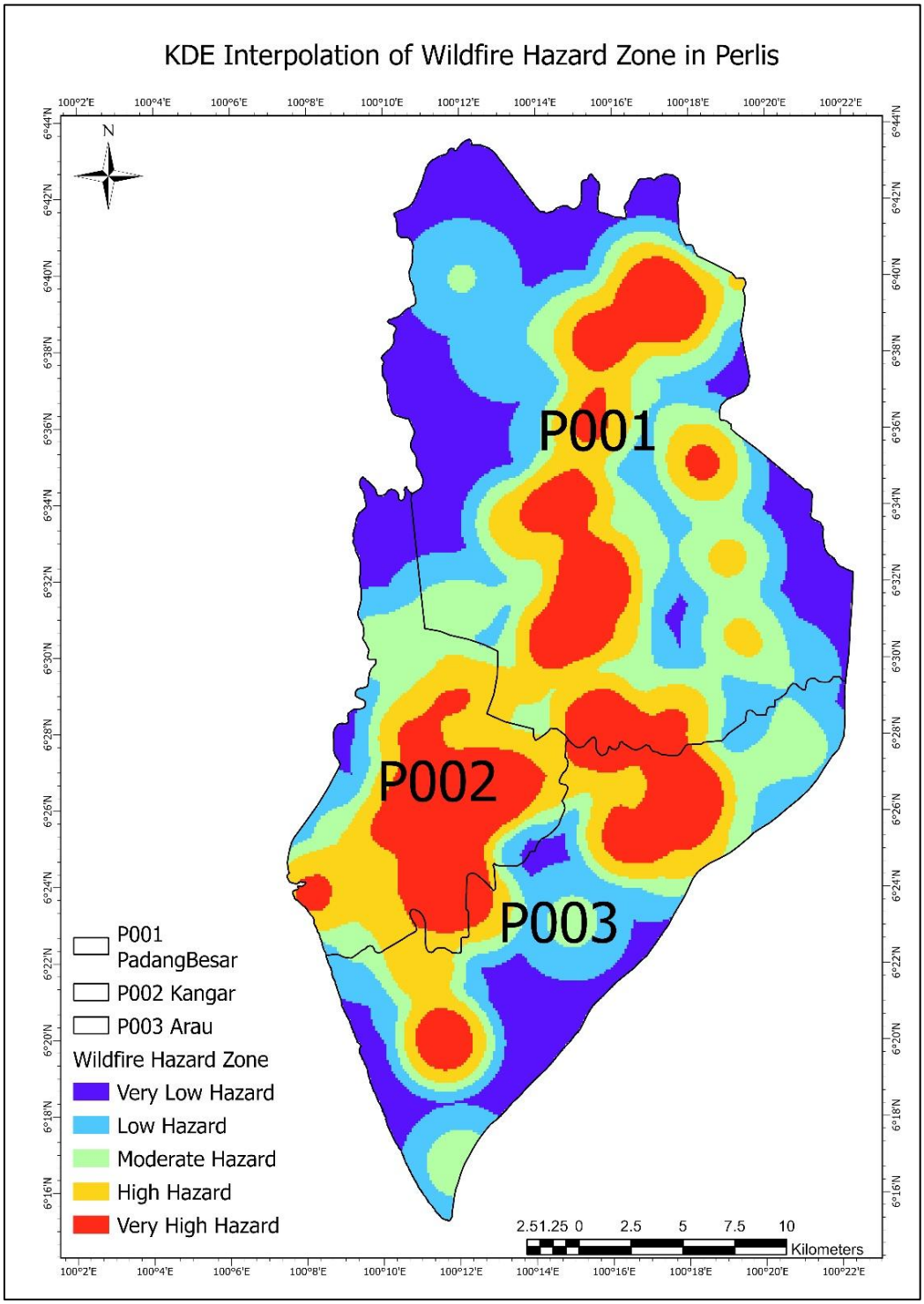

Figure 4.20 The Wildfire Hazard Zone Based On Fire Location In Perlis

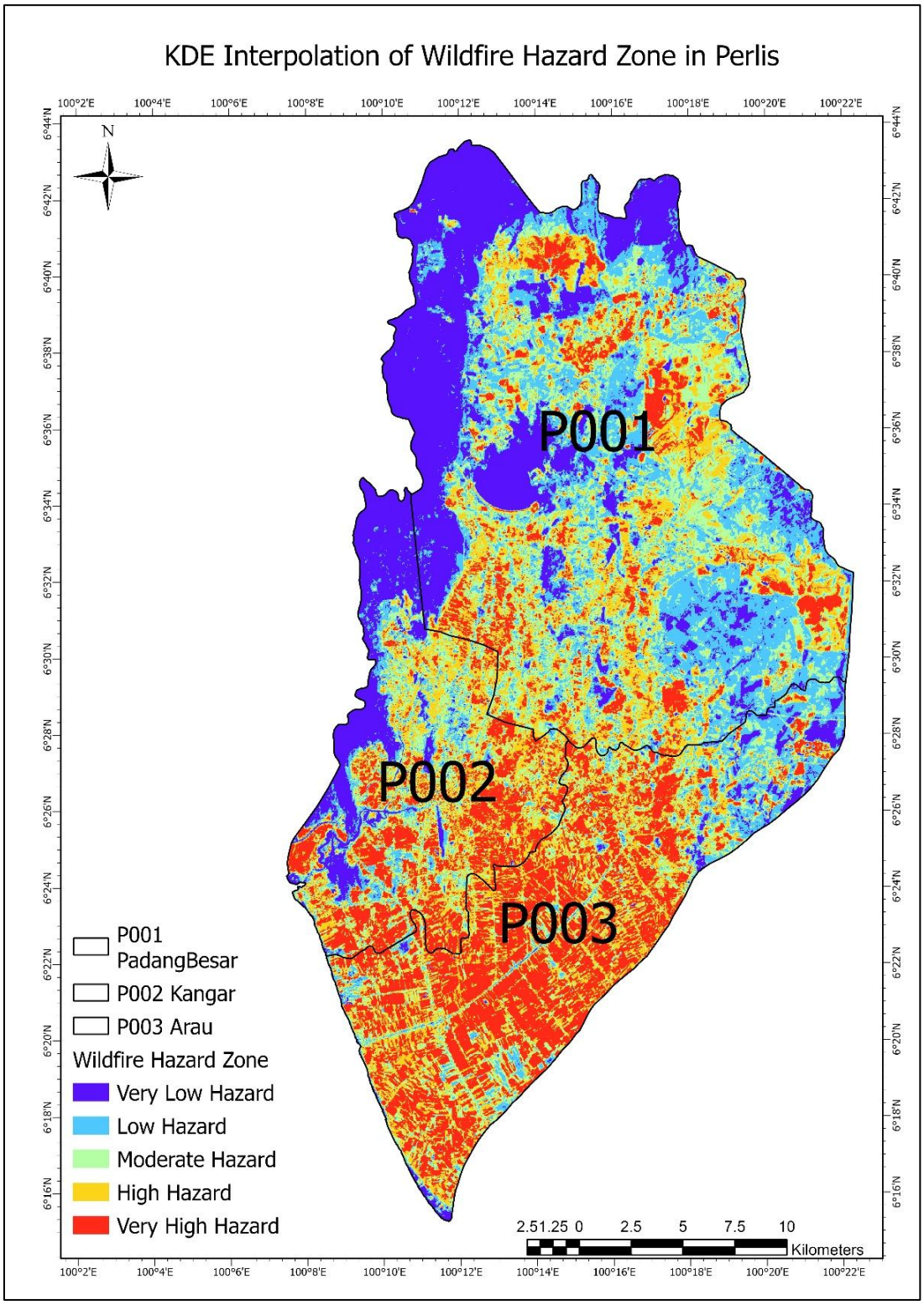

Figure 4.21 The Wildfire Hazard Zone Based On Spectral Indices Values In Perlis

4.5 Discussion

The results obtained in this study only revealed the sampling data conducted in March and do not explicitly state the impact on annual trends. The findings highlight that the increasing trend in wildfire occurrence coincides with the LST readings in March. The relationship between spectral indices and LST was examined to understand the environmental conditions that contribute to ignition. Consequently, an FHI was derived and applied to identify the hazard zone in the studied area.

4.5.1 Interpreting the Wildfire Occurrence Frequency and Variation of LST

Wildfire occurrence in Perlis shows an almost similar trend throughout the studied year, with the cases reported peaking in March and starting to decline in May, as shown in Figures 4.1 and 4.2. The findings revealed that an average of 72 cases were reported in March compared to other months in that year. The high number of cases may be related to the dry season during the southwest monsoon, which particularly took place in March. The prolonged drought and consistently high temperatures have increased the probability of wildfire occurrence in Perlis. In accordance with the present results, a previous study conducted to investigate the pattern of wildfire in Malaysia has demonstrated that a total of 518 hotspots were detected in March (Chew et al., 2022a). The findings of this study are also in agreement with a study conducted by Chew et al. (2022b), which noted that a clear pattern has been identified, indicating that the months of February, March, and April exhibit the maximum frequency of fire incidents in Pahang. Apart from Malaysia, Thailand also exhibits a similar pattern where the wildfire occurrence exhibited peak activity in March, accounting for 46%, with February at 21% and April at 20% (Talukdar et al., 2024). Similar findings have also been found in a study by Phantanaikasem et al. (2024) that highlighted the majority of wildfire activity transpired during the dry period, with March continuously identified as the period exhibiting the highest incidence over many years. The elevated number of wildfire cases in March was observed to be linked with the high LST values during the dry season.

The analysis found that the mean LST exhibited an average reading of 36°C in March for all studied years, indicating a strong correlation with wildfire occurrences, as revealed in Figures 4.4 to 4.6. The elevated surface temperatures may be associated with

prolonged droughts and increased solar radiation during the southwest monsoon and episodes of the El Niño event, which accelerate moisture loss in plants and soil. The likelihood of ignition increased when surface temperatures remained elevated for extended periods, particularly during arid seasons or droughts. Supporting this view, Kamal et al. (2019) write that the peak monthly LST was documented in March, averaging 34.5°C, from the year 2003 to 2018 in Peninsular Malaysia. Similarly, elevated LST readings were observed during the initial quarter of the year in Cameron Highlands, Pahang (Aik et al., 2020). A study by Tajudin et al. (2021) also noted that 41.47% of the Ulu Klang area had high LST values in March to April 2017, which were higher than 27°C. A consistent pattern of LST was also noticed from the year 2000 to 2022, where the LST increases at the beginning of the year and later declines towards the end of the year (Munawar et al., 2024). The results in this study are consistent with the study conducted by Muhammad et al. (2024), where the warmest months in a year are March, April, and May, with maximal temperatures ranging from 26 to 33°C. The regular warming pattern every year has influenced the occurrence of wildfires in Malaysia.

The significant increase in LST readings in March, to a certain degree, has contributed to the occurrence of wildfires. The elevated LST has increased the rate of moisture loss, leading to soil and vegetation dehydration. Dried vegetation is one of the most effective fuels for fire ignition. As noted by Vlassova et al. (2014), all categories of burn severity in the province of Cáceres, Spain, exhibit consistent mean LST values exceeding 30°C. Elevated temperatures enhanced the combustibility of vegetation during summer, since high temperatures correspond to low moisture levels (Chaparro, Piles, et al., 2016). A study by Stoyanova, Georgiev, & Neytchev (2022) also revealed that the wildfires occurring in Europe between July and September exhibited positive LST anomaly values. Likewise, Rafaqat et al. (2025) also hold the view that wildfires are positively correlated with average LST, and the year 2018 experienced the highest number of cases in Norway due to significant drought and abnormally high LST. Sensitivity analysis conducted by Bostani & Pourebrahim (2025) proved that variations in LST have a significant impact on the possibility of wildfire occurrence. However, using only LST was not sufficient to assess wildfire occurrence.

4.5.2 Describing the Correlation Between Spectral Indices and LST

Investigating the relation between LST and other spectral indices, such as NDVI, NDMI, NDWI, NDDI, and NBR, may facilitate measuring wildfire occurrence, particularly during the dry season. NDVI is a parameter used to assess vegetation health, and its relation with LST can reflect the impact of high temperatures, which can reduce vegetation health. To prove this fact, the NDVI was found to have a negative relationship with LST during March in Perlis, as illustrated in Figure 4.12. A possible explanation for this might be that the increase in LST dehydrates the vegetation faster and deteriorates vegetation health. A similar finding has been made by Sun & Kafatos (2007), where the rise in evaporation due to elevated LST leads to a decrease in the NDVI, consequently establishing a strong negative relationship between LST and NDVI. This view is also supported by Gorgani et al. (2013), where the results of correlation and regression coefficients between NDVI and LST are both negative. The analysis of emissivity and vegetation index obtained by Anbazhagan & Paramasivam (2016) for the years 1992, 2001, and 2010 revealed that an increase in LST correlates with a negative discrepancy in the NDVI value. An increase in NDVI value and decreased LST signify healthy vegetation regions, whereas decreased NDVI and increased LST suggest dehydrated vegetation regions (Ullah et al., 2023), where elevated temperatures are usually associated with diminished vegetation greenness.

In the context of wildfire occurrence, the relation between NDVI and LST was important since the indices reflect that dehydration of vegetation will heighten the probability of fire ignition. NDVI has demonstrated a negative correlation with fire severity and burned areas, while LST has a positive relationship with burned areas (Mamgain et al., 2023). According to the spatial pattern found by Li et al. (2024), wildfire occurrence is positively correlated with LST and negatively correlated with NDVI. Few regions in Italy also demonstrate a notable negative relationship between NDVI and LST, indicating that the vegetation experiences stress during the hot, dry summers, therefore rendering it more vulnerable to wildfire (Ghaderpour et al., 2025). The findings have demonstrated that the possibility of wildfire occurrence increases as the LST increases and vegetation dries. The evaporation of vegetation can be assessed using NDMI.

The relationship between NDMI and LST was essential to monitor the moisture level in vegetation as LST increases during the dry period. From Figure 4.13, it can be

seen that the NDMI is negatively related to LST. It seems possible that these results are due to high temperatures expediting the rate of moisture loss in soil and vegetation. The condition also leads to a decrease in the water level in nearby rivers and lakes, as rainfall influences the fluctuation in water level, as well as soil and vegetation moisture. Through the assessment of the moisture index and temperature conducted by Nejad & Zoratipour (2019), an inverse linear relationship was identified between NDMI and LST. According to Tan et al. (2020), the NDMI had a substantial effect and was inversely associated with the mean LST, as a rise in NDMI corresponded with a considerable decrease in the mean LST, indicating that water vapour exerted a substantial cooling influence on LST. Due to a rise in LST, the total volume of water bodies within the study area has decreased (Morshed et al., 2020). In a similar study, Taripanah & Ranjbar (2021) noted that in regions with elevated moisture levels, the LST value declined, showing the inverse relationship between LST and NDMI. A study conducted in Maharashtra, India, revealed that in August, an increase in LST results in the NDMI values declining from 0.301 to 0.019, indicating moisture stress, signifying drought or lack of water (Dapke et al., 2025). The results strengthen the hypotheses that LST imposes a significant influence on the rate of moisture loss in soil and vegetation.

Apart from that, LST also affects the NDWI values. The result in Figure 4.14 revealed that NDWI exhibits an inverse relation with LST. It can be assumed that the temperature increases to a certain degree may be able to evaporate the water bodies. In accordance with the present results, previous studies have demonstrated that water bodies exhibit positive NDWI values amid reduced LST (Bala et al., 2018). A similar finding was also reported by Guha et al. (2020), that the regression indicates an inverse spatial correlation between LST and NDWI, with the south-eastern region exhibiting increased LST and decreased NDWI. The study by Jothimani et al. (2021) found that a reduction in NDWI values signified the shrinking of water bodies due to increased LST. Likewise, Abdalkadhum et al. (2021) also noted that the correlation value between NDWI and LST is -0.93, showing a strong negative link between LST and NDWI. Lower LST values are recorded in regions with elevated NDWI values, as rivers and lakes significantly attenuate the harmful thermal radiation to the Earth's surface (Morsy & Hadi, 2022). The resultant decrease in NDWI values indicates that the areas are experiencing drought conditions.

The severity of drought in a particular region can be analysed using NDDI. The result of the relation between NDDI and LST in Figure 4.15 presents a positive

relationship. It can be deduced that the increase in LST readings has increased the severity of the drought in that area. This is because in hot weather, the soil and vegetation tend to dehydrate faster than usual, thus resulting in a high NDDI value. Supporting this view, Yang et al. (2017) write that the NDDI value exceeding 0.35 was found in the arid region where temperatures surpassed 37°C. In the linear regression model conducted by Du et al. (2018), the NDDI had a significant relationship with LST, indicated by a high R^2 value. As noted by Orimoloye et al. (2019), the results showed a generally negative relationship between NDDI and LST, with the built-up region producing the highest value, followed by the open surface. Similar points were also found by Arif & Susena (2024), that the elevated NDDI is concentrated in the southern region of the studied area, having a maximum temperature of 30.47ºC. Higher LST values often correlate with drought conditions, as elevated temperatures can contribute to increased evaporation of water and diminished soil moisture (Patel & Patel, 2024). Regions experiencing severe drought due to high temperatures are more susceptible to wildfire occurrence, which may cause severe burned areas.

The NBR was used to identify the burned areas and to assess their severity in the studied region. The result in Figure 4.16 demonstrates that the NBR was negatively related to LST. This indicates that unburned areas have a lower LST compared to burned areas. This result was supported by Fernández-Manso et al. (2020), who claim that the increased mean values of NBR and decreased levels of LST were observed due to considerable accessibility to water resulting from closeness to the river. A study by Alexander (2020) revealed that the most significant link with LST across the entire studied area is the inverse of the NBR. The Pearson correlation between LST and NBR carried out by Junaidi et al. (2021) implies a negative correlation in the relationship's direction. Additionally, Ezzaher et al. (2024) point out that the LST continued to rise, attaining its peak temperature of 50°C, while the NBR declined to -0.27, indicating a high severity level of vegetation burning related to the exceedingly elevated temperature.

4.5.3 Aligning the Fire Hazard Index in Predicting Wildfire Hazard Zones

The MLR was performed to assess the strength of each spectral index as a predictor of wildfire occurrence. From the statistics shown in Table 4.3, the most significant predictors of wildfire occurrence were LST, followed by NBR, NDVI, and

NDDI. This suggests that wildfire occurrence was most likely related to high temperatures and dehydrated vegetation. As mentioned by Oliveira et al. (2012), temperature is a good explanatory variable for fire occurrence, where most fires transpired at temperatures exceeding 20°C. A study by Darvishi et al. (2020) revealed that the multiple regression analysis used to ascertain the parameters influencing fire showed 63% confidence, with precipitation and monthly temperature as the most significant predictors. In a study by Manavalan et al. (2022), the OLS regression that has several independent variables was utilized, and the results revealed that the changes in LST have caused significant changes in NDVI and NDWI values.

The regression coefficients of the spectral indices are shown in Table 4.3, and the NBR and NDDI are the most significant influencing factors according to the coefficients' values. On the other hand, the model's least significant component was the LST. This result implies that during the extended hot and dry season, LST has reached its maximum threshold. It can be inferred that the vegetation was severely dehydrated, considering the satellite imagery used in this study was taken in March, which is the climax of the hot and dry season. Although LST is a major influence on fuel dehydration, other parameters, such as NDDI and NBR, are of greater significance in determining the fire risk in extremely dry areas. These results are consistent with a study conducted by Liu & Zhang (2015), which was carried out over the prolonged dry season, showing that the wind speed is the most important element, with a coefficient value of 12.21, while the highest temperature has the lowest coefficient value, at 0.064. According to a study conducted by Ntinopoulos et al. (2022), the Standardized Precipitation Index (SPI), which was used to study drought in a semi-arid region, has a higher coefficient value of 0.71, compared to temperature, with a value of 0.03. Additionally, Nguyen & Tong (2023) also showed that NDDI has the greatest weighting value of 0.30, whereas LST has 0.15 in their forest fire risk prediction map (FFRPM) equation. This FHI can be used to determine the index scale of the incident after a fire occurs because the NBR is the most significant variable, as mentioned by Anucharan et al. (2025), and the NBR has a high accuracy of 90.6% in detecting burned regions.

Meanwhile, the NDWI and NDMI have been identified as insignificant influencing factors in the model. This is because NDWI and NDMI are closely related to NDVI, resulting in redundancy that reduces the indices' statistical importance in model derivation. Indices such as NDDI, NBR, and NDVI already act as strong proxies for the fire hazard model, since a decrease in vegetation moisture often correlates with

a loss of vegetation greenness, which is reflected by NDVI value, and an increase in thermal stress is reflected by NDDI and LST. The model has extracted the moisture variance from NDVI and NDDI, rendering the coefficients for NDWI and NDMI statistically insignificant. These statements were aligned with Nejad & Zoratipour (2019), who stated that NDMI is found to be insignificant when integrated with dominant environmental predictors like LST and NDVI. Not only that, but Mohamed (2022) also notes that feature selection algorithms remove NDMI to prevent variance multicollinearity in the Weighted Least Squares Regression. Additionally, the formulation of NDWI is mathematically optimized to delineate open surface water bodies rather than terrestrial leaf moisture, making it useless for fire hazard estimation (Moisa et al., 2023). Thus, NDWI and NDMI are not significant influencing factors in the FHI model because of the existence of dominant indices such as LST, NDVI, NDDI, and NBR.

The coefficient values of multispectral indices used in the FHI for Perlis state may differ from other states because the statistical relationship between spectral indices and fire occurrences is highly dependent on local environmental conditions. Perlis is characterized by a relatively dry climate, distinct seasonal patterns, and massive agricultural and vegetation landscapes, which differ from those found in more humid and densely forested states such as Pahang, Johor, and Sabah. As a result, indices related to vegetation health, moisture content, and surface temperature, such as NDVI, NDMI, and LST, may contribute differently to fire hazard prediction, leading to variation in the regression coefficients. In addition, differences in topography, land-use practices, fuel characteristics, meteorological conditions, and historical fire patterns can alter the sensitivity of each index to wildfire occurrence. Consequently, the FHI require local calibration to accurately reflect the environmental conditions of the implemented states. This is consistent with a study by Zahran et al. (2020) that mentioned the predictive performance of spectral indices in fire occurrence modelling varies according to vegetation structure, climatic conditions, and landscape characteristics of the studied area.

The number of incidents recorded from the years 2014 to 2024 was found to be in accordance with the interpolated hazard zone map in Figure 4.19. The findings indicate that a few locations in the Padang Besar area, specifically at Titi Tinggi, Bukit Chabang Mari, and Chuping, have approximately 110, 20, and 160 cases, respectively. This figure also highlighted that the Kangar area has a larger “Very High Hazard” zone

at the main town, roughly 410 cases, and a smaller one at Kuala Perlis, around 40 cases. Meanwhile, in the Arau area, the “Very High Hazard” zone extends from the main town up to Mata Ayer, approximately 160 accumulated cases. Even though most of the cases took place near the main town, which was primarily made up of developed areas, there also existed secondary forests and bushes that were vulnerable to ignition, especially during the hot and dry weather. The secondary forest and shrubs close to residential areas were the exact locations of the reported wildfire occurrences, according to documentation obtained from the Perlis state Fire and Rescue Department. Figure 4.22 demonstrates the ground truth data of the fire occurrence at Chuping, approximately 6°32'15.27"N and 100°17'34.29"E, match with the hazard zone map. The fire that occurred in January 2026 signifies the beginning of the hot and dry season in Perlis. This research suggests that the occurrence of fire in these locations may have been due to the increased heat from the built-up elements and additional heat emitted from vehicles. Owing to the increase in carbon emissions, it is commonly accepted that densely populated places and built-up areas contribute to the rise of LST in the area. This is in line with the findings of Zahran et al. (2020), which indicate that areas with high population densities are more likely to experience fire occurrence. A study conducted by Moisa et al. (2023) also confirmed that the LST value increased significantly in developed areas, indicating that the release of carbon stock has contributed to temperature rises in the study area.



Figure 4.22 Post-Fire Image Taken On 28th January 2026 At Chuping, Perlis

In contrast, the “Very Low Hazard” zone was primarily located in the Nakawan Range's forested regions. This result may be explained by the high density of canopies and their high capacity to store water in forested areas, which slows down the rate of evaporation and reduces the LST reading. The dense canopy of a forest reflects and absorbs a significant amount of incoming solar radiation before reaching the ground, preventing the ground from being excessively heated. The conditions in a dense forest

are typically more humid, wind speeds are reduced due to the friction of the trees, and organic materials, such as decaying leaves and twigs, remain cooler and more humid than they would in an open environment. The high moisture content substantially hinders the ignition of a fire by a spark. The findings are consistent with the study conducted by Gupta & Shukla (2022), which found that the LST in forested areas is much lower compared to the average LST during the hot months. Similar findings were also reported by Rendana et al. (2023), where the low fire risk rating was found in the medium- to high-density forests. According to a study by Nguyen & Tong (2023), it is also confirmed that the mountains and forests constitute the majority of the area with the lowest fire danger. The local government might use these findings to create wildfire mitigation measures, particularly in hot and dry conditions.

CHAPTER 5
CONCLUSION

5.1 Introduction

The last chapter will summarize and conclude the presented aim, methodology, and results of this study. As explained in Chapter 1, this research aimed to estimate the wildfire hazard zone through geospatial analysis for Perlis state, and analyse the temporal pattern of LST and wildfire occurrences, particularly in fire-prone areas. This chapter will also include a few recommendations to be improved for future study. To achieve this goal, this study established three objectives, which are to examine the changing trend of LST and wildfire occurrence from the year 2014 to the year 2024, to determine the correlation between NDVI, NDWI, NDMI, NDDI, NBR, and LST for the year 2024, and to interpolate the potential wildfire occurrences within the state of Perlis using Kernel Density analysis. The main conclusions are outlined in this chapter, along with possible future study directions.

5.2 Conclusion

The detailed assessment of wildfire hazard zones by geospatial analysis confirms that wildfire risk is a dynamic phenomenon shaped by the interaction of multiple weather conditions and vegetation health. By defining the spatiotemporal pattern of wildfire occurrence and calculating LST from the years 2014 to 2024, the first objective was accomplished. The statistical data obtained from the Perlis state Fire and Rescue Department and Landsat 8 OLI/TIRS images downloaded from the USGS Earth Explorer website were utilized and pre-processed accordingly. The process begins with plotting the wildfire points and overlaid to the Perlis state political boundary to evaluate the spatial distribution of the incidents, and the Mann-Kendall test is employed to identify trends in the frequency of wildfires over time. Then, the LST was determined by applying the six-step processing, which includes the conversion of digital numbers into radiance, the determination of brightness temperature using top-of-atmosphere radiance, the determination of NDVI, the determination of proportional vegetation using NDVI, the determination of land surface emissivity using proportional vegetation,

and the determination of LST using brightness temperature and emissivity. The findings indicate that the Mann-Kendall test shows an increasing trend in wildfire occurrence from the years 2014 to 2024. Even though the annual trend fluctuated, the number of cases kept increasing, peaking in March every studied year. Meanwhile, the variation of LST demonstrates a high reading, with an average of 36°C, during the hot and dry weather in March. This evidence emphasizes that wildfire occurrence is strongly related to elevated LST and prolonged drought, which accelerates the dehydration rate of vegetation. This study also highlights that the majority of the wildfires occurred near built-up areas, in paddy fields, and grasslands with low canopy density. Although LST is an important parameter in assessing wildfire occurrence in a region, this study highlights that LST alone was not sufficient to predict wildfire susceptibility during the dry season.

The second objective was achieved through the determination of the selected spectral indices and the investigation of correlational analysis using the MLR method. In this study, there were six spectral indices used, which are LST, NDVI, NDMI, NDWI, NDDI, and NBR. The selected spectral indices were calculated using mathematical equations that utilize specific raw spectral reflectance bands, such as NIR and SWIR. These indices are produced at the pixel level, resulting in a continuous raster map where each cell represents a specific value. Subsequently, linear regression is employed to determine the strength and direction of the relationship between the spectral indices and LST. Pixel values from the LST map and the spectral indices are taken at random sampling points to create a matched dataset. The trend is then displayed in a scatter plot, and the coefficients of determination (R^2) are computed. The relation among these spectral indices captures the fundamental relationship between temperature, biomass density, and vegetation stress. The results of the correlation analysis revealed that the selected spectral indices were appropriate to map the wildfire hazard zone for Perlis state, with 70% overall suitability. The analysis further establishes that the LST is positively related to NDDI and negatively related to NDVI, NDWI, NDMI, and NBR. The relation indicates that as the LST increases, the dryness increases, vegetation condition deteriorates, moisture level decreases, and burning is more severe. The statistical correlation between spectral indices and LST shows that NBR is significantly related to LST, with an R^2 value of 0.621, while the other indices were moderately related to LST. This condition suggests that high temperatures intensify the burning, especially during the dry season.

This study has also successfully achieved the third objective by generating the FHI using multispectral indices and identifying the high-hazard zones for Perlis state. The wildfire cases from the years 2014 to 2024 were combined, and a density map was developed using the KDE method. This method accumulates the wildfire points in the form of continuous density. The KDE map visualizes wildfire concentrations, representing areas with a high probability of historical event recurrence. A multiple linear regression technique is employed to integrate multispectral indices into the FHI, illustrating the impact of each indicator on the hazard. The generated FHI model can identify high-hazard zones where vegetation was dehydrated and highly flammable by employing NDVI to assess vegetation condition, NDMI to assess canopy water content, and NDDI to evaluate dryness. The coefficient values of the model demonstrate that the most significant factors are NDDI and NBR with coefficient values of 13.876 and 19.112, respectively. Meanwhile, NDMI and NDWI are not significant in the model due to multicollinearity with other vegetation and thermal indices. This is because the model has extracted the moisture variance from NDVI and NDDI, rendering the coefficients for NDWI and NDMI statistically insignificant. The final hazard zone map is generated by applying the FHI to the studied area. The total values are categorized into groups ranging from “Very Low Hazard” to “Very High Hazard”, using data clustering techniques such as Natural Breaks (Jenks). The results demonstrate that the majority of the area in Perlis is highly susceptible during the hot and dry weather. The most concerning areas were identified in the principal town of Kangar, which recorded a total of 410 historical cases across the studied years, followed by Chuping with 160 cases. Meanwhile, the interpolation of the hazard zone based on the spectral index values illustrates that the most concerning type of land cover was paddy fields. Though there were limited cases reported involving wildfires at paddy fields, the high index value indicates that the areas were highly probable to ignite if precautionary actions were not taken. Therefore, it is recommended that the regional Fire and Rescue Department supervise the “Very High Hazard” zone, especially at Titi Tinggi, Chuping, and Padang Besar during the hot and dry weather to avoid devastating incidents.

This study provides valuable insight into wildfire occurrence, climatological conditions, and vegetation indices. The maps illustrating places with considerable fuel loads and very high LST assist firefighters in taking a proactive rather than reactive approach. The primary advantage of the hazard zone mapping is its capacity to assist in land use planning, such as limiting the construction of new residences in high-risk

zones, and also facilitating funding for initiatives that promote mitigation actions. Furthermore, it also helps communities become more cautious by determining exactly where the fire restriction zones are that must be properly obeyed in order to avoid massive property losses. The identification of the wildfire hazard zone enables various agencies to plan mitigation actions accordingly before the outbreak of wildfires. The Fire and Rescue Department may utilize the maps to delineate precise evacuation routes, establish staging areas for equipment, and facilitate water resources allocation during active wildfire control efforts. Besides, the State Forestry Department can refer to the hazard zones to minimize human activities in forested regions and monitor forest health to prevent minor wildfires from escalating into significant crown wildfires. The Town and Country Department may incorporate risk data into zoning reports to ensure that new infrastructure, such as power lines and hospitals, is constructed in safer locations.

5.3 Recommendations for Future Works

Upon the FHI model established in this study, future studies should aim to incorporate other variables, such as topographical factors and human factors, in projecting the probability of wildfire occurrence. The use of only spectral indices limits the understanding of fire occurrence caused by human factors and the propagation rate of the fire. Since this study revealed that most of the cases occurred in the developed areas, it is also recommended to incorporate social factors, human-induced wildfire, and the Normalized Difference Built-up Index (NDBI) to assess the social interference in wildfire occurrence and the intensity of urbanisation. Future studies may evaluate the effect of the Urban Heat Island (UHI) to ascertain the impact of built-up features on the increased temperature in developed areas. Additionally, future studies should explore the use of other models, such as Random Forest (RF) and Support Vector Machines (SVM), to determine the optimal weights of each spectral index. Future research should also be focused on improving the precision and predictive capacity of hazard models by integrating high-resolution satellite data with real-time monitoring technology. This study primarily depends on moderate-resolution sensors, which are Landsat 8 OLI/TIRS images. Future studies may utilize hyperspectral imagery and LiDAR data to more precisely identify vertical fuel structures and specific vegetation moisture levels, which are crucial for understanding fire dynamics.

REFERENCES

Abatzoglou, J. T., Balch, J. K., Bradley, B. A., & Kolden, C. A. (2018). Human-related ignitions concurrent with high winds promote large wildfires across the USA. *International Journal of Wildland Fire*, *27*(6), 377–386. https://doi.org/10.1071/WF17149

Abdalkadhum, A. J., Salih, M. M., & Jasim, O. Z. (2021). The Correlation Among Land Cover Spectral Indices and Surface Temperature Using Remote Sensing Techniques. *IOP Conference Series: Materials Science and Engineering*, *1090*(1), 012024. https://doi.org/10.1088/1757-899x/1090/1/012024

Abdo, H. G., Almohamad, H., Al-Dughairi, A. A., & Al-Mutiry, M. (2022). GIS-Based Frequency Ratio and Analytic Hierarchy Process for Forest Fire Susceptibility Mapping in the Western Region of Syria. *Sustainability (Switzerland)*, *14*(8). https://doi.org/10.3390/su14084668

Abdollahi, M., Islam, T., Gupta, A., & Hassan, Q. K. (2018). An advanced forest fire danger forecasting system: Integration of remote sensing and historical sources of ignition data. *Remote Sensing*, *10*(6). https://doi.org/10.3390/rs10060923

Adamek, M., Jankovska, Z., Hadincova, V., Kula, E., & Wild, J. (2018). Drivers of forest fire occurrence in the cultural landscape of Central Europe Drivers of forest fire occurrence in the cultural landscape of Central Europe. *Landscape Ecology*, *November*. https://doi.org/10.1007/s10980-018-0712-2

Adrianto, H. A., Spracklen, D. V., Arnold, S. R., Sitanggang, I. S., & Syaufina, L. (2020). Forest and land fires are mainly associated with deforestation in Riau Province, Indonesia. *Remote Sensing*, *12*(1), 1–12. https://doi.org/10.3390/RS12010003

Afghah, F., Razi, A., Chakareski, J., & Ashdown, J. (2019). Wildfire Monitoring in Remote Areas using Autonomous Unmanned Aerial Vehicles. *INFOCOM 2019 - IEEE Conference on Computer Communications Workshops, INFOCOM WKSHPS 2019*, *88*, 835–840. https://doi.org/10.1109/INFCOMW.2019.8845309

Aik, J., Ismail, M. H., & Muharam, F. M. (2020). Land Use / Land Cover Changes and the Relationship. *Land*, *9*(372), 1–23.

Alauddin, M. W., Anshori, M., Wicaksono, A. S., & Utaminingrum, F. (2018). Comparative Study based on Error Calculation in Multiple Linear Regression Coefficient for Forest Fires Prediction. *3rd International Conference on*

Sustainable Information Engineering and Technology, SIET 2018 - Proceedings, 115–120. https://doi.org/10.1109/SIET.2018.8693226

Aldiansyah, S., & Madani, I. (2024). Spatial model of wildfire susceptibility using Machine Learning approaches on Rawa Aopa Watumohai National Park, Indonesia. *GeoScape*, *18*(1), 1–20. https://doi.org/10.2478/geosc-2024-0001

Alexander, C. (2020). Normalised difference spectral indices and urban land cover as indicators of land surface temperature (LST). *International Journal of Applied Earth Observation and Geoinformation*, *86*(November 2019).

Alkhatib, A. A. A. (2014). A review on forest fire detection techniques. *International Journal of Distributed Sensor Networks*, *2014*. https://doi.org/10.1155/2014/597368

Allison, R. S., Johnston, J. M., Craig, G., & Jennings, S. (2016). Airborne optical and thermal remote sensing for wildfire detection and monitoring. *Sensors (Switzerland)*, *16*(8). https://doi.org/10.3390/s16081310

Amos, C., Petropoulos, G. P., & Ferentinos, K. P. (2019). Determining the use of Sentinel-2A MSI for wildfire burning & severity detection. *International Journal of Remote Sensing*, *40*(3), 905–930. https://doi.org/10.1080/01431161.2018.1519284

Anbazhagan, S., & Paramasivam, C. R. (2016). Statistical Correlation between Land Surface Temperature (LST) and Vegetation Index (NDVI) using Multi-Temporal Landsat TM Data. *International Journal of Advanced Earth Science and Engineering*, *5*(1), 333–346. https://doi.org/10.23953/cloud.ijaese.204

Anucharan, T., Sroprom, T., Chaikaew, N., & Iamchuen, N. (2025). Assessing Burn Severity and Vegetation Impact Using Sentinel-2 Satellite Imagery and Geospatial Analysis in Mae Ka Subdistrict, Mueang District, Phayao, Thailand. *International Journal of Geoinformatics*, *21*(4), 51–70.

Arif, N., & Susena, Y. (2024). Soil moisture mapping for drought monitoring in urban areas. *IOP Conference Series: Earth and Environmental Science*, *1314*(1). https://doi.org/10.1088/1755-1315/1314/1/012087

Ariffin, M., & Wan Yaacob, Wan Nor Amalina. (2017). Assessment of Knowledge, Attitude and Practice of Solid Waste Open Burning in Terengganu, Malaysia. *EnvironmentAsia*, *2*(1), 25–32.

Arisanty, D., Muhaimin, M., Rosadi, D., Saputra, A. N., Hastuti, K. P., & Rajiani, I. (2021). Spatiotemporal Patterns of Burned Areas Based on the Geographic

Information System for Fire Risk Monitoring. *International Journal of Forestry Research*, *2021*, 11–14. https://doi.org/10.1155/2021/2784474

Arndt, N., Vacik, H., Koch, V., Arpaci, A., & Gossow, H. (2013). Modeling human-caused forest fire ignition for assessing forest fire danger in Austria. *IForest*, *6*(6), 315–325. https://doi.org/10.3832/ifor0936-006

Artikanur, S., Widiatmaka, Setiawan, Y., & Marimin. (2022). Normalized Difference Drought Index (NDDI) computation for mapping drought severity in Bojonegoro Regency, East Java, Indonesia Normalized Difference Drought Index (NDDI) computation for mapping drought severity in Bojonegoro Regency, East Java, Indones. *Earth and Environmental Science*. https://doi.org/10.1088/1755-1315/1109/1/012027

Asha'ari, Z. H., & Badrunsham, A. S. (2014). Spatial Temporal Analysis of Forest Fire in Malaysia Using ATSR Satellite Measurement. *Bulletin of Environmental Science and Sustainable Management (e-ISSN 2716-5353)*, *2*(1), 8–11. https://doi.org/10.54987/bessm.v2i1.110

Babu, K. V. S., & Roy, A. (2019). Automation of Forest Fire Danger Index from the Near Real-Time Satellite Datasets. *Journal of Environmental Informatics Letters*, *2*(1), 1–9. https://doi.org/10.3808/jeil.201900015

Bala, R., Prasad, R., Yadav, V. P., & Sharma, J. (2018). A comparative study of land surface temperature with different indices on heterogeneous land cover using Landsat 8 data. *International Archives of the Photogrammetry, Remote Sensing and Spatial Information Sciences - ISPRS Archives*, *42*(5), 389–394. https://doi.org/10.5194/isprs-archives-XLII-5-389-2018

Bandara, S., Navaratnam, S., & Rajeev, P. (2023). Bushfire Management Strategies: Current Practice, Technological Advancement and Challenges. *Fire*, *6*(11). https://doi.org/10.3390/fire6110421

Bankert, R. L., Solbrig, J. E., Lee, T. F., & Miller Cira, S. D. (2011). Automated lightning flash detection in nighttime visible satellite data. *Weather and Forecasting*, *26*(3), 399–408. https://doi.org/10.1175/WAF-D-10-05002.1

Bao, S., Xiao, N., Lai, Z., Zhang, H., & Kim, C. (2015). Optimizing watchtower locations for forest fire monitoring using location models. *Fire Safety Journal*, *71*(December 2013), 100–109. https://doi.org/10.1016/j.firesaf.2014.11.016

Barbero, R., Curt, T., Ganteaume, A., Maillé, E., Jappiot, M., & Bellet, A. (2019). Simulating the effects of weather and climate on large wildfires in France. *Natural*

Hazards and Earth System Sciences, *19*(2), 441–454. https://doi.org/10.5194/nhess-19-441-2019

Barmpoutis, P., Papaioannou, P., Dimitropoulos, K., & Grammalidis, N. (2020). A review on early forest fire detection systems using optical remote sensing. *Sensors (Switzerland)*, *20*(22), 1–26. https://doi.org/10.3390/s20226442

Baykal, T. M. (2025). Performance assessment of GIS-based spatial clustering methods in forest fire data. In *Natural Hazards* (Vol. 121, Issue 7). Springer Netherlands. https://doi.org/10.1007/s11069-025-07135-0

Bhattacharya, O., Sinha, S., Mishra, V. N., Kumari, M., Falah, F., Hasher, B., Barman, J., & Zhran, M. (2025). Results in Engineering Harnessing geospatial tools to map the forest fire : Risk zonation in Pauri. *Results in Engineering*, *25*(November 2024), 103694. https://doi.org/10.1016/j.rineng.2024.103694

Bitek, D., Sanli, fusun balik, & Erenoglu, r. cuneyt. (2024). Forest Fire Analysis with Landsat Satellite Images : 2023 Gökçeada Forest Fire (Türkiye) FOREST FIRE ANALYSIS WITH LANDSAT SATELLITE IMAGES : 2023 GÖKÇEADA ISLAND FOREST FIRE (TÜRKİYE). *International Symposium on Applied Geoinformatics*, *May*, 132–136.

Bonnier, A., Finné, M., & Weiberg, E. (2019). Examining Land-Use through GIS-Based Kernel Density Estimation: A Re-Evaluation of Legacy Data from the Berbati-Limnes Survey. *Journal of Field Archaeology*, *44*(2), 70–83. https://doi.org/10.1080/00934690.2019.1570481

Bostani, A. M., & Pourebrahim, S. (2025). Integrated fire risk assessment using time-series satellite data and multi-criteria decision-making techniques. *Environmental and Sustainability Indicators*, *28*(July), 100916. https://doi.org/10.1016/j.indic.2025.100916

Burapapol, K., & Nagasawa, R. (2016). Mapping Soil Moisture as an Indicator of Wildfire Risk Using Landsat 8 Images in Sri Lanna National Park, Northern Thailand. *Journal of Agricultural Science*, *8*(10), 107. https://doi.org/10.5539/jas.v8n10p107

Cardil, A., De-Miguel, S., Silva, C. A., Reich, P. B., Calkin, D., Brancalion, P. H. S., Vibrans, A. C., Gamarra, J. G. P., Zhou, M., Pijanowski, B. C., Hui, C., Crowther, T. W., Hérault, B., Piotto, D., Salas-Eljatib, C., Broadbent, E. N., Almeyda Zambrano, A. M., Picard, N., Aragao, L. E. O. C., … Liang, J. (2020). Recent deforestation drove the spike in Amazonian fires. *Environmental Research Letters*,

15(12). https://doi.org/10.1088/1748-9326/abcac7

Chan, C. C., Alvi, S. A., Zhou, X., Durrani, S., Wilson, N., & Yebra, M. (2024). A Survey on IoT Ground Sensing Systems for Early Wildfire Detection: Technologies, Challenges, and Opportunities. *IEEE Access*, *12*(October), 172785–172819. https://doi.org/10.1109/ACCESS.2024.3501336

Chaparro, D., Piles, M., Vall-Llossera, M., & Camps, A. (2016). Surface moisture and temperature trends anticipate drought conditions linked to wildfire activity in the Iberian Peninsula. *European Journal of Remote Sensing*, *49*, 955–971. https://doi.org/10.5721/EuJRS20164950

Chaparro, D., Vall-llossera, M., Piles, M., Camps, A., Rudiger, C., & Riera-tatch, R. (2016). Predicting the Extent of Wildfires Using Remotely Sensed Soil Moisture and Temperature Trends. *IEEE JOURNAL*, *9*(6), 2818–2829. https://doi.org/10.1109/JSTARS.2016.2571838

Charizanos, G., & Demirhan, H. (2023). Bayesian prediction of wildfire event probability using normalized difference vegetation index data from an Australian forest. *Ecological Informatics*, *73*(November 2022). https://doi.org/10.1016/j.ecoinf.2022.101899

Chas-Amil, M. L., Nogueira-Moure, E., Prestemon, J. P., & Touza, J. (2022). Spatial patterns of social vulnerability in relation to wildfire risk and wildland-urban interface presence. *Landscape and Urban Planning*, *228*(April), 104577. https://doi.org/10.1016/j.landurbplan.2022.104577

Chew, Y. J., Ooi, S. Y., Pang, Y. H., & Lim, Z. Y. (2023). Investigating the Relationship between the Influencing Fire Factors and Forest Fire Occurrence in the Districts of Rompin, Pekan, and Kuantan in the State of Pahang, Malaysia, Using Google Earth Engine. *International Journal on Advanced Science Engineering Information Technology*, *13*(5), 1733–1741. https://doi.org/10.18517/ijaseit.13.5.19026

Chew, Y. J., Ooi, S. Y., Pang, Y. H., & Wong, K. S. (2022a). A Review of Forest Fire Combating Efforts, Challenges and Future Directions in Peninsular Malaysia, Sabah, and Sarawak. *Forests*, *13*(9), 1–37. https://doi.org/10.3390/f13091405

Chew, Y. J., Ooi, S. Y., Pang, Y. H., & Wong, K. S. (2022b). Trend Analysis of Forest Fire in Pahang, Malaysia from 2001-2021 with Google Earth Engine Platform. *Journal of Logistics, Informatics and Service Science*, *9*(4), 15–26. https://doi.org/10.33168/LISS.2022.0402

Childs, C. (2004). Interpolating Surfaces in ArcGIS Spatial Analyst. *Encyclopedia of*

GIS, 556–556. https://doi.org/10.1007/978-3-319-17885-1_100368

Chowdhury, E. H., & Hassan, Q. K. (2015). Development of a new daily-scale forest fire danger forecasting system using remote sensing data. *Remote Sensing*, *7*(3), 2431–2448. https://doi.org/10.3390/rs70302431

Cimdins, R., Krasovskiy, A., & Kraxner, F. (2022). Regional Variability and Driving Forces behind Forest Fires in Sweden. *Remote Sensing*, *14*(22). https://doi.org/10.3390/rs14225826

Clarke, H., Gibson, R., Cirulis, B., Bradstock, R. A., & Penman, T. D. (2019). Developing and testing models of the drivers of anthropogenic and lightning-caused wildfire ignitions in south-eastern Australia. *Journal of Environmental Management*, *235*(January), 34–41. https://doi.org/10.1016/j.jenvman.2019.01.055

Çolak, E., & Sunar, F. (2020). Evaluation of forest fire risk in the Mediterranean Turkish forests: A case study of Menderes region, Izmir. *International Journal of Disaster Risk Reduction*, *45*(July 2019), 101479. https://doi.org/10.1016/j.ijdrr.2020.101479

Collins, K. M., Penman, T. D., & Price, O. F. (2016). Some wildfire ignition causes pose more risk of destroying houses than others. *PLoS ONE*, *11*(9), 1–18. https://doi.org/10.1371/journal.pone.0162083

Collins, L., Bradstock, R. A., & Penman, T. D. (2014). Can precipitation influence landscape controls on wildfire severity' A case study within temperate eucalypt forests of south-eastern Australia. *International Journal of Wildland Fire*, *23*(1), 9–20. https://doi.org/10.1071/WF12184

Cordero, R. R., Feron, S., Damiani, A., Carrasco, J., Karas, C., Wang, C., Kraamwinkel, C. T., & Beaulieu, A. (2024). Extreme fire weather in Chile driven by climate change and El Niño–Southern Oscillation (ENSO). *Scientific Reports*, *14*(1), 1–12. https://doi.org/10.1038/s41598-024-52481-x

Costafreda-Aumedes, S., Comas, C., & Vega-Garcia, C. (2017). Human-caused fire occurrence modelling in perspective: A review. *International Journal of Wildland Fire*, *26*(12), 983–998. https://doi.org/10.1071/WF17026

Dai, K. Y., Liu, G. R., Lim, K. M., & Gu, Y. T. (2003). Comparison between the radial point interpolation and the Kriging interpolation used in meshfree methods. *Computational Mechanics*, *32*(1–2), 60–70. https://doi.org/10.1007/s00466-003-0462-z

Dampage, U., Bandaranayake, L., Wanasinghe, R., Kottahachchi, K., & Jayasanka, B. (2022). Forest fire detection system using wireless sensor networks and machine learning. *Scientific Reports*, *12*(1), 1–11. https://doi.org/10.1038/s41598-021-03882-9

Dapke, P. P., Nagare, S. M., Quadri, S. A., Bandal, S. B., Gaikwad, R. M., & Baheti, M. R. (2025). Seasonal Analysis of Vegetation, Moisture, Urbanization, and Land Surface Temperature (LST) Using NDVI, NDMI, NDWI, and NDBI Indices: A Case Study of Sillod, Maharashtra. *IEEE International Conference on "Computational, Communication and Information Technology", ICCCIT 2025*, 753–760. https://doi.org/10.1109/ICCCIT62592.2025.10928110

Daraz, U., Bojnec, Š., & Khan, Y. (2024). Socio-Economic Determinants of Human Negligence in Wildfire Incidence: A Case Study from Pakistan's Peri-Urban and Rural Areas. *Fire*, *7*(11). https://doi.org/10.3390/fire7110377

Darvishi, L., Daryaei, M. G., & Abouzar, H. S. K. (2020). Comparison of Statistical Modeling and AHP Methods in Fire Risk Assessment in Oak Forests of Iran. *Journal of Forest Research*, *9*(2), 229. https://doi.org/10.35248/2168-9776.20.9.229

Devisscher, T., Anderson, L. O., Aragão, L. E. O. C., Galván, L., & Malhi, Y. (2016). Increased wildfire risk driven by climate and development interactions in the Bolivian Chiquitania, Southern Amazonia. *PLoS ONE*, *11*(9), 1–29. https://doi.org/10.1371/journal.pone.0161323

Diffenbaugh, N. S., Konings, A. G., & Field, C. B. (2021). Atmospheric variability contributes to increasing wildfire weather but not as much as global warming. *Proceedings of the National Academy of Sciences of the United States of America*, *118*(46), 1–3. https://doi.org/10.1073/pnas.2117876118

Dong, W. S., Ismailluddin, A., Yun, L. S., Ariffin, E. H., Saengsupavanich, C., Abdul Maulud, K. N., Ramli, M. Z., Miskon, M. F., Jeofry, M. H., Mohamed, J., Mohd, F. A., Hamzah, S. B., & Yunus, K. (2024). The impact of climate change on coastal erosion in Southeast Asia and the compelling need to establish robust adaptation strategies. *Heliyon*, *10*(4), e25609. https://doi.org/10.1016/j.heliyon.2024.e25609

Du, T. L. T., Du Bui, D., Nguyen, M. D., & Lee, H. (2018). Satellite-based, multi-indices for evaluation of agricultural droughts in a highly dynamic tropical catchment, Central Vietnam. *Water (Switzerland)*, *10*(5). https://doi.org/10.3390/w10050659

Eagleston, H., Bester, M., Yusuf, J., Damodaran, A., & Reno, M. J. (2025). Systemic Drivers of Electric-Grid-Caused Catastrophic Wildfires: Implications for Resilience in the United States. *Challenges*, *16*(1), 13. https://doi.org/10.3390/challe16010013

Emang, G. P., Touge, Y., & Kazama, S. (2019). ASSESSING NDVI BASED PHENOLOGY IN DIFFERENT FIRE SEVERITY IN THE KAMAISHI 2017 FOREST FIRE. *Journal of Japan Society of Civil Engineers*, *75*(5), 135–140.

Ezzaher, F. E., Ben Achhab, N., Raissouni, N., Naciri, H., & Chahboun, A. (2024). *Normalized Burn Ratio and Land Surface Temperature Pre- and Post-Mediterranean Forest Fires*. 3. https://doi.org/10.3390/ecrs2023-15829

Fasullo, J. T., Otto-Bliesner, B. L., & Stevenson, S. (2018). ENSO's Changing Influence on Temperature, Precipitation, and Wildfire in a Warming Climate. *Geophysical Research Letters*, *45*(17), 9216–9225. https://doi.org/10.1029/2018GL079022

Fernández-Manso, A., Quintano, C., & Roberts, D. A. (2020). Can Landsat-derived variables related to energy balance improve understanding of burn severity from current operational techniques? *Remote Sensing*, *12*(5). https://doi.org/10.3390/rs12050890

Fernandez-Pello, A. C. (2017). Wildland fire spot ignition by sparks and firebrands. *Fire Safety Journal*, *91*, 2–10. https://doi.org/10.1016/j.firesaf.2017.04.040

Findlay, M., Peaslee, D., Stetter, J. R., Waller, S., & Smallridge, A. (2022). Distributed Sensors for Wildfire Early Warnings. *Journal of The Electrochemical Society*, *169*(2), 020553. https://doi.org/10.1149/1945-7111/ac5344

Fisal, N. S. M., Lintangah, W., & Ismenyah, M. (2017). Community Awareness & Challenges in Forest Fire Prevention: a Case Study At Peat Swamp Forest, Klias Forest Reserve, Beaufort, Sabah, Malaysia. *International Journal of Agriculture, Forestry and Plantation*, *5*, 86–91.

Ghaderpour, E., Bozzano, F., Mugnozza, G. S., & Mazzanti, P. (2025). Analyses of MODIS Land Cover/Use and Wildfires in Italian Regions Since 2001. *Land*, *14*(7), 1–20. https://doi.org/10.3390/land14071443

Gharakhanlou, N. M., & Perez, L. (2025). Spatial Susceptibility Mapping of Boreal Forest Fires: Insights from Quebec's Historical and Future Trends (1980-2050). *Advances in Cartography and GIScience of the ICA*, *5*(August), 1–9. https://doi.org/10.5194/ica-adv-5-20-2025

Ghazali, N. N., Saraf, N. M., Rauf, A., Rasam, A., Othman, A. N., Salleh, S. A., & Saad, N. (2025). Forest Fire Severity Level Using dNBR Spectral Index. *International Geomatic*, *34*, 89–101. https://doi.org/10.32604/rig.2025.057562

Gizatullin, A. T., & Alekseenko, N. A. (2022). Prediction of Wildfires Based on the Spatio-Temporal Variability of Fire Danger Factors. *Geography, Environment, Sustainability*, *15*(2), 31–37. https://doi.org/10.24057/2071-9388-2021-139

Gorgani, S. A., Panahi, M., & Rezaie, F. (2013). The Relationship between NDVI and LST in the urban area of Mashhad, Iran. *International Conference on Civil Engineering Architecture & Urban Sustainable Development*, *November*. https://www.researchgate.net/publication/265601825_The_Relationship_between_NDVI_and_LST_in_the_urban_area_of_Mashhad_Iran

Govil, K., Welch, M. L., Ball, J. T., & Pennypacker, C. R. (2020). Preliminary results from a wildfire detection system using deep learning on remote camera images. *Remote Sensing*, *12*(1). https://doi.org/10.3390/RS12010166

Granville, K., Woolford, D. G., Dean, C. B., Boychuk, D., & McFayden, C. B. (2023). On the selection of an interpolation method with an application to the Fire Weather Index in Ontario, Canada. *Environmetrics*, *34*(2), 1–23. https://doi.org/10.1002/env.2758

Gray, M. E., Zachmann, L. J., & Dickson, B. G. (2018). A weekly, continually updated dataset of the probability of large wildfires across western US forests and woodlands. *Earth System Science Data*, *10*(3), 1715–1727. https://doi.org/10.5194/essd-10-1715-2018

Grillakis, M., Voulgarakis, A., Rovithakis, A., Seiradakis, K. D., Koutroulis, A., Field, R. D., Kasoar, M., Papadopoulos, A., & Lazaridis, M. (2022). Climate drivers of global wildfire burned area. *Environmental Research Letters*, *17*(4). https://doi.org/10.1088/1748-9326/ac5fa1

Guan, R. (2023). Predicting Forest Fire with Linear Regression and Random Forest. *Highlights in Science, Engineering and Technology*, *44*, 1–7. https://doi.org/10.54097/hset.v44i.7159

Guha, S., Govil, H., & Besoya, M. (2020). An investigation on seasonal variability between LST and NDWI in an urban environment using Landsat satellite data. *Geomatics, Natural Hazards and Risk*, *11*(1), 1319–1345. https://doi.org/10.1080/19475705.2020.1789762

Guiop-Servan, R. E., Cotrina-Sanchez, A., Puerta-Culqui, J., Oliva-Cruz, M., &

Barboza, E. (2025). Remote Sensing for Wildfire Mapping: A Comprehensive Review of Advances, Platforms, and Algorithms. *Fire*, *8*(8), 1–23. https://doi.org/10.3390/fire8080316

Guo, F., Innes, J. L., Wang, G., Ma, X., Sun, L., Hu, H., & Su, Z. (2014). Historic distribution and driving factors of human-caused fires in the Chinese boreal forest between 1972 and 2005. *Journal of Plant Ecology*, *8*(5), 480–490. https://doi.org/10.1093/jpe/rtu041

Guo, F., Wang, G., Su, Z., Liang, H., Wang, W., Lin, F., & Liu, A. (2016). What drives forest fire in Fujian, China ? Evidence from logistic regression and Random Forests What drives forest fire in Fujian, China ? Evidence from logistic regression and Random Forests. *International Journal of Wildland Fire*, *April*. https://doi.org/10.1071/WF15121

Gupta, P., & Shukla, D. P. (2022). Google Earth Engine-Based Temporal Analysis of Indices Used for Forest Fire Study in Mizoram, India. *XXIV ISPRS Congress*, *XLIII*(June), 493–499.

Hatchett, B. J., Nauslar, N. J., & Brown, T. J. (2024). Comparing ground-based lightning detection networks near wildfire points-of-origin. *Natural Hazards*, *120*(14), 13617–13626. https://doi.org/10.1007/s11069-024-06741-8

Heidari, F. B., & Arfania, R. (2022). Wildfire Susceptibility Mapping using NBR Index and Frequency Ratio Model. *Geoconservation Research*, *5*(1), 240–260. https://doi.org/10.30486/gcr.2022.1961153.1107

Herawati, H., González-olabarria, J. R., Wijaya, A., Martius, C., Purnomo, H., & Andriani, R. (2015). Tools for Assessing the Impacts of Climate Variability and Change on Wildfire Regimes in Forests. *Forests*, *6*, 1476–1499. https://doi.org/10.3390/f6051476

Holden, Z. A., Swanson, A., Luce, C. H., Jolly, W. M., Maneta, M., Oyler, J. W., Warren, D. A., Parsons, R., & Affleck, D. (2018). Decreasing fire season precipitation increased recent western US forest wildfire activity. *Proceedings of the National Academy of Sciences of the United States of America*, *115*(36), E8349–E8357. https://doi.org/10.1073/pnas.1802316115

Honary, R., Shelton, J., & Kavehpour, P. (2025). A Review of Technologies for the Early Detection of Wildfires. *ASME Open Journal of Engineering*, *4*, 1–13. https://doi.org/10.1115/1.4067645

Hoyt, W. T., Leierer, S. J., & Millington, M. (2006). Analysis and interpretation of

findings using multiple regression techniques. *Rehabilitation Counseling Bulletin*, *49*(4), 223–233. https://doi.org/10.1177/00343552060490040401

Jain, P., & Flannigan, M. D. (2017). Comparison of methods for spatial interpolation of fire weather. *Canadian Journal of Forest Research*, *47*(12), 1646–1658. https://tspace.library.utoronto.ca/bitstream/1807/80338/1/cjfr-2017-0101.pdf

Jamaruppin, M. E. Bin, Bayuaji, L., Ab Ghani, N. B., Rahman, M. A., Akashah, F. W., & Shah, A. (2016). Forest Fire Occurrence Analysis Based on Land Brightness Temperature using Landsat Data (Study Area: Jalan Kuantan–Pekan, Pahang, Malaysia). *The National Conference for Postgraduate Research*, 798–805.

Jothimani, M., Gunalan, J., Duraisamy, R., & Abebe, A. (2021). Study the Relationship Between LULC, LST, NDVI, NDWI and NDBI in Greater Arba Minch Area, Rift Valley, Ethiopia. *Proceedings of the 3rd International Conference on Integrated Intelligent Computing Communication & Security (ICIIC 2021)*, *4*(Iciic), 183–193. https://doi.org/10.2991/ahis.k.210913.023

Junaidi, S. N., Khalid, N., Othman, A. N., Hamid, J. R. A., & Saad, N. M. (2021). Analysis of the Relationship between Forest Fire and Land Surface Temperature using Landsat 8 OLI/TIRS Imagery. *IOP Conference Series: Earth and Environmental Science*, *767*(1). https://doi.org/10.1088/1755-1315/767/1/012005

Kadir, E. A., Alomainy, A., Daud, H., Maharani, W., Muhammad, N., & Syafitri, N. (2023). Multi Sensor Network System for Early Detection and Prediction of Forest Fires in Southeast Asia. *2023 33rd International Telecommunication Networks and Applications Conference, ITNAC 2023*, 190–195. https://doi.org/10.1109/ITNAC59571.2023.10368547

Kadir, E. A., Irie, H., Rosa, S. L., & Othman, M. (2019). Modelling of wireless sensor networks for detection of land and forest fire hotspots. *Telkomnika (Telecommunication Computing Electronics and Control)*, *17*(6), 2772–2781. https://doi.org/10.12928/TELKOMNIKA.v17i6.12971

Kamal, N. I. A., Ash'aari, Z. H., & Abdullah, A. M. (2019). Spatio-temporal variability of heat exposure in peninsular Malaysia using land surface temperature. *Disaster Advances*, *12*(12), 1–9.

Karurung, W. S., Lee, K., & Lee, W. (2025). Assessment of forest fire vulnerability prediction in Indonesia: Seasonal variability analysis using machine learning techniques. *International Journal of Applied Earth Observation and Geoinformation*, *138*(February), 104435.

https://doi.org/10.1016/j.jag.2025.104435

Khairil, M., Jeganathan, cheryl stephen, Razman, muhammad rizal, Syed Zakaria, sharifah zarina, & Arifin, K. (2018). The Communication on Enforcement of Open Burning Cases in Malaysia. *International Journal on Information*, *21*(5), 1549–1553. https://www.researchgate.net/publication/329223109

Khan, M. F., Hamid, A. H., Rahim, H. A., Maulud, K. N. A., Latif, M. T., Nadzir, M. S. M., Sahani, M., Qin, K., Kumar, P., Varkkey, H., Faruque, M. R. I., Guan, N. C., Ahmadi, S. P., & Yusoff, S. (2020). El Niño-driven haze over the Southern Malaysian Peninsula and Borneo. *Science of the Total Environment*, *730*. https://doi.org/10.1016/j.scitotenv.2020.139091

Kim, J., Kim, T., Lee, Y. E., & Im, S. (2025). Spatial and temporal variability of forest fires in the Republic of Korea over 1991–2020. *Natural Hazards*, *121*(8), 9801–9821. https://doi.org/10.1007/s11069-025-07169-4

Kolanek, A., Szymanowski, M., & Raczyk, A. (2021). Human activity affects forest fires: The impact of anthropogenic factors on the density of forest fires in Poland. *Forests*, *12*(6), 1–21. https://doi.org/10.3390/f12060728

Kong, B. (2024). A Comparative Analysis of Machine Learning Models for Wildfire Prediction. *The National High School Journal of Science*.

Koutsias, N., Balatsos, P., & Kalabokidis, K. (2014). Fire occurrence zones: Kernel density estimation of historical wildfire ignitions at the national level, Greece. *Journal of Maps*, *10*(4), 630–639. https://doi.org/10.1080/17445647.2014.908750

Krueger, E. S., Levi, M. R., Achieng, K. O., Bolten, J. D., Carlson, J. D., Coops, N. C., Holden, Z. A., Magi, B. I., Rigden, A. J., & Ochsner, T. E. (2022). Using soil moisture information to better understand and predict wildfire danger: a review of recent developments and outstanding questions. *International Journal of Wildland Fire*, *32*(2), 111–132. https://doi.org/10.1071/wf22056

Krüll, W., Tobera, R., Willms, I., Essen, H., & Von Wahl, N. (2012). Early forest fire detection and verification using optical smoke, gas and microwave sensors. *Procedia Engineering*, *45*, 584–594. https://doi.org/10.1016/j.proeng.2012.08.208

Kuduyu, I. (2023). *BOTSWANA UNIVERSITY OF AGRICULTURE AND NATURAL RESOURCES DEPARTMENT OF AGRICULTURAL AND BIO-SYSTEMS ENGINEERING- By Issa Kaduyu Student ID : 202000794*. *January*.

Kumar, M., Ojha, N., & Singh, N. (2021). Atmospheric aerosols from open burning in South and Southeast Asia. *Asian Atmospheric Pollution: Sources, Characteristics*

and Impacts, *January*, 75–96. https://doi.org/10.1016/B978-0-12-816693-2.00001-9

Kuter, N., Yenilmez, F., & Kuter, S. (2011). Forest fire risk mapping by kernel density estimation. *Croatian Journal of Forest Engineering*, *32*(2), 599–610.

Lan, Y., Wang, J., Hu, W., Kurbanov, E., Cole, J., Sha, J., Jiao, Y., & Zhou, J. (2023). Spatial pattern prediction of forest wildfire susceptibility in Central Yunnan Province, China based on multivariate data. *Natural Hazards*, *116*(1), 565–586. https://doi.org/10.1007/s11069-022-05689-x

Lan, Z., Su, Z., Guo, M., Alvarado, E. C., Guo, F., Hu, H., & Wang, G. (2021). Are climate factors driving the contemporary wildfire occurrence in China? *Forests*, *12*(4). https://doi.org/10.3390/f12040392

Lanorte, A., Nolè, G., & Cillis, G. (2024). Application of Getis-Ord Correlation Index (Gi) for Burned Area Detection Improvement in Mediterranean Ecosystems (Southern Italy and Sardinia) Using Sentinel-2 Data. *Remote Sensing*, *16*(16). https://doi.org/10.3390/rs16162943

Li, H., Vulova, S., Rocha, A. D., & Kleinschmit, B. (2024). Spatio-temporal feature attribution of European summer wildfires with Explainable Artificial Intelligence (XAI). *Science of the Total Environment*, *916*(January). https://doi.org/10.1016/j.scitotenv.2024.170330

Li, J., Huang, D., Chen, C., Liu, Y., Wang, J., Shao, Y., Wang, A., & Li, X. (2024). Prediction of Forest-Fire Occurrence in Eastern China Utilizing Deep Learning and Spatial Analysis. *Forests*, *15*(9). https://doi.org/10.3390/f15091672

Li, S., & Banerjee, T. (2021). Spatial and temporal pattern of wildfires in California from 2000 to 2019. *Scientific Reports*, *11*(1), 1–17. https://doi.org/10.1038/s41598-021-88131-9

Liu, D., & Zhang, Y. (2015). Research of regional forest fire prediction method based on multivariate linear regression. *International Journal of Smart Home*, *9*(1), 13–22. https://doi.org/10.14257/ijsh.2015.9.1.02

Liu, W., Wang, S., Zhou, Y., Wang, L., & Zhang, S. (2010). Analysis of forest potential fire environment based on GIS and RS. *2010 18th International Conference on Geoinformatics, Geoinformatics 2010*, *200704027*, 1–6. https://doi.org/10.1109/GEOINFORMATICS.2010.5567966

Lourenco, L., Fernandes, S., Nunes, A., Bento-goncalves, A., & Vieira, A. (2013). Determination of forest fire causes in Portugal (1996-2010). *Flamma*, *4*(March),

171–175.

Lovreglio, R., Leone, V., Giaquinto, P., & Notarnicola, A. (2010). Wildfire cause analysis: Four case-studies in southern Italy. *IForest*, *3*(JANUARY), 8–15. https://doi.org/10.3832/ifor0521-003

Lu, J., Zhou, T., Li, B., & Wu, C. (2018). Scale Analysis and Correlation Study of Wildfire and the Meteorological Factors That Influence It. *Mathematical Problems in Engineering*, *2018*. https://doi.org/10.1155/2018/5739805

Ma, C., Pu, R., Downs, J., & Jin, H. (2022). Characterizing Spatial Patterns of Amazon Rainforest Wildfires and Driving Factors by Using Remote Sensing and GIS Geospatial Technologies. *Geosciences (Switzerland)*, *12*(6). https://doi.org/10.3390/geosciences12060237

Ma, W., Feng, Z., Cheng, Z., Chen, S., & Wang, F. (2020). Identifying forest fire driving factors and related impacts in China using random forest algorithm. *Forests*, *11*(5). https://doi.org/10.3390/F11050507

Mamgain, S., Roy, A., Karnatak, H. C., & Chauhan, P. (2023). Satellite-based long-term spatiotemporal trends of wildfire in the Himalayan vegetation. *Natural Hazards*, *116*(3), 3779–3796. https://doi.org/10.1007/s11069-023-05835-z

Manepalli, U., Bham, G., & Kandada, S. (2011). Evaluation of Hotspots Identification Using Kernel Density. *The 3rd International Conference on Road Safety and Simulation*, *1750*, 1–17.

Mansoor, S., Farooq, I., Kachroo, M. M., Mahmoud, A. E. D., Fawzy, M., Popescu, S. M., Alyemeni, M. N., Sonne, C., Rinklebe, J., & Ahmad, P. (2022). Elevation in wildfire frequencies with respect to climate change. *Journal of Environmental Management*, *301*(April 2021), 113769. https://doi.org/10.1016/j.jenvman.2021.113769

Mat Deli, M. (2023). Forest Fire Incident Forecasting System In Permanent Reserved Forest In Peninsular Malaysia Using Big Data Analytics. *Sustainable Energy and Environment Review*, *1*(1), 1–13. https://doi.org/10.59762/seer92471204112023110314305 3

Mitchener, L. J., & Parker, A. J. (2005). Climate, Lightning, and Wildfire in the National Forests of the Southeastern United States: 1989-1998. *Physical Geography*, *26*(2), 147–162. https://doi.org/10.2747/0272-3646.26.2.147

Mohamed, T. B. (2022). Wildfire Effects on Vegetation Moisture, Using Remote Sensing Techniques: Case Study of Ain Marah Al-Jabal Al-Akhdar, Libya. *Libyan*

Journal of Ecological & Environmental Sciences and Technology, *4*(2), 51–59. https://doi.org/10.63359/tp2kd393

Mohapatra, A., & Trinh, T. (2022). Early Wildfire Detection Technologies in Practice—A Review. *Sustainability (Switzerland)*, *14*(19). https://doi.org/10.3390/su141912270

Mohaymany, A. S., Shahri, M., & Mirbagheri, B. (2013). GIS-based method for detecting high-crash-risk road segments using network kernel density estimation. *Geo-Spatial Information Science*, *16*(2), 113–119. https://doi.org/10.1080/10095020.2013.766396

Mohd Jaafar, W. S. W., Maulud, K. N. A., Muhmad Kamarulzaman, A. M., Raihan, A., Sah, S. M., Ahmad, A., Maizah Saad, S. N., Mohd Azmi, A. T., Syukri, N. K. A. J., & Khan, W. R. (2020). The influence of deforestation on land surface temperature-A case study of Perak and Kedah, Malaysia. *Forests*, *11*(6). https://doi.org/10.3390/F11060670

Moisa, M. B., Gabissa, B. T., Wedajo, Y. N., Gurmessa, M. M., Deribew, K. T., Negasa, G. G., Negassa, M. D., & Gemeda, D. O. (2023). Analyzing the correlation of forest and wetland with land surface temperature by using geospatial technology: a case of Yayo district, Southwestern Ethiopia. *Geocarto International*, *38*(1). https://doi.org/10.1080/10106049.2023.2256300

Moreno, M., Bertolín, C., Arlanzón, D., Ortiz, P., & Ortiz, R. (2023). Climate change, large fires, and cultural landscapes in the Mediterranean basin: An analysis in southern Spain. *Heliyon*, *9*(6), 1–19. https://doi.org/10.1016/j.heliyon.2023.e16941

Morshed, S. R., Abdul Fattah, M., Amin Rimi, A., & Nazmul Haque, M. (2020). Surface Temperature Dynamics in Response To Land Cover Transformation. *Journal of Civil Engineering, Science and Technology*, *11*(2), 94–110. https://doi.org/10.33736/jcest.2616.2020

Morsy, S., & Hadi, M. (2022). Impact of land use/land cover on land surface temperature and its relationship with spectral indices in Dakahlia Governorate, Egypt. *International Journal of Engineering and Geosciences*, *7*(3), 272–282. https://doi.org/10.26833/ijeg.978961

Morton, D. C., Defries, R. S., Randerson, J. T., Giglio, L., Schroeder, W., & van der Werf, G. R. (2008). Agricultural intensification increases deforestation fire activity in Amazonia. *Global Change Biology*, *14*(10), 2262–2275.

https://doi.org/10.1111/j.1365-2486.2008.01652.x

Mpakairi, K. S., Ndaimani, H., & Kavhu, B. (2020). Exploring the utility of Sentinel-2 MSI derived spectral indices in mapping burned areas in different land-cover types. *Scientific African*, *10*, e00565. https://doi.org/10.1016/j.sciaf.2020.e00565

Muhammad, M. K. I., Hamed, M. M., Harun, S., Sa'adi, Z., Sammen, S. S., Al-Ansari, N., Shahid, S., & Scholz, M. (2024). Heatwaves in Peninsular Malaysia: a spatiotemporal analysis. *Scientific Reports*, *14*(1), 1–16. https://doi.org/10.1038/s41598-024-53960-x

Munawar, M., McNeil, R., Jani, R., Nur, E. M., & McNeil, D. (2024). Variation and Forecasting of Land Surface Temperature in Malaysia. *Pertanika Journal of Science and Technology*, *32*(6), 2723–2735. https://doi.org/10.47836/pjst.32.6.16

Mundo, I. A., Wiegand, T., Kanagaraj, R., & Kitzberger, T. (2013). Environmental drivers and spatial dependency in wildfire ignition patterns of northwestern Patagonia. *Journal of Environmental Management*, *123*, 77–87. https://doi.org/10.1016/j.jenvman.2013.03.011

Musri, I., Ainuddin, A. N., Hyrul, M. H. I., Hazandy, A. H., Azani, A. M., & Mitra, U. (2020). Post-forest fire management at tropical peat swamp forest: A review of Malaysian experience on rehabilitation and risk mitigation. *IOP Conference Series: Earth and Environmental Science*, *504*(1). https://doi.org/10.1088/1755-1315/504/1/012017

Naftal, B. M., Kija, H., Piel, A. K., Naftal, B., Kija, H. K., William, C., Noe, C., Anderson, D., & Stewart, F. A. (2022). Spatial and temporal pattern of wildfires in the Masito-Ugalla Ecosystem (2008-2019), Tanzania. *Journal of Environmental Science*, *16*(7), 12–19. https://doi.org/10.9790/2402-1607021219

Narayanaraj, G., & Wimberly, M. C. (2012). Influences of forest roads on the spatial patterns of human- and lightning-caused wildfire ignitions. *Applied Geography*, *32*(2), 878–888. https://doi.org/10.1016/j.apgeog.2011.09.004

Nejad, M. F., & Zoratipour, A. (2019). Assessment of LST and NDMI indices using MODIS and Landsat images in Karun riparian forest. *Journal of Forest Science*, *65*(1), 27–32. https://doi.org/10.17221/121/2018-JFS

Nelson, R. M. (2002). An effective wind speed for models of fire spread. *International Journal of Wildland Fire*, *11*(2), 153–161. https://doi.org/10.1071/WF02031

Neto, V. P. S., Leite, R. V., Santos, V. J. Dos, Alves, S. D. C., Castro, J. D. S., Torres, F. T. P., & Calijuri, M. L. (2022). Burning Susceptibility Modeling to Reduce

Wildfire Impacts : A GIS and Multivariate Statistics Approach. *Conservation of Nature*, *29*(1), 1–12.

Nguyen, T. T. N., & Tong, T. H. (2023). WILDFIRE RISKS IN THE SOUTHWEST OF KY SON DISTRICT, NGHE AN PROVINCE – A MULTI-CRITICAL MODEL. *Journal of Science and Technique*, 7–18. https://doi.org/10.56651/lqdtu.jst.v6.n01.662.sce

NourEldeen, N., Mao, K., Yuan, Z., Shen, X., Xu, T., & Qin, Z. (2020). Analysis of the spatiotemporal change in land surface temperature for a long-term sequence in Africa (2003-2017). *Remote Sensing*, *12*(3). https://doi.org/10.3390/rs12030488

Ntinopoulos, N., Spiliotopoulos, M., Vasiliades, L., & Mylopoulos, N. (2022). Contribution to the Study of Forest Fires in Semi-Arid Regions with the Use of Canadian Fire Weather Index Application in Greece. *Climate*, *10*(10). https://doi.org/10.3390/cli10100143

Nugraha, M. G., Mozasurya, E. D., Hidayat, M., & Saptoadi, H. (2023). Evaluation of combustion characteristics in biomass residues open burning. *Materials Today: Proceedings*, *87*, 45–50. https://doi.org/10.1016/j.matpr.2023.02.098

Nunes, Adelia N. (2012). Regional variability and driving forces behind forest fires in Portugal: an overview of the last three decades (1980 - 2009). *Elsevier Applied Geography*, *34*, 576–586. https://doi.org/10.1016/j.apgeog.2012.03.002

Oad, vipin kumar, Szymkiewicz, A., Khan, nabeel ali, Ashraf, S., Nawaz, R., Elnashar, A., Saad, S., & Qureshi, abdul hannan. (2023). Remote Sensing Applications : Society and Environment. Time series analysis and impact assessment of the temperature changes on the vegetation and the water availability : A case study of Bakun-Murum Catchment Region in Malaysia. *Remote Sensing Application: Society and Environment*, *29*(December 2022).

Oliveira, S., Oehler, F., San-Miguel-Ayanz, J., Camia, A., & Pereira, J. M. C. (2012). Modeling spatial patterns of fire occurrence in Mediterranean Europe using Multiple Regression and Random Forest. *Forest Ecology and Management*, *275*, 117–129. https://doi.org/10.1016/j.foreco.2012.03.003

Öncü, G., & Çorumluoğlu, Ö. (2023). Determination of Spatial Distribution of Damage Intensity of Tınazlı -Izmir Forest Fire Using Remote Sensing Indexing Techniques. *International Journal of Environment and Geoinformatics*, *10*(2), 151–158.

Orimoloye, I. R., Ololade, O. O., Mazinyo, S. P., Kalumba, A. M., Ekundayo, O. Y.,

Busayo, E. T., Akinsanola, A. A., & Nel, W. (2019). Spatial assessment of drought severity in Cape Town area, South Africa. *Heliyon*, *5*(7). https://doi.org/10.1016/j.heliyon.2019.e02148

Parajuli, A., Gautam, A. P., Sharma, S. P., Bhujel, K. B., Sharma, G., Thapa, P. B., Bist, B. S., & Poudel, S. (2020). Forest fire risk mapping using GIS and remote sensing in two major landscapes of Nepal. *Geomatics, Natural Hazards and Risk*, *11*(1), 2569–2586. https://doi.org/10.1080/19475705.2020.1853251

Partheepan, S., Sanati, F., & Hassan, J. (2023). Autonomous Unmanned Aerial Vehicles in Bushfire Management: Challenges and Opportunities. *Drones*, *7*(1), 1–34. https://doi.org/10.3390/drones7010047

Parvar, Z., Saeidi, S., & Mirkarimi, S. (2024). Integrating meteorological and geospatial data for forest fire risk assessment. *Journal of Environmental Management*, *358*(March). https://doi.org/10.1016/j.jenvman.2024.120925

Pasukphun, N. (2018). Environmental Health Burden of Open Burning in Northern Thailand: a Review. *PSRU Journal of Science and Technology*, *3*(3), 11–28.

Patel, R., & Patel, A. (2024). "Evaluating the impact of climate change on drought risk in semi-arid region using GIS technique." *Results in Engineering*, *21*(March). https://doi.org/10.1016/j.rineng.2024.101957

Pathak, G., Nichter, M., Hardon, A., Moyer, E., Latkar, A., Simbaya, J., Pakasi, D., Taqueban, E., & Love, J. (2023). Plastic pollution and the open burning of plastic wastes. *Global Environmental Change*, *80*(January). https://doi.org/10.1016/j.gloenvcha.2023.102648

Patil, P. P., Jagtap, M. P., Khatri, N., Madan, H., Abhiram, A., & Patodia, T. (2024). Case Studies in Chemical and Environmental Engineering Exploration and advancement of NDDI leveraging NDVI and NDWI in Indian semi-arid regions : A remote sensing-based study. *Case Studies in Chemical and Environmental Engineering*, *9*(December 2023).

Pausas, J. G., & Keeley, J. E. (2021). Wildfires and global change. *Frontiers in Ecology and the Environment*, *19*(7), 387–395. https://doi.org/10.1002/fee.2359

Pelletier, N., Millard, K., & Darling, S. (2023). Wildfire likelihood in Canadian treed peatlands based on remote-sensing time-series of surface conditions. *Remote Sensing of Environment*, *296*(July). https://doi.org/10.1016/j.rse.2023.113747

Peña-molina, E., Moya, D., Marino, E., Tom, L., Fajardo-cantos, Á., Gonz, J., Lucas-borja, M. E., & Heras, J. De. (2024). Fire Vulnerability, Resilience, and Recovery

Rates of Mediterranean Pine Forests Using a 33-Year Time Series of Satellite Imagery. *Remote Sensing*, *16*, 1–21.

Pérez-Invernón, F. J., Gordillo-Vázquez, F. J., Huntrieser, H., & Jöckel, P. (2023). Variation of lightning-ignited wildfire patterns under climate change. *Nature Communications*, *14*(1). https://doi.org/10.1038/s41467-023-36500-5

Phantanaikasem, P., Pannawan, A., Jamroen, C., & Surinkaew, T. (2024). Potential Impacts of Wildfire on Distribution Networks in Thailand: A Data-Driven Assessment Using Hotspot Analysis. *2024 IEEE 22nd Student Conference on Research and Development, SCOReD 2024*, 39–43. https://doi.org/10.1109/SCOReD64708.2024.10872680

Quan, X., Xie, Q., He, B., Luo, K., & Liu, X. (2021). Integrating remotely sensed fuel variables into wildfire danger assessment for China. *International Journal of Wildland Fire*, *30*(10), 807–821. https://doi.org/10.1071/WF20077

Rafaqat, W., Sanchez, P., Botnen, D., & Fernandez-Anez, N. (2025). Analysing historical events and current management strategies of wildfires in Norway. *Scientific Reports*, *15*(1), 1–17. https://doi.org/10.1038/s41598-025-08760-2

Rajan, N M, & Shanmugam, J. (2018). Estimation of Forest Fire Spread by Modeling in GIS Platform. *Indian Journal of Science and Technology*, *11*(February). https://doi.org/10.17485/ijst/2018/v11i6/119650

Rajan, Nambi Manavalan, Neelamegam, P., & Thatheyus, A. J. (2022). Multiple linear and non-linear regression analyses of various soil and terrain indices concerning their efficiency in the determination of temporal changes in LST values within Trichy district of Tamil Nadu, India. *Environmental Monitoring and Assessment*, *194*(138), 1–15. https://doi.org/10.1007/s10661-022-09796-x

Rajendran, S. P., & Vani, K. (2024). Early Detection of Forest Fire Based on Lightning Activity and Climatic Factors Using Deep Learning. *45th Asian Conference on Remote Sensing, ACRS 2024*, *Acrs*, 1–15.

Rashkovetsky, D., Mauracher, F., Langer, M., & Schmitt, M. (2021). Wildfire Detection from Multisensor Satellite Imagery Using Deep Semantic Segmentation. *IEEE Journal of Selected Topics in Applied Earth Observations and Remote Sensing*, *14*, 7001–7016. https://doi.org/10.1109/JSTARS.2021.3093625

Razali, S. M., & Nuruddin, A. A. (2012). A method of mapping forest fuel types in peat swamp forest. *African Journal of Agricultural Research*, *7*(12), 1901–1909. https://doi.org/10.5897/AJAR11.1456

Rendana, M., Idris, W. M. R., Rahim, S. A., Abdo, H. G., Almohamad, H., Al Dughairi, A. A., & Albanai, J. A. (2023). Current and future land fire risk mapping in the southern region of Sumatra, Indonesia, using CMIP6 data and GIS analysis. *SN Applied Sciences*, *5*(8). https://doi.org/10.1007/s42452-023-05432-6

Rodney, R. M., Swaminathan, A., Calear, A. L., Christensen, B. K., Lal, A., Lane, J., Leviston, Z., Reynolds, J., Trevenar, S., Vardoulakis, S., & Walker, I. (2021). Physical and Mental Health Effects of Bushfire and Smoke in the Australian Capital Territory 2019–20. *Frontiers in Public Health*, *9*(October), 1–13. https://doi.org/10.3389/fpubh.2021.682402

Rossi, F., & Becker, G. (2019). Creating forest management units with Hot Spot Analysis (Getis-Ord Gi*) over a forest affected by mixed-severity fires. *Australian Forestry*, *82*(4), 166–175. https://doi.org/10.1080/00049158.2019.1678714

Roy, D. P., De Lemos, H., Huang, H., Giglio, L., Houborg, R., & Miura, T. (2024). Multi-resolution monitoring of the 2023 Maui wildfires, implications and needs for satellite-based wildfire disaster monitoring. *Science of Remote Sensing*, *10*(May), 100142. https://doi.org/10.1016/j.srs.2024.100142

Sadasivuni, R., Cooke, W. H., & Bhushan, S. (2013). Wildfire risk prediction in Southeastern Mississippi using population interaction. *Ecological Modelling*, *251*, 297–306. https://doi.org/10.1016/j.ecolmodel.2012.12.024

Salavati, G., Saniei, E., Ghaderpour, E., & Hassan, Q. K. (2022). Wildfire Risk Forecasting Using Weights of Evidence and Statistical Index Models. *Sustainability (Switzerland)*, *14*(7), 1–15. https://doi.org/10.3390/su14073881

Setiawan, I., Mahmud, A. R., Mansor, S., Mohamed Shariff, A. R., & Nuruddin, A. A. (2004). GIS-grid-based and multi-criteria analysis for identifying and mapping peat swamp forest fire hazard in Pahang, Malaysia. *Disaster Prevention and Management: An International Journal*, *13*(5), 379–386. https://doi.org/10.1108/09653560410568507

Shahriar, S., El-Said, M. M., Z., Safwanah N. M., S., Kho J., H., Lee, N. N. D. H. M. F., & Hasim, N. H. H. (2019). Risk assessment for forest fire in Brunei Darussalam. *MATEC Web of Conferences*, *258*, 05033. https://doi.org/10.1051/matecconf/201925805033

Sharma, S. K., Aryal, J., & Rajabifard, A. (2022). Remote Sensing and Meteorological Data Fusion in Predicting Bushfire Severity : A Case Study from Victoria, Australia. *Remote Sensing*, *14*, 1–27.

Shi, K., & Touge, Y. (2022). Characterization of global wildfire burned area spatiotemporal patterns and underlying climatic causes. *Scientific Reports*, *12*(1), 1–17. https://doi.org/10.1038/s41598-021-04726-2

Shi, Z., Feng, Y., Stewart, M. G., & Gao, W. (2024). Virtual modelling-based fragility assessment of structures under bushfire propagation. *Reliability Engineering and System Safety*, *245*(October 2023), 110000. https://doi.org/10.1016/j.ress.2024.110000

Shrestha, N. (2020). Detecting Multicollinearity in Regression Analysis. *American Journal of Applied Mathematics and Statistics*, *8*(2), 39–42. https://doi.org/10.12691/ajams-8-2-1

Shuo, Z., Jingyu, Z., Zhengxiang, Z., & Jianjun, Z. (2021). Identifying the density of grassland fire points with kernel density estimation based on spatial distribution characteristics. *Open Geosciences*, *13*(1), 796–806. https://doi.org/10.1515/geo-2020-0265

Sim, M. S., Wee, S. J., Alcantara, E., & Park, E. (2023). Deforestation as the Prominent Driver of the Intensifying Wildfire in Cambodia, Revealed through Geospatial Analysis. *Remote Sensing*, *15*(13). https://doi.org/10.3390/rs15133388

Simpson, G., & Wu, Y. H. (2014). Accuracy and effort of interpolation and sampling: Can GIS help lower field costs? *ISPRS International Journal of Geo-Information*, *3*(4), 1317–1333. https://doi.org/10.3390/ijgi3041317

Singh, H., & Srivastava, S. K. (2025). Identification of forest fire-prone region in Lamington National Park using GIS-based multicriteria technique: validation using field and Sentinel-2-based observations. *Geocarto International*, *40*(1). https://doi.org/10.1080/10106049.2025.2462484

Sinha, A., Nikhil, S., Ajin, R. S., Danumah, J. H., Saha, S., Costache, R., Rajaneesh, A., & Sajinkumar, K. S. (2023). Wildfire Risk Zone Mapping in Contrasting Climatic Conditions : An Approach Employing AHP and F-AHP Models. *Fire*, *6*(2023).

Song, Y., Xu, C., Li, X., & Oppong, F. (2024). Lightning-Induced Wildfires: An Overview. In *Fire* (Vol. 7, Issue 3, pp. 1–28). https://doi.org/10.3390/fire7030079

Stoyanova, J. S., Georgiev, C. G., & Neytchev, P. N. (2022). Satellite Observations of Fire Activity in Relation to Biophysical Forcing Effect of Land Surface Temperature in Mediterranean Climate. *Remote Sensing*, *14*(7). https://doi.org/10.3390/rs14071747

Strelec, G., Kunneke, A., & Jooste, F. (2022). Method for detection and identification of lightning strokes likely to cause wildfires. *ICLP 2022 - 36th International Conference on Lightning Protection*, *January*, 632–636. https://doi.org/10.1109/ICLP56858.2022.9942469

Suhaimi, A. M. (2024). Perlis kekal negeri terpanas suhu boleh cecah 40 darjah celcius. *Kosmo*.

Sun, D., & Kafatos, M. (2007). Note on the NDVI-LST relationship and the use of temperature-related drought indices over North America. *Geophysical Research Letters*, *34*(24), 1–4. https://doi.org/10.1029/2007GL031485

Sun, Y., Wang, X., Zhang, C., & Zuo, M. (2023). Multiple Regression : Methodology and Applications. *Science, Engineering and Technology*, *49*, 542–548.

Syphard, A. D., & Keeley, J. E. (2015). Location, timing and extent of wildfire vary by cause of ignition. *International Journal of Wildland Fire*, *24*(1), 37–47. https://doi.org/10.1071/WF14024

Sze, J. S., Jefferson, & Lee, J. S. H. (2019). Evaluating the social and environmental factors behind the 2015 extreme fire event in Sumatra, Indonesia. *Environmental Research Letters*, *14*(1). https://doi.org/10.1088/1748-9326/aaee1d

Tajudin, N., Ya'acob, N., Ali, D. M., & Adnan, N. A. (2021). Soil moisture index estimation from Landsat 8 images for prediction and monitoring landslide occurrences in Ulu Kelang, Selangor, Malaysia. *International Journal of Electrical and Computer Engineering*, *11*(3), 2101–2108. https://doi.org/10.11591/ijece.v11i3.pp2101-2108

Talukdar, N. Rahman, Ahmad, F., Goparaju, L., Choudhury, P., Qayum, A., & Rizvi, J. (2024). Forest fire in Thailand : Spatio-temporal distribution and future risk assessment. *Natural Hazards Research*, *4*(1), 87–96. https://doi.org/10.1016/j.nhres.2023.09.002

Tan, J., Yu, D., Li, Q., Tan, X., & Zhou, W. (2020). Spatial relationship between land-use/land-cover change and land surface temperature in the Dongting Lake area, China. *Scientific Reports*, *10*(1), 1–9. https://doi.org/10.1038/s41598-020-66168-6

Taripanah, F., & Ranjbar, A. (2021). Quantitative analysis of spatial distribution of land surface temperature (LST) in relation to ecohydrological, terrain and socio-economic factors based on Landsat data in a mountainous area. *Advances in Space Research*, *68*(9), 3622–3640. https://doi.org/10.1016/j.asr.2021.07.008

Thakali, L., Kwon, T. J., & Fu, L. (2015). Identification of crash hotspots using kernel density estimation and kriging methods: a comparison. *Journal of Modern Transportation*, *23*(2), 93–106. https://doi.org/10.1007/s40534-015-0068-0

Thangavel, K., Spiller, D., Sabatini, R., Amici, S., Sasidharan, S. T., Fayek, H., & Marzocca, P. (2023). Autonomous Satellite Wildfire Detection Using Hyperspectral Imagery and Neural Networks: A Case Study on Australian Wildfire. *Remote Sensing*, *15*(3). https://doi.org/10.3390/rs15030720

Tran, T. T. K., Janizadeh, S., Bateni, S. M., Jun, C., Kim, D., Trauernicht, C., Rezaie, F., Giambelluca, T. W., & Panahi, M. (2024). Improving the prediction of wildfire susceptibility on Hawai‘i Island, Hawai‘i, using explainable hybrid machine learning models. *Journal of Environmental Management*, *351*(July 2023), 119724. https://doi.org/10.1016/j.jenvman.2023.119724

Trang, P. T., Andrew, M. E., Chu, T., & Enright, N. J. (2022). Forest fire and its key drivers in the tropical forests of northern Vietnam. *International Journal of Wildland Fire*, *31*, 213–229. https://doi.org/10.1071/WF21078

Treneska, S., & Stojkoska, B. R. (2021). Wildfire detection from UAV-collected images using transfer learning. *Conference: 18th International Conference on Informatics and Information Technologies*. https://www.researchgate.net/publication/353732371

Trinh, L. H., & Vu, D. T. (2019). Application of remote sensing technique for drought assessment based on normalized difference drought index, a case study of Bac Binh district, Binh Thuan province (Vietnam). *Russian Journal of Earth Sciences*, *19*(2). https://doi.org/10.2205/2018ES000647

Tzoumas, G., Pitonakova, L., Salinas, L., Scales, C., Richardson, T., & Hauert, S. (2023). Wildfire detection in large-scale environments using force-based control for swarms of UAVs. *Swarm Intelligence*, *17*(1–2), 89–115. https://doi.org/10.1007/s11721-022-00218-9

Ullah, W., Ahmad, K., Ullah, S., Tahir, A. A., Javed, M. F., Nazir, A., Abbasi, A. M., Aziz, M., & Mohamed, A. (2023). Analysis of the relationship among land surface temperature (LST), land use land cover (LULC), and normalized difference vegetation index (NDVI) with topographic elements in the lower Himalayan region. *Heliyon*, *9*(2), e13322. https://doi.org/10.1016/j.heliyon.2023.e13322

Van, L. N., & Lee, G. (2025). Investigating the Relationship Between Topographic Variables and Wildfire Burn Severity. *Geographies*, *5*(3).

https://doi.org/10.3390/geographies5030047

Vasilakos, C., Kalabokidis, K., Hatzopoulos, J., & Matsinos, I. (2009). Identifying wildland fire ignition factors through sensitivity analysis of a neural network. *Natural Hazards*, *50*(1), 125–143. https://doi.org/10.1007/s11069-008-9326-3

Velayati, A. H., Boloorani, A. D., Kiavarz, M., Samani, N. N., & Alavipanah, S. K. (2024). Spatiotemporal analysis of wildfire in the Tigris and Euphrates basin: A remote sensing-based wildfire potential mapping. *Remote Sensing Applications: Society and Environment*, *34*(December 2023), 101150. https://doi.org/10.1016/j.rsase.2024.101150

Veraverbeke, S., Sedano, F., Hook, S. J., Randerson, J. T., Jin, Y., & Rogers, B. M. (2014). Mapping the daily progression of large wildland fires using MODIS active fire data. *International Journal of Wildland Fire*, *23*(5), 655–667. https://doi.org/10.1071/WF13015

Vlassova, L., Perez-cabello, F., Mimbrero, M. R., montorio lloveria, R., & Garcia-martin, A. (2014). Analysis of the Relationship between Land Surface Temperature and Wildfire Severity in a Series of Landsat Images. *Remote Sensing*, *6*, 6136–6162. https://doi.org/10.3390/rs6076136

Wee, S. J., Park, E., Alcantara, E., & Lee, J. S. H. L. (2024). Exploring Multi-Driver Influences on Indonesia's Biomass Fire Patterns from 2002 to 2019 through Geographically Weighted Regression. *Journal of Geovisualization and Spatial Analysis*, *2016*, 1–18. https://doi.org/10.1007/s41651-023-00166-w

Weinstein, D. A., & Woodbury, P. B. (2010). Review of methods for developing probabilistic risk assessments. *Advances in Threat Assessment and Their Application to Forest and Rangeland Management*, *1*, 285–302.

Wu, S. (2021). The Temporal-Spatial Distribution and Information-Diffusion- Based Risk Assessment of Forest Fires in China. *Sustainability*, *13*.

Xing, H., Fang, K., Yao, Q., Zhou, F., Ou, T., Liu, J., Zhou, S., Jiang, S., Chen, Y., Bai, M., & Chen, J. M. (2023). Impacts of changes in climate extremes on wildfire occurrences in China. *Ecological Indicators*, *157*(September). https://doi.org/10.1016/j.ecolind.2023.111288

Ya'acob, N., Jamil, I. A. A., Aziz, N. F. A., Yusof, A. L., Kassim, M., & Naim, N. F. (2022). Hotspots Forest Fire Susceptibility Mapping for Land Use or Land Cover using Remote Sensing and Geographical Information Systems (GIS). *IOP Conference Series: Earth and Environmental Science*, *1064*(1).

https://doi.org/10.1088/1755-1315/1064/1/012029

Ya'Acob, N., Jamil, I. A. A., Aziz, N. F. A., Yusof, A. L., Kassim, M., & Naim, N. F. (2022). Hotspots Forest Fire Susceptibility Mapping for Land Use or Land Cover using Remote Sensing and Geographical Information Systems (GIS). *IOP Conference Series: Earth and Environmental Science*, *1064*(1). https://doi.org/10.1088/1755-1315/1064/1/012029

Yang, X., Jin, X., & Zhou, Y. (2021). Wildfire risk assessment and zoning by integrating MaxEnt and GIS in Hunan Province, China. *Forests*, *12*(10). https://doi.org/10.3390/f12101299

Yang, Y., Cao, C., Pan, X., Li, X., & Zhu, X. (2017). Downscaling land surface temperature in an arid area by using multiple remote sensing indices with random forest regression. *Remote Sensing*, *9*(8). https://doi.org/10.3390/rs9080789

Yu, P., Xu, R., Abramson, M. J., Li, S., & Guo, Y. (2020). Bushfires in Australia: a serious health emergency under climate change. *The Lancet Planetary Health*, *4*(1), e7–e8. https://doi.org/10.1016/S2542-5196(19)30267-0

Yu, W., & Ai, T. (2014). A visualização e análise de facilidades urbanas, usando o método POIS por meio da densidade de Kernel restringida. *Boletim de Ciencias Geodesicas*, *20*(4), 902–926. https://doi.org/10.1590/S1982-21702014000400050

Zahran, E. S. M. M., Shams, S., & Said, S. N. Matullah B. M. (2020). Validation of forest fire hotspot analysis in GIS using forest fire contributory factors. *Systematic Reviews in Pharmacy*, *11*(12), 249–255. https://doi.org/10.31838/srp.2020.12.40

Zhang, F., Zhao, P., Xu, S., Wu, Y., Yang, X., & Zhang, Y. (2020). Integrating multiple factors to optimize watchtower deployment for wildfire detection. *Science of the Total Environment*, *737*, 139561. https://doi.org/10.1016/j.scitotenv.2020.139561

Zhang, P., Hu, X., & Ban, Y. (2022). Wildfire-S1S2-Canada: A Large-Scale Sentinel-1/2 Wildfire Burned Area Mapping Dataset Based on the 2017-2019 Wildfires in Canada. *International Geoscience and Remote Sensing Symposium (IGARSS)*, *2022-July*, 7954–7957. https://doi.org/10.1109/IGARSS46834.2022.9884275

Zhao, Y., Ma, J., Li, X., & Zhang, J. (2018). Saliency detection and deep learning-based wildfire identification in UAV imagery. *Sensors (Switzerland)*, *18*(3). https://doi.org/10.3390/s18030712

APPENDICES

APPENDIX 1

The processing report of Ordinary Least Squares (OLS) using the ArcGIS software

OLS Diagnostics

Input Features:	PointFire_CollectEvents	Dependent Variable:	ICOUNT
Number of Observations:	77	Akaike's Information Criterion (AICc) [d]:	322.211907
Multiple R-Squared [d]:	0.135679	Adjusted R-Squared [d]:	0.061595
Joint F-Statistic [e]:	1.831411	Prob(>F), (6,70) degrees of freedom:	0.105397
Joint Wald Statistic [e]:	15.095008	Prob(>chi-squared), (6) degrees of freedom:	0.019531*
Koenker (BP) Statistic [f]:	9.169571	Prob(>chi-squared), (6) degrees of freedom:	0.164264
Jarque-Bera Statistic [g]:	14.493726	Prob(>chi-squared), (2) degrees of freedom:	0.000712*

The Number Of Reported Wildfire Cases From The Year 2014 To 2024 In Perlis

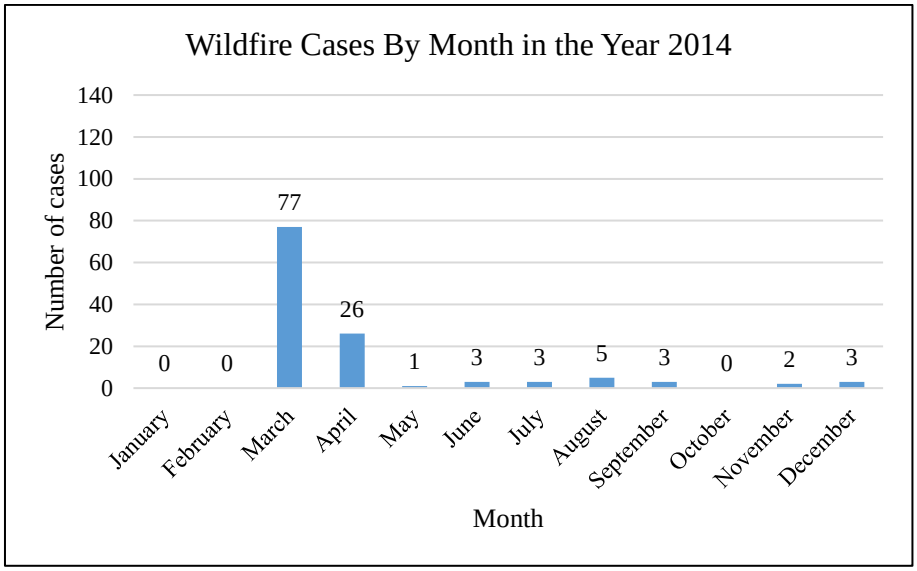

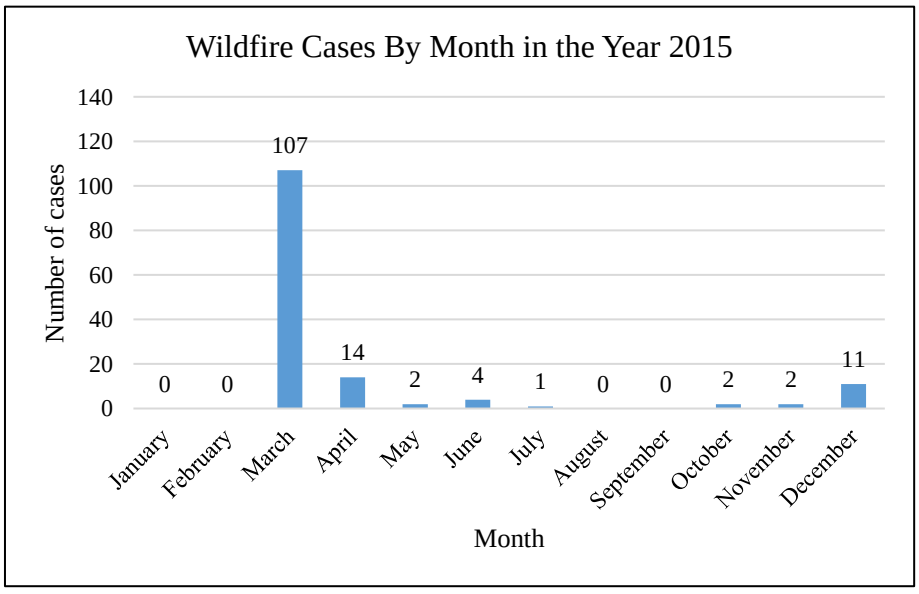

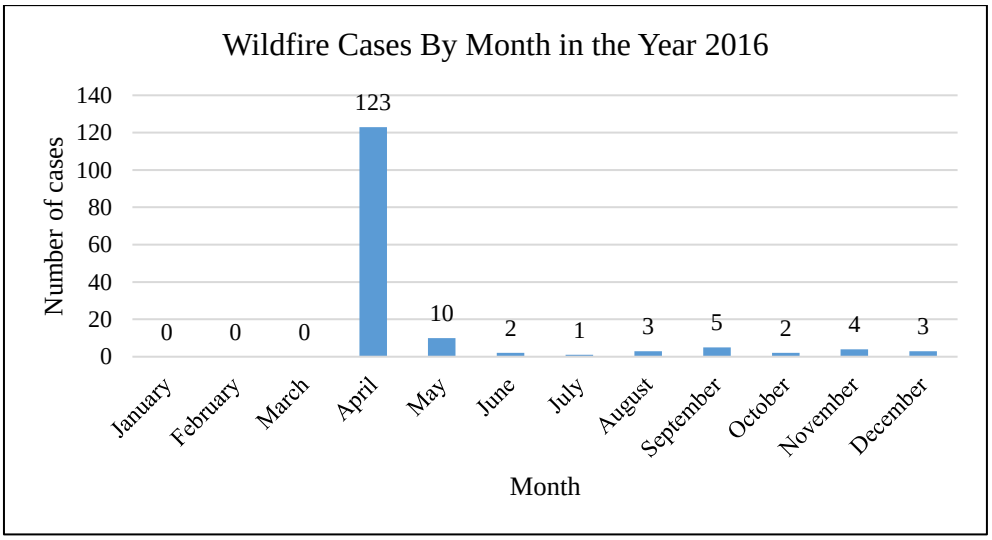
Wildfire Cases By Month in the Year 2016
Number of cases
140
120
100
80
60
40
20
0
0
0
0
123
10
2
1
3
5
2
4
3
January
February
March
April
May
June
July
August
September
October
November
December
Month

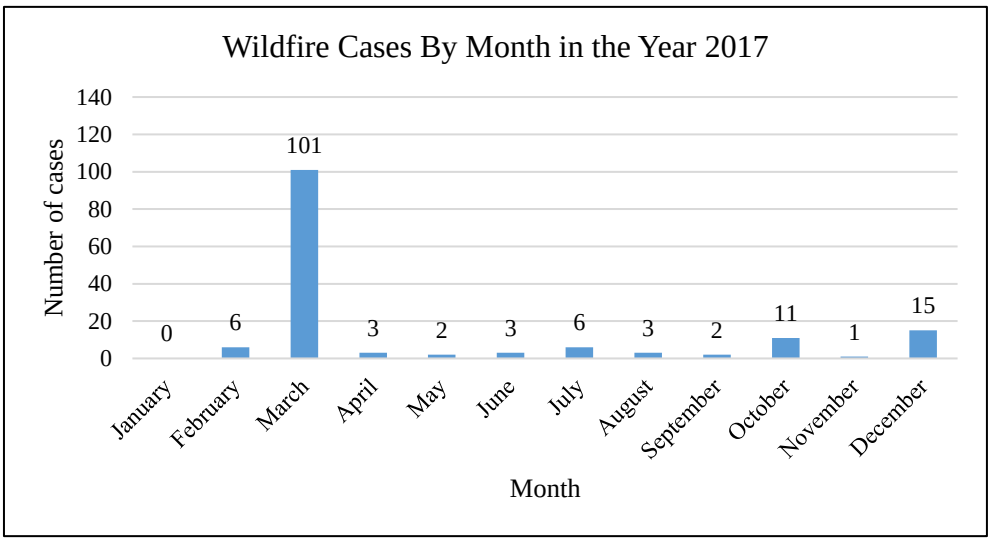
Wildfire Cases By Month in the Year 2017
Number of cases
140
120
100
80
60
40
20
0
0
6
101
3
2
3
6
3
2
11
1
15
January
February
March
April
May
June
July
August
September
October
November
December
Month

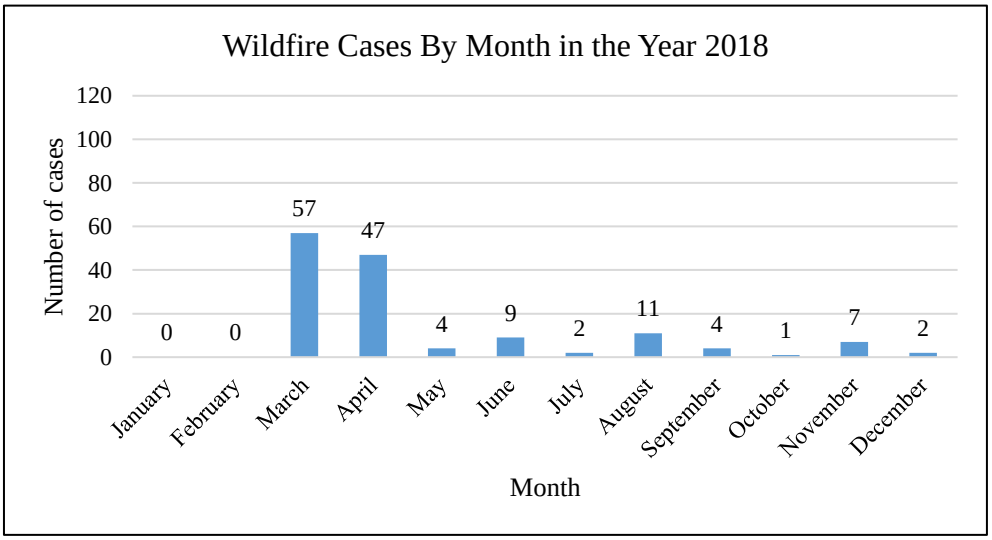
Wildfire Cases By Month in the Year 2018
Number of cases
120
100
80
60
40
20
0
0
0
57
47
4
9
2
11
4
1
7
2
January
February
March
April
May
June
July
August
September
October
November
December
Month

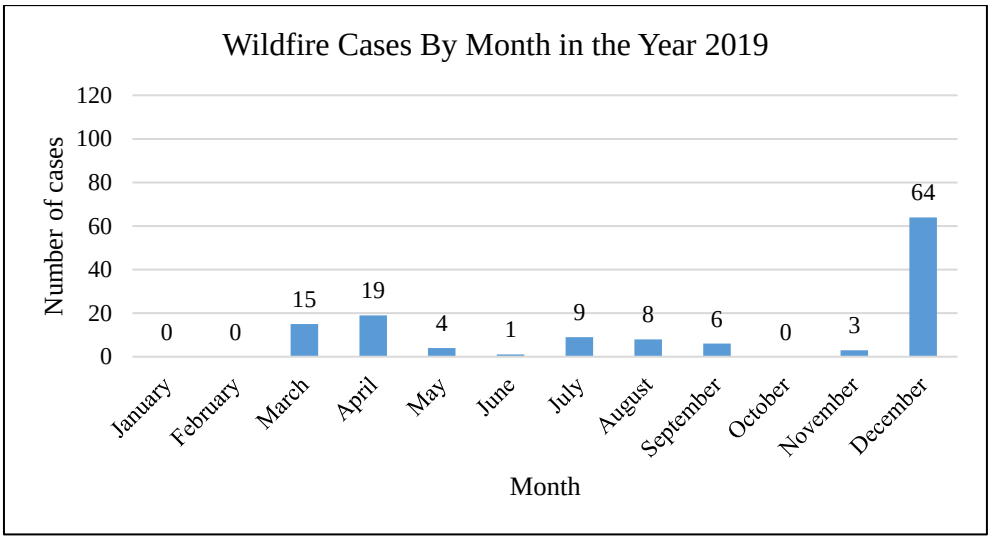
Wildfire Cases By Month in the Year 2019
Number of cases
120
100
80
60
40
20
0
0
0
15
19
4
1
9
8
6
0
3
64
January
February
March
April
May
June
July
August
September
October
November
December
Month

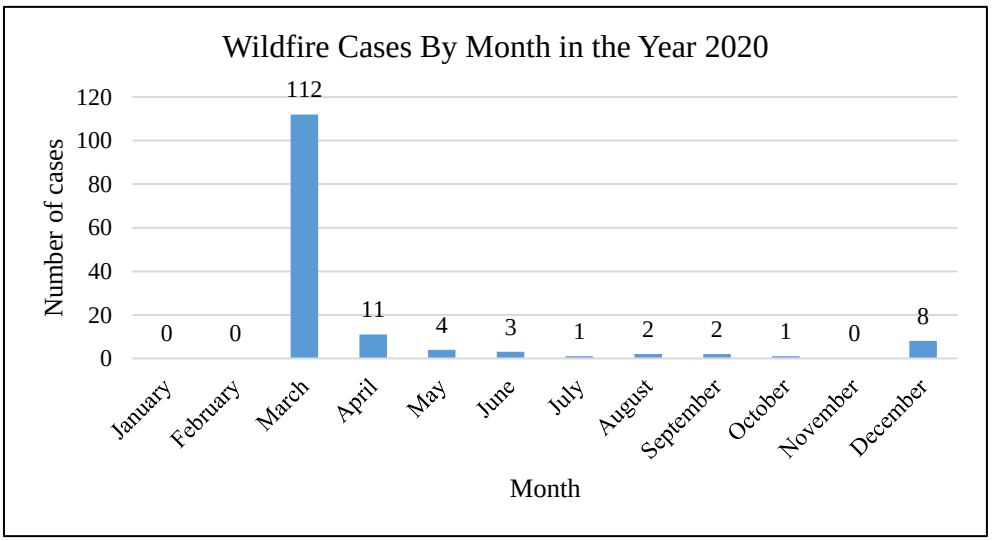
Wildfire Cases By Month in the Year 2020
Number of cases
120
100
80
60
40
20
0
0
0
112
11
4
3
1
2
2
1
0
8
January
February
March
April
May
June
July
August
September
October
November
December
Month

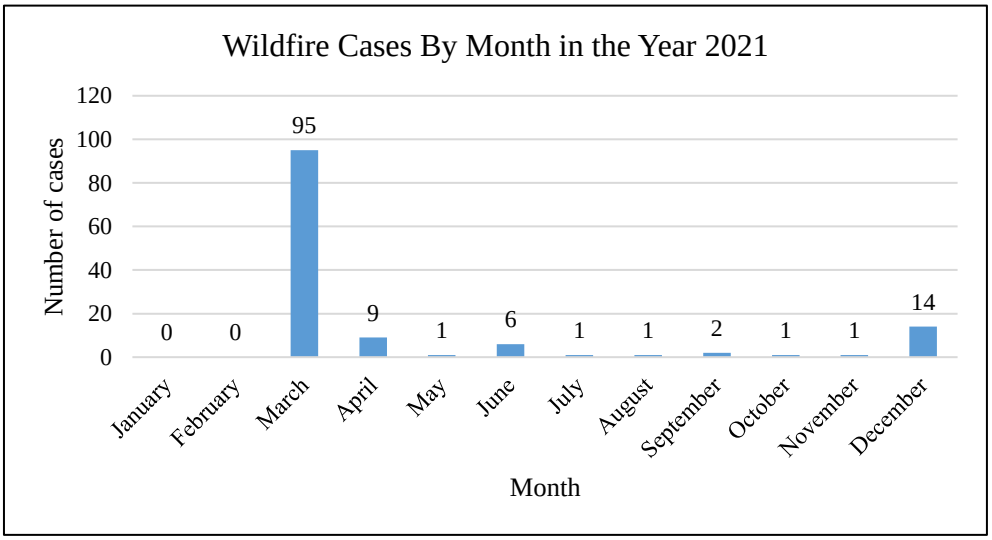
Wildfire Cases By Month in the Year 2021
Number of cases
120
100
80
60
40
20
0
0
0
95
9
1
6
1
1
2
1
1
14
January
February
March
April
May
June
July
August
September
October
November
December
Month

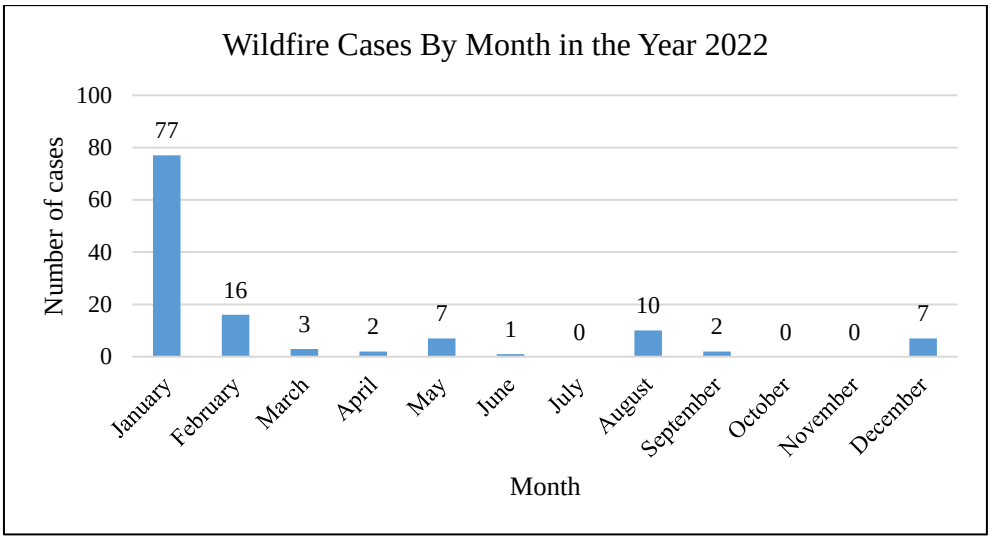
Wildfire Cases By Month in the Year 2022
Number of cases
100
80
60
40
20
0
77
16
3
2
7
1
0
10
2
0
0
7
January
February
March
April
May
June
July
August
September
October
November
December
Month

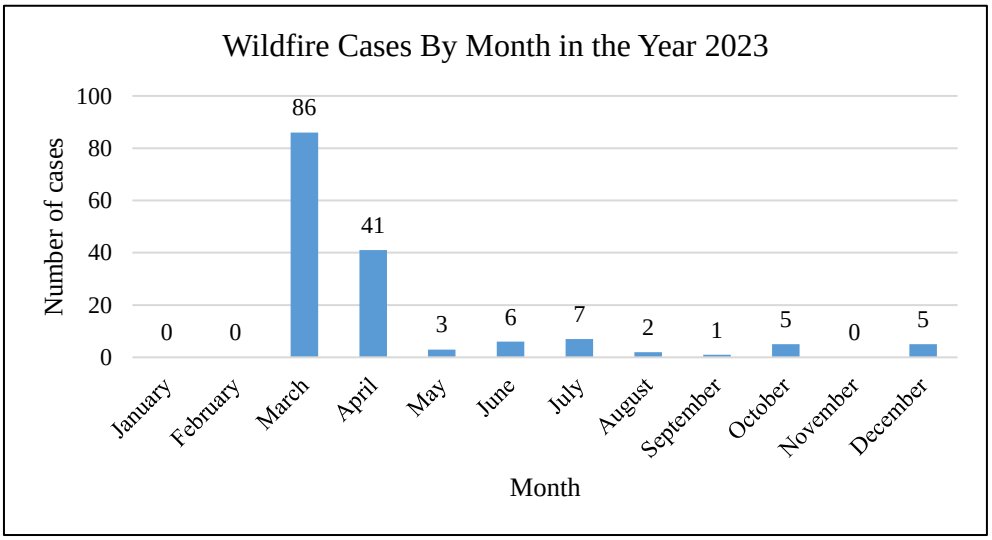
Wildfire Cases By Month in the Year 2023
Number of cases
100
80
60
40
20
0
0
0
86
41
3
6
7
2
1
5
0
5
January
February
March
April
May
June
July
August
September
October
November
December
Month

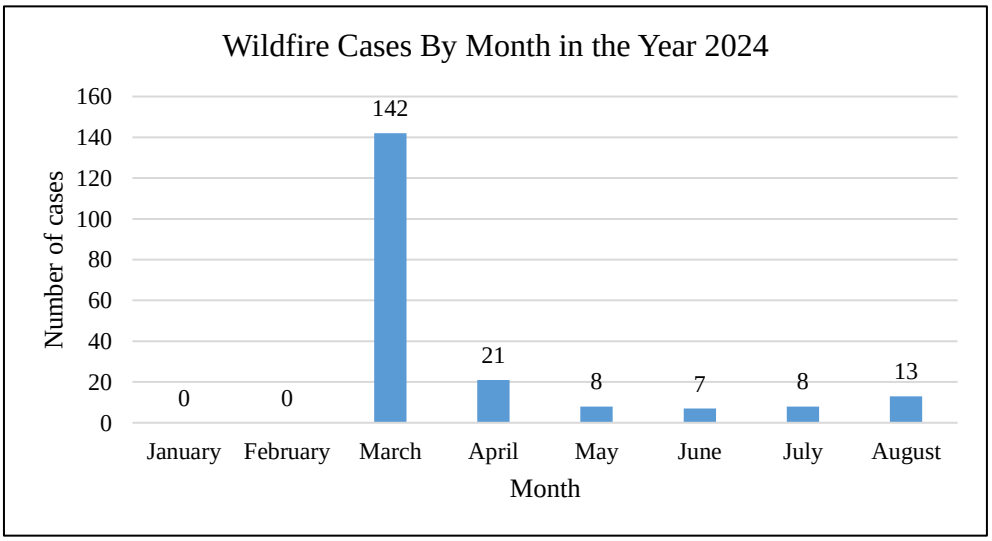
Wildfire Cases By Month in the Year 2024
Number of cases
160
140
120
100
80
60
40
20
0
0
0
142
21
8
7
8
13
January
February
March
April
May
June
July
August
Month

AUTHOR'S PROFILE



Afiqah Zahidah Binti Anwarzaini is a student of the Bachelor of Science Surveying and Geomatics (Hons.) in 2020 from UiTM Perlis Branch. Her MSc thesis involves the generation of FHI using MLR analysis and the identification of wildfire hazard zones for Perlis state, incorporating several spectral indices such as LST, NDVI, NDWI, NDMI, NDDI, and NBR.

LIST OF PUBLICATIONS

N. B. M. Tarmizi, A. Z. B. Anwarzaini, and M. F. B. M. Fisol, "Maximum Likelihood Classifier Analysis of UAV Image Classification Post-Fire Area Estimation," *2025 IEEE 16th Control and System Graduate Research Colloquium (ICSGRC)*, Shah Alam, Malaysia, 2025, pp. 222-227, doi: 10.1109/ICSGRC65918.2025.11159749.

Anwarzaini, A. Z., & Tarmizi, N. M. (2025). Spatiotemporal Analysis Of Wildfire Occurrence In Perlis From 2014 To 2024. *Journal Of Tourism, Hospitality And Environment Management (JTHEM)*, *10*(42), 21–38. https://doi.org/10.35631/JTHEM.1042003

Anwarzaini, A. Z., & Tarmizi, N. M. (2026). Development of Fire Hazard Index through Multispectral Indices and Geospatial Analysis. International Journal of Research and Innovation in Social Science (IJRISS), 10(2).

Anwarzaini, A. Z., & Tarmizi, N. M. (2026). Tropical Climate Fire Hazard Index (FHI). Innovation Series Quarterly, 2(1), 109-117.